

UNIVERSITY OF OKLAHOMA

GRADUATE COLLEGE

BIOLOGICAL IMPLICATIONS OF THE REACTIONS OF THIOCYANATE
(SCN⁻) WITH SMALL MOLECULE, MACROMOLECULE AND CELLULAR
CHLORAMINES

A DISSERTATION

SUBMITTED TO THE GRADUATE FACULTY

in partial fulfillment of the requirements for the

Degree of

DOCTOR OF PHILOSOPHY

By

BHEKI ALEX XULU

Norman, Oklahoma

2011

BIOLOGICAL IMPLICATIONS OF THE REACTIONS OF THIOCYANATE
(SCN⁻) WITH SMALL MOLECULE, MACROMOLECULE AND CELLULAR
CHLORAMINES

A DISSERTATION APPROVED FOR THE
DEPARTMENT OF CHEMISTRY AND BIOCHEMISTRY

BY

Dr. Michael Ashby, Chair

Dr. George Richter-Addo

Dr. Paul Cook

Dr. Kenneth Nicholas

Dr. David Nagle

ACKNOWLEDGEMENTS

To my major advisor **Dr Michael Ashby**, I would like to express my sincere gratitude for letting me be part of your research team. Thanks for your leadership and support throughout my graduate career. You explained to me your research themes and encouraged me to develop my own research questions and always gave me sound guidance on how to investigate them. **Jennifer Beal**, thanks for training me on how to use the stopped-flow instrument and for the willingness to listen as I rambled on about my projects. **Dr Susan Nimmo**, I appreciate your time and patience as you trained me on how to use the NMR instruments. **Dr Dario Ramirez and Sandra Gomez-Megiba**, thanks for welcoming me with open arms to your laboratory and for teaching me how to do some of the biological experiments. **Dr Randy Hewes**, thanks for the training on how to operate the fluorescence microscope. I would be remiss if I failed to recognize former members of the Ashby group, **Dr Peter Nagy, Dr Lemma Wordegiorgis, Dr Xiaoguang Wang, Dr Hisanori Ueki and Dr Irina Chvyrkova** all postdocs in my lab. Although I may not have worked directly with some of you, I learned a lot from watching you as you worked on your projects. To the entire **Chemistry Office Staff**, thank you for the valuable support. I owe a great deal of gratitude to **Arlene Crawford** who one day as I walked into the chemistry office, looked at me and said Alex, I've been here for many years now and I will let you in on the secret of how to make it in this place. With humility and grace she said "learn to roll

with the punches”, I would not be telling the truth if I claim to have understood what she meant at the time, however, as years passed by, I began to understand the wisdom of those words and they have helped me a great deal in my journey. To **Garry Chapmann**, you are a great friend, please don't ever change. To my family and friends, words cannot explain how much I appreciate you. A special thanks to my brother and friend **Progress Mathews**, I always knew I could rely on you.

TABLE OF CONTENTS

Acknowledgements	iv
Table of Contents	vi
List of Tables	xi
List of Figures	xii
Abstract	xviii
Chapter 1: Framework for the research	1
1.1 Statement of problems and objectives	1
1.2 Phagocytosis	2
1.3 Oxidative burst	4
1.4 Chloramines	8
1.5 Hypothiocyanite (OSCN ⁻)	10
1.6 Glutathione reductase (GR)	13
1.7 Fluorescence microscopy for cell imaging	14
1.8 Summary	17
1.9 References	21
Chapter 2: Experimental methods	33
2.1 Reagents	33
2.2 Sample preparation	34
2.2.1 Hypochlorite (OCl ⁻)	34
2.2.2 Taurine chloramine (TauCl)	34
2.2.3 Reaction of TauCl with SCN ⁻ and quantification of OSCN ⁻	34
2.2.4 Taurine dichloramine (TauCl ₂)	35

2.2.5	Synthesis of 5-thio-2-nitrobenzoic acid (TNB)	35
2.2.6	Hypothiocyanite (OSCN ⁻)	35
2.2.7	Ubiquitin chloramines (Ub*Cl)	36
2.2.8	Reaction of Ub*Cl with SCN ⁻ and quantification of OSCN ⁻	37
2.2.9	Chlorination of <i>E. coli</i> and quantification of oxidizing equivalents	37
2.2.10	Reaction of chlorinated MG1655 with SCN ⁻ and Quantification of OSCN ⁻	38
2.2.11	Synthesis of the Rhodamine derivative 1	38
2.2.12	Assay for the GOR reduction of GSSG	39
2.3	Instrumentation and data analysis	39
2.3.1	UV/Visible spectroscopy	39
2.3.2	Fluorescence spectroscopy	40
2.3.3	pH measurements	40
2.3.4	Stopped-flow studies	40
2.3.5	Confocal microscopy	40
2.3.6	Cell assay and Protocol	41
2.4	References	44

Chapter 3: Small molecular, macromolecular and cellular chloramines react with thiocyanate to give the human defense factor hypothiocyanite	46
3.1 Introduction	46
3.2 Results and discussion	49
3.2.1 Reaction of small molecular chloramines with thiocyanate	49
3.2.2 Reaction of protein chloramines with thiocyanate	56
3.2.3 Reaction of Cellular Chloramines with thiocyanate	62
3.2.4 Biological significance of the reduction of chloramines by SCN^- and OSCN^-	65
3.3 Conclusions	67
3.4 References	71
CHAPTER 4: Formation of stable organic dichloramines and their reactivities towards thiols and other antioxidants	77
4.1 Introduction	77
4.2 Results and discussion	82
4.2.1 The chemical stability of dichloramines	82
4.2.2 Reactions of TauCl_2 with thiols, ascorbate, methionine and lysine	83
4.2.3 pH dependency of the reaction of TauCl_2 with TNB	

and ascorbate	87
4.2.4 Kinetics of the reaction of TauCl_2 with TNB	99
4.2.4.1 Concentration dependencies	99
4.2.4.2 pH dependency	102
4.2.4.3 Proposed mechanism	103
4.2.5 Possible biological significance	103
4.4 Conclusions	106
4.5 References	107
CHAPTER 5: Repair of cellular damage and recovery of enzyme activity by SCN^- following treatment with HOCl	115
5.1 Introduction	115
5.2 Results and discussion	118
5.2.1 In vitro study of the reactions of the probe with HOCl and chloramines	118
5.2.2 Cellular imaging studies with A549 cancer cells	122
5.2.3 Inhibition glutathione reductase (GR) and the recovery of enzyme activity after SCN^- treatment	126
5.3 Detection of apoptosis and necrosis by flow cytometry	132
5.4 Possible biological significance of these findings	134
5.5 Conclusions	135
5.6 References	137

LIST OF TABLES

Table 2.1:	Protocol adopted for treatment of A549 cells (controls and experiments)	43
Table 4.1:	Stabilities of monochloramines and dichloramines of amino acids	82
Table 4.2:	Pseudo-second-order rate constants for the reactions of TauCl_2 with thiols, methionine, ascorbate and lysine at pH 7.4.	87

LIST OF FIGURES

Figure 1.1:	Phases of phagocytosis	3
Figure 1.2:	Neutrophil oxidative burst	4
Figure 1.3:	Proposed mechanism for the oxidation of protein-derived tryptophan by HO ₂ SCN ⁻	12
Figure 1.4:	Synthesis of the rhodamine-hydroxamic acid probe (1)	16
Figure 3.1:	UV-vis spectra obtained for the reactions of TauCl (50 μM) with SCN ⁻ (50-250 μM) in phosphate buffer (100 mM, pH 7.4) at 20 °C. The spectra were recorded with a 1 meter fiber optic cell. The chemical yield of OSCN ⁻ is indicated versus [SCN ⁻] ₀	50
Figure 3.2:	UV-vis spectra obtained for the reactions of TauCl (80 μM) with SCN ⁻ (0.5-5.0 mM) in phosphate buffer (100 mM, pH 7.4) at 20 °C. The spectra were recorded with a 1 meter fiber optic cell. The chemical yield of OSCN ⁻ is indicated versus [SCN ⁻] ₀	51
Figure 3.3:	Chemical yield of OSCN ⁻ for [SCN ⁻] = 10 mM and [TauCl] ₀ = 0.25, 0.50, 1.0, and 2.0 mM in phosphate buffer (100 mM, pH 7.4) at 20 °C.	52
Figure 3.4:	Concentrations determined at 252 nm (solid circles, λ _{max} for TauCl) and 376 nm (open circles, λ _{max} for OSCN ⁻) versus time for the reaction of [TauCl] ₀ = 0.74 mM and [OSCN ⁻] ₀ = 0.74 mM in phosphate buffer (100 mM, pH 7.4) at 20 °C. The OSCN ⁻ was prepared by the LPO-catalyzed oxidation of 5 mM SCN ⁻ by 5 mM H ₂ O ₂ to give a 3.5 mM stock solution of OSCN ⁻ (determined spectrophotometrically). The solid lines are imperfect nonlinear least-squares fit of the experimental data (for clarity, 1% and 10% shown for TauCl and OSCN ⁻ , respectively) using a mixed second-order rate equation $k = (1.182 \pm 0.002) \times 10^3$ and $(2.84 \pm 0.03) \times 10^3 \text{ M}^{-1}\text{s}^{-1}$ at 276 and 376 nm, respectively). The dashed line is the expected absorption change for a second-order absorption decay for $k = 128.6 \pm 0.1 \text{ M}^{-1} \text{ s}^{-1}$ (the independently measured rate constant for the reaction of TauCl and SCN ⁻ under the same reaction conditions).	55

- Figure 3.5: Observed absorbance decrease at 412 nm for the reaction of OSCN^- ($4 \mu\text{M}$, produced by the LPO-catalyzed oxidation of SCN^- by H_2O_2) with TNB ($56 \mu\text{M}$) at pH 7.4 and $I = 1.0 \text{ M}$. A first-order fit (red) and 20% of the data (black circles) are illustrated 57
- Figure 3.6: Observed absorbance decrease at 412 nm for the reaction of OSCN^- ($5.5 \mu\text{M}$, produced by the uncatalyzed oxidation of SCN^- by TauCl) with TNB ($56 \mu\text{M}$) at pH 7.4 and $I = 1.0 \text{ M}$. A first-order fit (red) and 10% of the data (black circles) are illustrated 58
- Figure 3.7: Observed biexponential (decrease-decrease) absorbance decrease at 412 nm for the reaction of Ub^*Cl ($6 \mu\text{M}$, based upon the amount of HOCl used) with TNB ($68 \mu\text{M}$) at pH 7.4 and $I = 1.0 \text{ M}$. A biexponential fit (red) and 10% of the data (black circles) are illustrated 61
- Figure 3.8: Observed absorbance decrease at 412 nm for the reaction of TauCl ($208 \mu\text{M}$) with TNB ($16 \mu\text{M}$) at pH 7.4 and $I = 1.0 \text{ M}$. A first-order fit (red) and 2% of the data (black circles) are illustrated 62
- Figure 3.9: Observed absorbance decrease at 412 nm for the reaction of Ub^*Cl ($6.75 \mu\text{M}$) with SCN^- (0.5 mM) for 20 minutes, followed by reaction with TNB ($58.66 \mu\text{M}$) at pH 7.4 and $I = 1.0 \text{ M}$. A first-order fit (red) and 10% of the data (black circles) are illustrated 63
- Figure 3.10: Absorbance decrease at 412 nm for the reaction of chlorinated *E. coli* ($6 \mu\text{M}$, based upon the HOCl used) with TNB ($60.8 \mu\text{M}$) at pH 7.4 and $I = 1.0 \text{ M}$. A biexponential fit (red) and 10% of the data (black circles) are illustrated. The kinetics are apparently multi-phasic 65
- Figure 3.11: Observed absorbance decrease at 412 nm for the reaction of chlorinated *E. coli* ($6 \mu\text{M}$, based upon the HOCl used) with SCN^- (2.5 mM) for 12 minutes, followed by reaction with TNB ($58.66 \mu\text{M}$) at pH 7.4 and $I = 1.0 \text{ M}$. A first-order fit (red) and 50% of the data (black circles) are illustrated 66
- Figure 4.1: Observed absorbance decrease at 412 nm for the

	reaction of TauCl_2 (40 μM) with TNB (4 μM) at pH 7.4 and $I = 1.0$ M. A first-order fit (red) and 10% of the data (black circles) are illustrated	84
Figure 4.2:	Observed absorbance decrease at 265 nm for the reaction of TauCl_2 (200 μM) with ascorbic acid (16 μM) at pH 7.4 and $I = 1.0$ M. A first-order fit (red) and 10% of the data (black circles) are illustrated	85
Figure 4.3:	pH-rate profile for the reaction of TauCl_2 with TNB	88
Figure 4.4:	Observed absorbance decrease at 412 nm for the reaction of TauCl_2 (40 μM) with TNB (4 μM) at pH 5.9 and $I = 1.0$ M. A first-order fit (red) and 10% of the data (black circles) are illustrated	89
Figure 4.5:	Observed absorbance decrease at 412 nm for the reaction of TauCl_2 (40 μM) with TNB (4 μM) at pH 6.2 and $I = 1.0$ M. A first-order fit (red) and 10% of the data (black circles) are illustrated	90
Figure 4.6:	Observed absorbance decrease at 412 nm for the reaction of TauCl_2 (40 μM) with TNB (4 μM) at pH 6.7 and $I = 1.0$ M. A first-order fit (red) and 10% of the data (black circles) are illustrated	91
Figure 4.7:	Observed absorbance decrease at 412 nm for the reaction of TauCl_2 (40 μM) with TNB (4 μM) at pH 7.1 and $I = 1.0$ M. A first-order fit (red) and 10% of the data (black circles) are illustrated	92
Figure 4.8:	pH-rate profile for the reaction of TauCl_2 with ascorbate	94
Figure 4.9:	Observed absorbance decrease at 265 nm for the reaction of TauCl_2 (200 μM) with ascorbic acid (16 μM) at pH 7.2 and $I = 1.0$ M. A first-order fit (red) and 10% of the data (black circles) are illustrated	95
Figure 4.10:	Observed absorbance decrease at 265 nm for the reaction of TauCl_2 (200 μM) with ascorbic acid (16 μM) at pH 6.9 and $I = 1.0$ M. A first-order fit (red) and 10% of the data (black circles) are illustrated	96
Figure 4.11:	Observed absorbance decrease at 265 nm for the reaction of TauCl_2 (200 μM) with ascorbic acid (16 μM) at pH 6.8 and $I = 1.0$ M. A first-order fit (red) and 10%	

of the data (black circles) are illustrated	97
Figure 4.12: Observed absorbance decrease at 265 nm for the reaction of TauCl_2 (200 μM) with ascorbic acid (16 μM) at pH 5.0 and $I = 1.0$ M. A first-order fit (red) and 10% of the data (black circles) are illustrated	98
Figure 4.13: $[\text{TauCl}_2]$ dependence of the rate law under pseudo-first order conditions	100
Figure 4.14: $[\text{TNB}]$ dependence of the rate law under pseudo-first order conditions	101
Figure 4.15: Dependence of the observed second-order rate constant k_{eff} ($\text{M}^{-1}\text{s}^{-1}$) for the reaction of TauCl_2 with TNB on $[\text{H}^+]$ at $\text{pH} > 5.5$	102
Figure 5.1: HOCl-induced oxidation of the fluorescent probe	116
Figure 5.2: Fluorescence response of the probe (10 μM) 10 min after the addition of (a) 50 μM ; (b) 100 μM HOCl, NH_2Cl and $^-\text{SO}_3\text{CH}_2\text{CH}_2\text{NHCl}$	121
Figure 5.3: Fluorescence images of A549 cells (A) untreated; (B) treated with 50 μM HOCl; (C) treated with 100 μM HOCl	122
Figure 5.4: Fluorescence images of A549 cells (A) untreated; (B) treated with 50 μM HOCl; (C) treated with 50 μM SCN^- subsequent to treatment with 50 μM HOCl; (D-F) the corresponding transmission images	124
Figure 5.5: Morphological changes to A549 cells (A) control (untreated); (B) exposed to 50 μM HOCl; (C) exposed to 50 μM SCN^- ; (D) exposed to 50 μM SCN^- subsequent to treatment with 50 μM HOCl; (E) exposed to 50 μM OSCN^- ; (F) exposed to 50 μM SCN^- and then treated with 50 μM HOCl	125
Figure 5.6: Scheme of the GR active site	127
Figure 5.7: Kinetic traces at $\lambda = 340\text{nm}$ depicting the GOR-catalyzed reduction of GSSG by NADPH. Conditions: (A) $[\text{GSSG}]_0 = 1$ mM, $[\text{NADPH}]_0 = 0.1$ mM, $[\text{GR}] = 0.025$ U/mL, $[\text{iP}] = 0.1$ M, pH 7.4 and $T = 25$ $^\circ\text{C}$; (B) GR incubated with 40 μM HOCl for 20 min and then treated with 160 μM SCN^- for another 20 min. (c) GR incubated with 40 μM HOCl for 20 min and then treated with iP for an additional	

	20 min. Each line represents an average of five data sets and only 10% of the data are illustrated	129
Figure 5.8:	Enzyme activity estimated using the rate of change in the A_{340} and the molar absorptivity (6.22×10^{-3} nmol/mL) of GR. (a) Uncatalyzed: 0, (b) HOCl modified: 0.405, (c) SCN^- treated: 2.25 and control: 4.82 (mU/mL)	130
Figure 5.9:	Proportion between living, apoptotic and necrotic cells after 20 min incubation with HOCl	132
Figure 5.10:	Proportion between living, apoptotic and necrotic cells after 20 min incubation with HOCl	133

ABSTRACT

Hypochlorous acid (HOCl) is one of the major neutrophil-derived oxidants used to kill invading pathogens. However, excess or misplaced production of HOCl can damage host tissue as it reacts indiscriminately with biological molecules such as amino acids. Chloramines are a major product of the reaction between HOCl and amino acids. As they decompose, protein-bound chloramines can permanently damage proteins by altering their structures and function. Thiocyanate (SCN^-) reacts efficiently with HOCl and thus is able to limit its propensity to inflict host tissue damage. The concentration of SCN^- in human physiologic fluids varies depending on the source of fluid and the individuals dietary and smoking habits. For example, normal human blood plasma has micromolar levels of SCN^- while the oral cavity has millimolar concentrations.

The first chapter of this dissertation covers the objectives of the research and the introduction of the important themes. The second chapter summarizes the experimental methods and the analytical techniques used to conduct the research. The third chapter of this dissertation is focused on the reaction of SCN^- with chloramines. We found that SCN^- reacts efficiently with chloramines in small molecules, in proteins, and in *Escherichia coli* cells to give OSCN^- and the parent amine. We also observed that chloramines react faster with OSCN^- than SCN^- . This suggests that the reductions of chloramines by SCN^- and OSCN^- have potential biological significance as they may repair some of the damage inflicted by HOCl on proteins.

Under slightly acidic pH conditions, chloramines disproportionate to dichloramines. In the fourth chapter, the reactivity of dichloramines towards thiols was examined. We found that at equimolar concentrations, the dichloramines react much faster with thiols than monochloramines. Chlorotaurine reacts with thiols with a (pH-dependent) pseudo-second order rate constant of $10^2 \text{ M}^{-1}\text{s}^{-1}$ while the rate constant for dichlorotaurine is $10^6 \text{ M}^{-1}\text{s}^{-1}$ at pH 7.4. These results suggest that the more stable dichloramines (e.g. those on lysine residues and on taurine) may be playing a role, at least in part, in the killing of phagocytosed bacteria.

The fifth chapter of this dissertation evaluates the biological significance of the reaction of SCN^- with chloramines. To achieve this goal, we investigated the extent to which SCN^- restored the activity of glutathione reductase (GR) and also how it affected the population of viable A549 lung cancer cells after treatment with HOCl. Under certain conditions, we found that approximately half of GR activity that was inactivated by a large molar excess of HOCl was recovered after incubation with SCN^- . We speculate that the cysteine active site of the protein was protected from irreversible over-oxidation by its hydrophobicity. The observed reversibility upon reaction with thiocyanate is attributed to a chlorinated key histidine. The viability studies of A549 cells incubated with HOCl for 20 min and then with SCN^- show a significant increase in the proportion of live cells and a decrease in the proportion of necrotic cells. We surmise based on these results that early SCN^- intervention (≤ 20 min) after the exposure of A549 cells to low

concentrations of HOCl can repair and reverse some of the damage. Overall, the results of the investigation described in this dissertation indicate that SCN^- may play a more active role in quenching chloramines in vivo than has been previously appreciated.

CHAPTER 1: FRAMEWORK FOR THE RESEARCH

1.1 Statement of problems and objectives

Neutrophils whose main responsibility is to defend the host against invasion by foreign microbes are increasingly being suspected to play a mediatory role in the exacerbation of inflammatory diseases (1). As part of their ammunition, they release a concoction of reactive oxygen species that are capable of destroying the invading microbes (2). It has however been reported (3) that neutrophils lack or have very little innate ability to distinguish between foreign and normal cells and relies on other parts of the immune system to pick its targets. As a consequence of misidentification (3), normal host tissue damage occur thus aggravating inflammatory diseases such as rheumatoid arthritis, atherosclerosis and cystic fibrosis (3-5). It is therefore not surprising that finding therapeutic agents to prevent neutrophils from engaging in host tissue damage has become a subject of extensive research in recent years (3). Despite all these initiatives, the mechanism of tissue destruction and of the killing of invading microbes are still not fully understood. This lack of understanding is due in part to the complex nature of the reactive species in the neutrophil's armor (2-3). It is believed that hypochlorous acid (HOCl) produced by the myeloperoxidase (MPO) catalysed oxidation of chloride by hydrogen peroxide is the main defense factor employed by neutrophils against microbes (2, 6-7). Some studies have raised doubts about this claim pointing to the highly non-specific reactivity of HOCl, which potentially limits its effect/impact to the surface of the microbe (2, 8-11). More recent studies have suggested that it is the secondary reactive species produced by HOCl that

are responsible for the eventual killing of microbes (12-14). The main goal of this research was to investigate the reactions of chloramines (small molecular, macromolecular and cellular) with thiocyanate. We wanted to ascertain whether these interactions resulted in the repair of HOCl induced damage to proteins and restoration of enzyme activity. To aid with our investigation, we employed chlorotaurine, ubiquitin, glutathione reductase, *E. coli* and A549 cancer cells as models. A more detailed summary of this work is given in section 1.8 below.

1. 2 Phagocytosis

Phagocytes generally refer to white blood cells, which provide a front line of defense against invading microorganisms (15). They are critical for fighting infections and subsequent immunity (15-16). Their responsibility includes hunting, ingesting and destroying bacteria, viruses and dead or injured cells (15-16). The actual process of engulfing particles is called phagocytosis. Although there are many cells in the human body capable of phagocytosis, macrophages (which are derived from monocytes) and neutrophils (or polymorphonuclear neutrophilic leukocytes) are the two that are considered more efficient (15). Macrophages are the first to recognize the foreign agents and have been found to also play a key role in alerting the rest of the immune system to the invaders (15). Phagocytes were first described by the Russian Zoologist, Metchnikoff in the 1880s after observing that specialized cells were involved in defense against microbial infections (16). He was later (in 1908) awarded a Nobel Prize in physiology or medicine for his discovery. There are several stages in

phagocytosis, and the key ones include: (i) identification and hunting of the foreign intruder (ii) adherence to and ingestion of the intruder, (iii) digestion of the intruder, (iv) discharge of waste material.

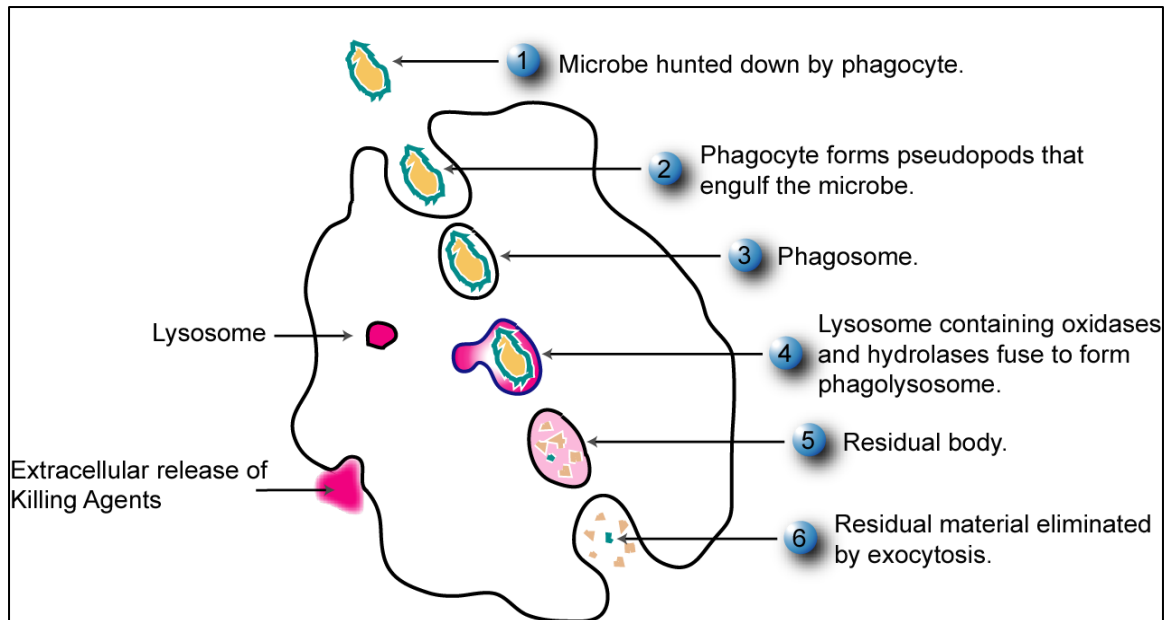


Figure 1.1. Phases of phagocytosis

Soon after entering the host tissues, the intruders begin to replicate. This is accompanied by the release of chemicals that are immediately detected by phagocytes (17). The phagocytes are then recruited to the site of infection. Upon reaching the site of infection, they attach to the surface of the foreign material and the cell membrane becomes involuted thereby forming pseudopods which engulfs the material forming a vacuole known as a phagosome (17). Inside the cell, the phagosome fuses with lysosomes to form a phagolysosome. The lysosome contains digestive enzymes (lysozyme, lipases and proteases,

RNAses and DNAses) which kill most bacteria within 30 minutes. After digestion, residual material is then discharged out of the cell (17).

1.3 Oxidative burst

It has been reported (6-7, 18-19) that the consumption of molecular oxygen by neutrophils increases during phagocytosis of microbial intruders, an event commonly known as oxidative burst. This leads to the production of a variety of reactive oxygen species (ROS) and reactive nitrogen species (RNS) which are unleashed upon the ingested microbe (Figure 1.2) (6-7, 18-19).

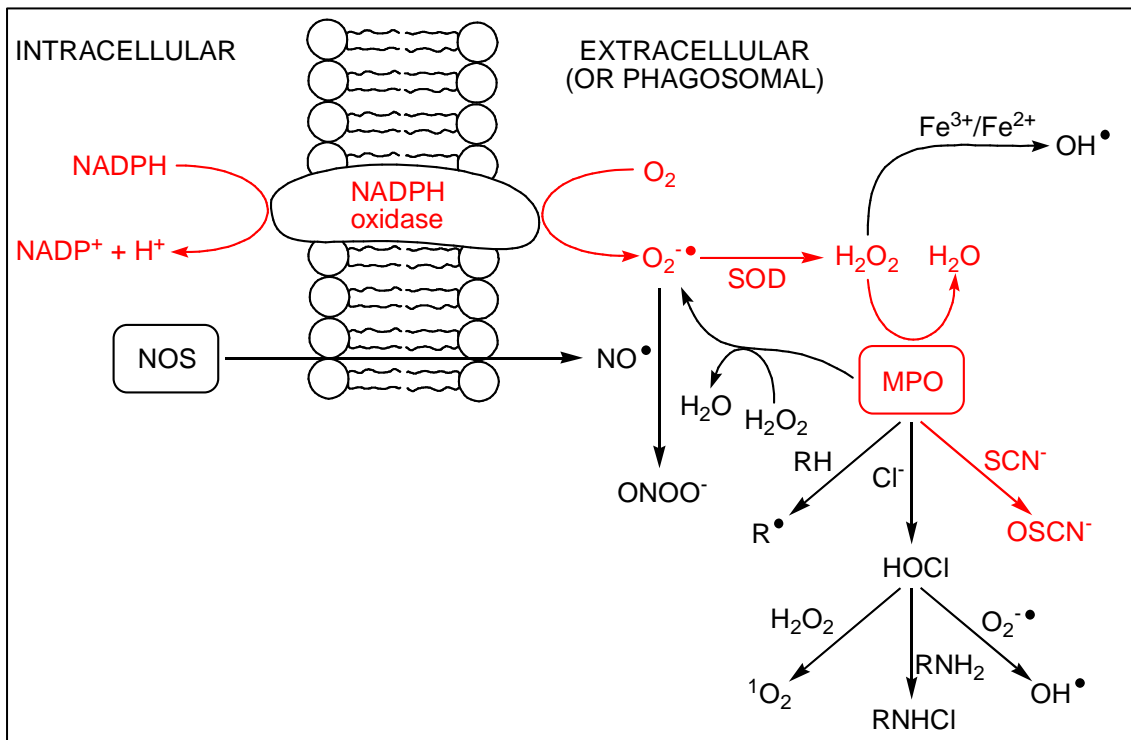


Figure 1.2. Neutrophil oxidative burst

The cascade of reactive species is initiated by NADPH oxidase, a dormant membrane-bound enzyme that is activated during oxidative burst. Upon activation, NADPH catalyzes the one-electron reduction of molecular oxygen to superoxide radical ($O_2^{\bullet-}$) (Eq.1) (6-7, 18-19). Superoxide is a mild and somewhat selective oxidant that is relatively unreactive towards most biological substrates.



In addition to ROS, neutrophils produce RNS such as nitric oxide ($\cdot NO$). Nitric oxide is produced endogenously by nitric oxide synthase (NOS) through the conversion of L-arginine to L-citrulline (Eq. 2).



Nitric oxide reacts with superoxide at rates close to the diffusion limit (23-25) to produce peroxynitrite ($ONOO^-$) (Eq. 3), a reaction catalyzed by nitric oxide synthase (NOS) (20-25). Peroxynitrite is very cytotoxic and its reactivity towards biological substrates is similar to that of $\cdot OH$ (22).



The majority of superoxide radical is converted to hydrogen peroxide (H_2O_2) (Eq. 4), through a disproportionation reaction catalyzed by superoxide dismutase

(SOD) (6-7, 18-19). Hydrogen peroxide can engage in both one-electron and two-electron reactions but has been found to react slowly with most biological molecules including thiols and antioxidants (26).



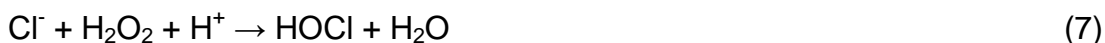
However, H_2O_2 reacts efficiently with iron (and/or copper) to produce the more damaging hydroxyl radical ($\cdot\text{OH}$), a reaction that is known as Fenton chemistry (27) (Eq. 5). The hydroxyl radical is an extremely reactive species and reacts immediately with many biomolecules at close to diffusion limited rates of reactions ($\sim 10^9 \text{ M}^{-1}\text{s}^{-1}$) (20, 28). The concentrations of free iron and copper in biological fluids are extremely low as most are bound in proteins for storage and transportation (20). This significantly limits the formation of $\cdot\text{OH}$ via the Fenton reaction. The other mechanism by which the hydroxyl radical can be produced is via the reaction of HOCl with superoxide (Eq. 6).



The production of the hydroxyl radical by neutrophils however remains a subject of debate (29-33). This is because it is extremely reactive and evidence presented for its existence is based on identification of potential secondary

products which can be produced by other oxidants such as superoxide and hypochlorous acid (29-33).

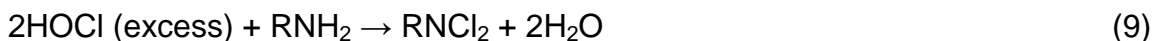
Myeloperoxidase (MPO), is a major heme enzyme that is released by neutrophils into phagosomal compartments and extracellularly (34). MPO has the unique capability to catalyze the oxidation of Cl^- by H_2O_2 to produce HOCl (Eq. 7). Depending on the physiological environment, some studies have reported that up to 80% of hydrogen peroxide produced by neutrophils is converted to micromolar to low millimolar HOCl (35-37). HOCl is a powerful oxidizing agent and is believed to be a potent bactericidal agent on a per-mole basis produced by neutrophils (28).



The MPO- H_2O_2 system can also oxidize Br^- and the pseudohalide SCN^- to produce corresponding hypohalous acids (HOBr and HOSCN) (35-37). HOCl can react with amines to produce chloramines. Typically, the concentrations of the halides and pseudo-halides in plasma are (100-140 mM) $[\text{Cl}^-]$, (20-100 μM) $[\text{Br}^-]$ and ($\leq 120 \mu\text{M}$) $[\text{SCN}^-]$ (38-40).

1.4 Chloramines

HOCl is known to be very reactive towards a number of important biological molecules including proteins, DNA, lipids and antioxidants (28). However, because of their high concentration, proteins which are major constituents in cells, tissue and biological fluids are likely to be the major targets (8). Extensive kinetic data for the reactions of HOCl with biological molecules have been published (9-11, 41-42). These studies reveal that sulfur and amino groups are preferred HOCl kinetic targets (9-11, 41-42). These functional groups are present in proteins in the form of lysine, histidine, cysteine and methionine side chains. The following second-order rate constants for the reaction of HOCl with these functional groups have been reported cysteine and methionine ($k > 10^7 \text{ M}^{-1}\text{s}^{-1}$), histidine ($k \sim 10^5 \text{ M}^{-1}\text{s}^{-1}$) and lysine ($k \sim 5 \times 10^3 \text{ M}^{-1}\text{s}^{-1}$) (9-11, 41-42). The reaction of HOCl with amino compounds produces secondary oxidants known as (mono- and di-) chloramines. Chloramines retain the oxidizing equivalence of HOCl and thus can undergo secondary reactions. Relative to HOCl, chloramines are typically milder reactants and more selective towards thiols.



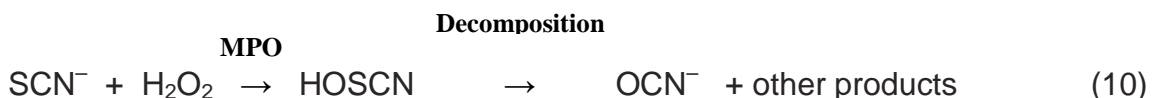
Despite being key HOCl-derived intermediates, the possible contribution of chloramines in the pathogenesis of inflammatory diseases has not been fully explored. A few studies have reported the second-order rate constants for the

reaction of selected chloramines with important biological molecules (12-13, 43). Peskin and Winterbourn observed that chloramines vary in their chemical reactivities towards thiols, with N-acetyl lysine and glycine chloramines being more reactive than taurine chloramine (12). The reaction of chloramines with the various low molecular weight thiols was dependent on the pK_a of the thiol group. The reactivity of other chloramines particularly histidine and histamine chloramines have subsequently been investigated (13, 43-45). It was found that histidine side-chain (imidazole) chloramine may be responsible for the oxidative attack on other protein components through secondary chlorine transfer reactions (44). The second-order rate constants determined for the reaction of histidine chloramine with protein components were found to be among the fastest that have been reported (46-47). Typically, the reactivity of histidine chloramine towards thiols was only 5-10 times less than that for HOCl, compared to other chloramines (lysine, taurine etc.) which are 25-50 times less reactive than HOCl. Encouraged by the results of histidine chloramine, other studies hypothesized that similar reactions were possible with histamine chloramine (13, 43, 45). Histamine which is stored in granules of mast cells at concentrations as high as 100 mM is released at sites of inflammation and thus has a potential to intercept some of the neutrophil HOCl thereby forming histamine chloramine (13, 43, 45). Relatively higher rate constants were measured for the reaction of histamine chloramine with thiols than taurine, lysine and glycine chloramines (13, 43, 45). Some studies have also investigated the ability of chloramines to inactivate thiol proteins (14, 48-49). It was reported by these studies that owing to its selectivity

for thiols, chloramines are more effective than HOCl at inactivating enzymes. In the absence of target molecules in the vicinity of chloramines, they ultimately decompose to radical intermediates and aldehydes (50-51).

1.5 Hypothiocyanite (OSCN⁻)

Thiocyanate (SCN⁻), a pseudohalide serving as a preferred substrate for MPO is present in some biological fluids including saliva and stomach lining fluid at high concentrations (52-53). Plasma concentrations of SCN⁻ in smokers are substantially higher (54). Other dietary sources of SCN⁻ which may result in elevated plasma concentrations include cabbage, broccoli, almond, corn, cassava and horseradish (55-56). Members of the peroxidase family including lactoperoxidase, salivary, gastric, eosinophil are all capable of catalyzing the formation of OSCN⁻ from H₂O₂ and SCN⁻ (54). Wang et al. have proposed that the peroxidase catalyzed reaction produces OCN⁻ in addition to OSCN⁻ which they have hypothesized is responsible for the carbamylation of proteins (Eq. 10) (54).



Several studies have shown that OSCN⁻ can also be produced non-enzymatically through the oxidation of SCN⁻ with HOCl and HOBr (Eq. 10) (57-58). Hypohalous acids (HOCl, HOBr) including the pseudo-hypohalite HOSCN form part of the human immune system. It has also been suggested by a number of

studies that excessive production of these oxidants leads to host tissue damage and thereby play an active role in inflammatory diseases including atherosclerosis, arthritis, cystic fibrosis, kidney disease and some cancers (59).



Unlike HOCl and HOBr which seem to indiscriminately attack a variety of cellular targets, HOSCN appears to be more selective towards thiol groups (60-61). Hawkins et al. published a study in which they investigated the reactions of HOSCN with thiols and other targets (62). They reported observing that free tryptophan and peptide-containing tryptophan were unreactive towards HOSCN. Only tryptophan residues in enzymes appeared to be favored HOSCN targets (62). It must be noted however that the authors indicated that the identification of the reaction products and the proposed mechanism for the reaction of HOSCN with tryptophan were tentative and required further investigation (62). Surprisingly, tryptophan oxidation was observed even in the presence of glutathione, which suggests that this reaction may be competitive in vivo. Interestingly, they also noticed that the products of this oxidation reaction were stable and thus proposed that they could be used as biomarkers for HOSCN mediated attack on proteins. The proposed mechanism for the oxidation reaction is shown in Figure 1.3. It indicates that the two major products due to the HOSCN attack on the pyrrole ring of tryptophan are dioxindolyalanine or N-

formylkynurenine (NFK). The formation of these products is believed to result in the loss of protein integrity via unfolding.

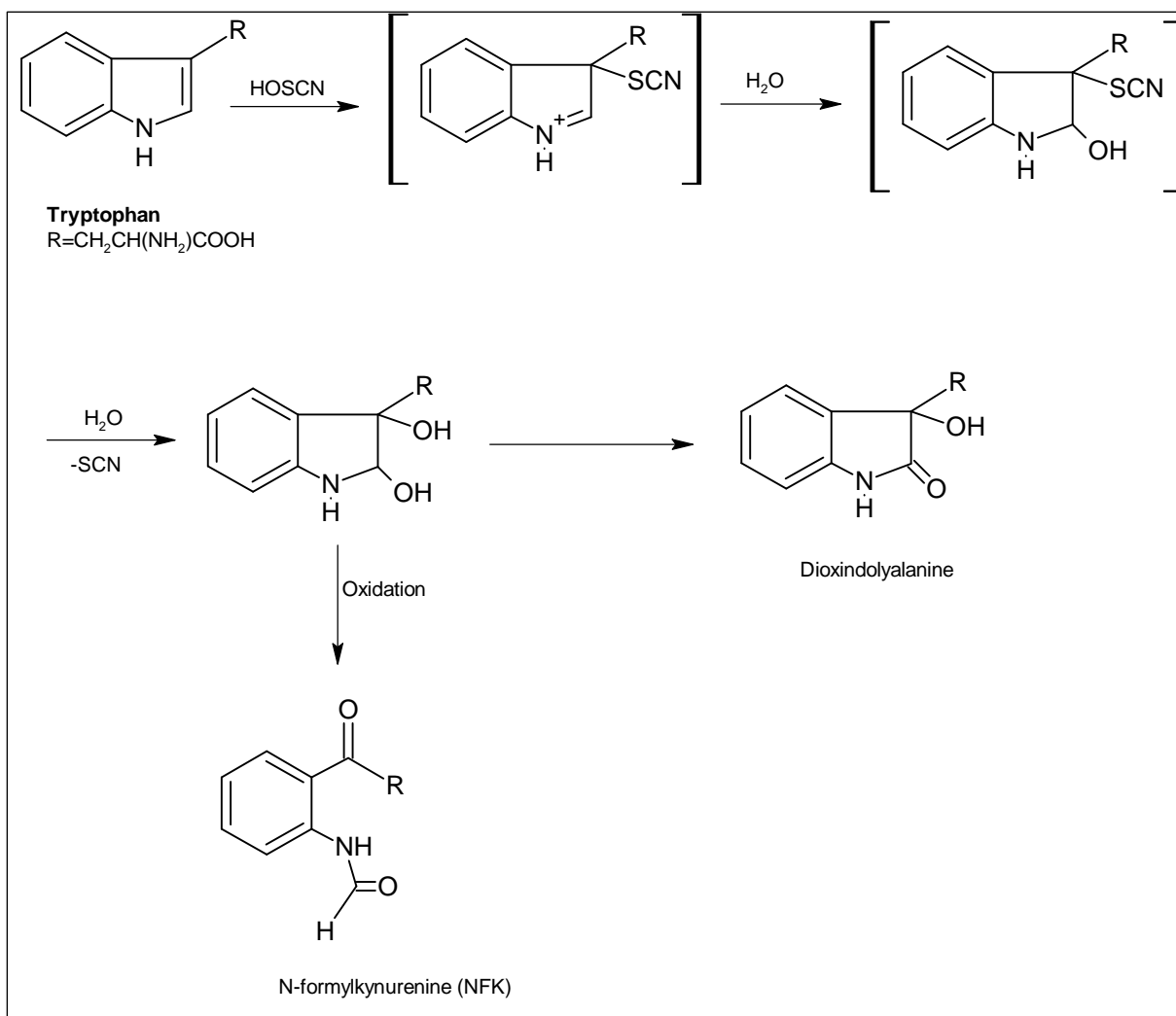


Figure 1.3. Proposed mechanism for the oxidation of protein-derived tryptophan by HOSCN

1.6 Glutathione reductase (GR)

Glutathione (GSH), is the most abundant non-protein bound thiols in eukaryotes and some prokaryotes (59-60, 63-64). One of the prominent roles of GSH is to ensure the protection of cells against oxidative damage, i.e. it acts as an antioxidant (59-60, 63-64). High concentrations of reduced glutathione in the cells are maintained by glutathione reductase (GR), a crucial housekeeping enzyme. GR catalyzes the reduction of oxidized glutathione (GSSG) to the sulfhydryl form (GSH) by NADPH. It is a member of a growing family of homodimeric flavoprotein disulfide oxidoreductases. Research on GR began with Meldrum and Tarr who observed that GSSG was reduced by rat blood and they showed that NADPH was a cofactor in this system (65). Since then a number of investigators have succeeded in purifying GR from a variety of sources including microorganisms, plants and animals (66-69). GR is a homodimeric enzyme with a molecular weight of 100 kDa (67). It is believed that the dimeric nature of GR is critical for its function as both subunits contributes to its catalytic activity. One of the subunits is responsible for a reductive-half and the other for the oxidative-half of the reaction. During the reductive half-reaction, FAD is reduced by NADPH and the reducing equivalence is then transferred to the redox-active disulfide. In the oxidative half-reaction, the resulting dithiol reacts with oxidized glutathione (GSSG), reducing it to two GSH. GR contains in its active site an acid catalyst (His467) which has a pKa of 9.2 and whose responsibility is to protonate the first glutathione that is released (67-68). The stability of GR has been tested in many organisms and it was found to be one of the most thermostable enzymes

(70-71). The inhibition of GR activity under conditions of oxidative stress creates an imbalance between prooxidant and antioxidant species which in turn may contribute to the genesis of many diseases (59).

1.7 Fluorescence microscopy for cell imaging

During the last three decades, fluorescence microscopy has seen a level of growth that has enabled it to emerge as a powerful and widely used imaging tool for biological research (72). This has resulted in the development of a significant number of various cation and anion fluorescent probes (73-75). Because of their important role in biology and in the environment, transition elements have been the main focus of the new probes (76-81). To explore fully the contribution of ROS in human diseases, new fluorophores affording an accurate detection of ROS in living cells are needed. The major drawback for most fluorescent probes is their susceptibility to auto-oxidation and their inability to distinguish between various ROS (76-81). Given the fact that different ROS are likely to play a unique role in the pathogenesis of inflammatory conditions, selective detection of specific ROS is required (4-5). Recently, fluorescent probes designed for the detection of the ROS especially HOCl and H₂O₂ have attracted considerable attention (82-86). Some of the most popular fluorescent dyes developed for HOCl detection are sulfonaphthoaminophenyl fluorescein (SNAPF), dipyrromethene boron difluoride (BODIPY) and rhodamine-based derivatives (87-89). Most of these probes have displayed reasonable selectivity for HOCl over other ROS; however, probes with better selectivity and sensitivity are still sought after. Tae et al. have recently

developed a new rhodamine-hydroxamic acid-based probe which they claim has superior sensitivity and selectivity for HOCl (90). Spectroscopic probes usually have two units: (1) a signaling unit, one whose properties are changed upon the reaction with the analyte, (2) a recognition unit, one responsible for the selective reaction with the analyte (73). The new probe was synthesized from rhodamine 6G (signaling unit) and thus contains the nonfluorescent spirocyclic form with hydroxamic acid incorporated into the rhodamine amide system. In phosphate buffer at pH 7.4, the probe forms a colorless solution but instantly develops a pink color upon coming in contact with HOCl. The color change is associated with the oxidation of the hydroxamic acid component (recognition unit) which leads to the ring opened fluorescent form (1). Unlike the HOCl probe reported by Nagano et al. whose synthetic route was rather complicated, the new probe can be synthesized by a simple three step synthetic procedure (Figure 1.4).

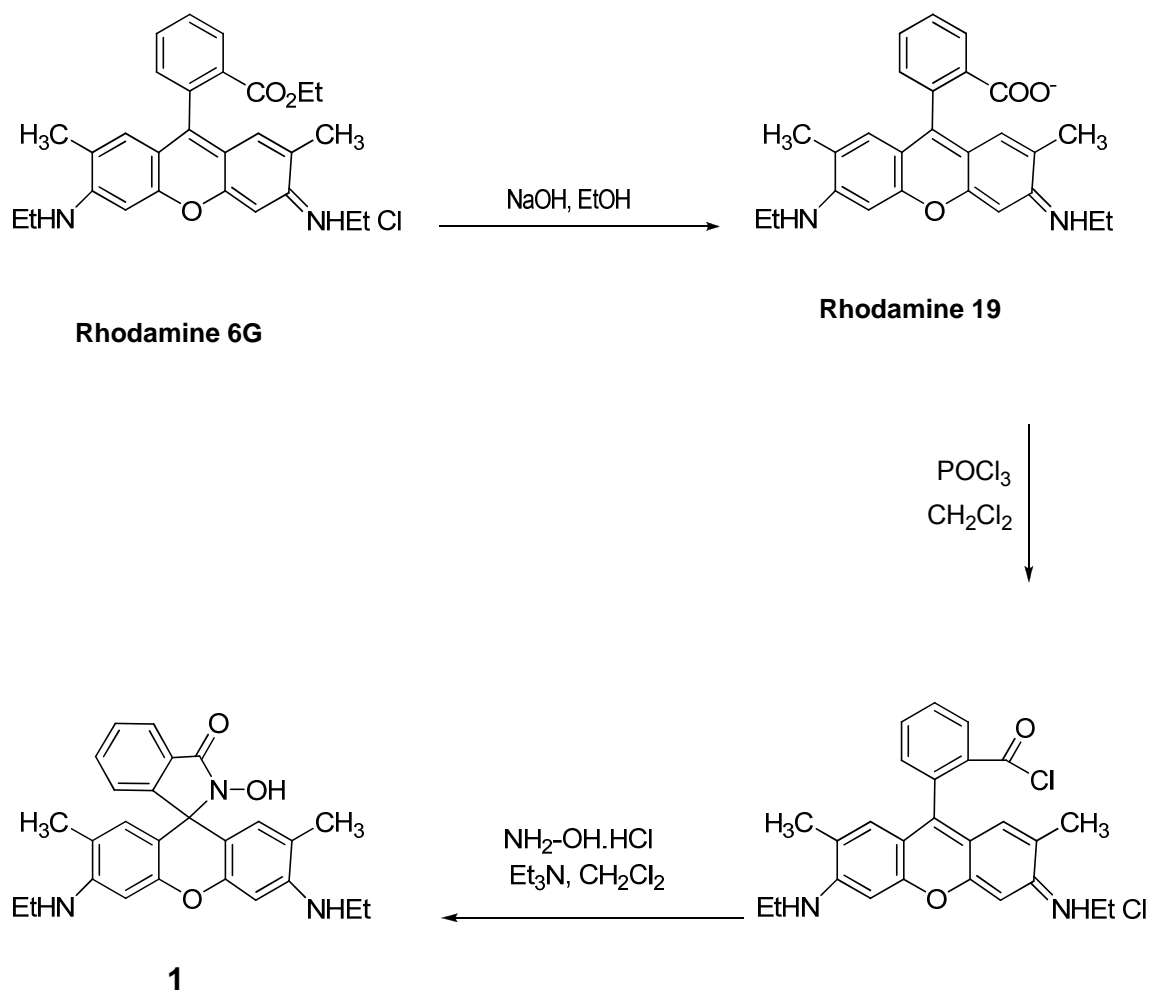


Figure 1.4. Synthesis of the rhodamine-hydroxamic acid probe (1)

1.8 Summary of this work

The work constituting this dissertation is comprised of several independent but related projects. Some parts of the research work on A549 cells were performed in collaboration with Dr Dario Ramirez. Although the chapters are interlinked, each contains its own introduction of important concepts.

Chapter 1 presents the framework for the research describes in broad terms the objectives of the research work and also the introduction of the main themes. Its purpose is to introduce the reader to the basic concepts of this research work.

Chapter 2 summarizes the experimental methods cover the sample preparation and analytical techniques used to conduct this research. Since the bulk of the reagents used in each project were similar, we decided to put them together in one chapter. These procedures are not repeated within each chapter.

Chapter 3 describes our finding that small molecular, macromolecular and cellular chloramines reacted effectively with thiocyanate to give the human defense factor hypothiocyanite. The identity of the product(s) of the reaction of chloramines with thiocyanate has eluded many researchers who ended-up speculating them to be the unstable chlorine thiocyanate (ClSCN) which rapidly decomposes to thiocyanogen (SCN)₂ (91). In this study, using two independent approaches we were able to demonstrate for the first time that the product of the reaction of chloramines with thiocyanate is hypothiocyanite (OSCN⁻). One of the

techniques we used in our endeavor was to look for the unique UV-visible spectroscopic signature of OSCN⁻ ($\lambda_{\text{max}} = 376 \text{ nm}$, $\epsilon = 26.5 \text{ M}^{-1}\text{cm}^{-1}$) (92). We suspect that the main reason why prior attempts to identify this product fell short is its very low extinction coefficient. We were able to overcome this challenge by using the Ocean Optics UBC2000 CCD spectrometer equipped with a 1 meter WPI fiber optic cell. We were able to substantiate the UV-visible spectroscopic data by developing a kinetic model in which the product of the reaction of chloramines with SCN⁻ was reacted with TNB. The kinetic model exploited the highly selective reactivity of OSCN⁻ with thiols. The kinetic approach made it possible to detect OSCN⁻ in cases where a direct spectroscopic measurement could not be used, such as those involving protein and cellular chloramines. One of the most surprising findings of this study was that OSCN⁻ reacts faster with chloramines than does SCN⁻. We surmise based on our data that the reaction of chloramines with SCN⁻ and OSCN⁻ may repair some damage inflicted by HOCl on proteins.

Chapter 4 describes the kinetics and the mechanism of the reactions of dichloramines (e.g. dichlorotaurine) with thiols (e.g. TNB). While the potential contribution of monochloramines in the killing of invading bacteria has been receiving a lot of attention (2, 14, 91), the role played by dichloramines remains largely un-explored. As a result of their low stability, it was reported recently that when they decompose, organic dichloramines form more toxic inorganic chloramines (93). The fate of the more stable dichloramines (e.g. dichlorotaurine)

was left to speculation including possibly decomposing to organic radicals. To our knowledge, the rate constant(s) for the reaction of dichlorotaurine with thiols have not been measured. The main finding of this study was that the reaction of dichlorotaurine with thiols is pH-dependent and at pH 7.4 it reacts ~ 1000 times faster with thiols than chlorotaurine. The mechanistic data for the reaction of dichlorotaurine with thiols are consistent with the reaction proceeding via the deprotonated thiolate (nucleophile) and dichlorotaurine acting as an electrophile. The stopped-flow studies, show that the reaction under first-order conditions is fast with a second order-rate constant of $1.1 \times 10^6 \text{ M}^{-1}\text{s}^{-1}$ for the TNB thiolate and $1.3 \times 10^6 \text{ M}^{-1}\text{s}^{-1}$ for the cysteine and glutathione thiolates at pH 7.4. These rate constants are only three-orders of magnitude lower than that for the reaction of HOCl with cysteine thiolate $1.2 \times 10^9 \text{ M}^{-1}\text{s}^{-1}$ which clearly indicates that these reactions are fast.

Chapter 5 addresses the reaction of thiocyanate with A549 cellular chloramines and glutathione reductase (GR) chloramine which resulted in an increase in the fraction of viable cells and the recovery of the enzyme activity. Using the rhodamine probe and confocal fluorescence microscopy, we were able to show that SCN^- was effective at quenching cellular chloramines. Cellular chloramine showed strong red fluorescence and no fluorescence was observed after the cells were treated with SCN^- . The preliminary flow cytometry data supports the confocal data as it suggests that the reaction of cellular chloramines with SCN^- repairs the damage caused by HOCl and thus ensures cell survival. The positive

effects of SCN^- on cellular chloramines were only observed when cells were incubated with HOCl for 20 min. The fraction of necrotic cells in the samples that were incubated with HOCl for 1 h remained high and relatively unchanged after the addition of SCN^- . When GR which was inactivated with excess HOCl was subsequently incubated with SCN^- , about 47 % of its activity was recovered. As explained in detail later, we surmise that this was due to the reaction of SCN^- with the chloramine on the histidine residue in the active site which is directly involved in the catalytic activity of GR.

1.9 References

1. Klebanoff, S. J. (2005) Myeloperoxidase: friend and foe, *J. Leukocyte Biol.* 77, 598-625.
2. Winterbourn, C. C., Kettle, J.A., Hampton, M.B. (1998) Inside the neutrophil phagosome: oxidants, myeloperoxidase, and bacterial killing, *Blood* 92, 3007-3017.
3. Weiss, S. J. (1989) Tissue destruction by neutrophils, *N. Engl. J. Med.* 320, 365-376.
4. Halliwell, B., Gutteridge, J (1999) *Free radicals in biology and medicine*, Oxford, Clarendon Press.
5. Wiseman, H., Halliwell, B. (1996) Damage to DNA by reactive oxygen and nitrogen species : role in inflammatory disease and progression to cancer, *Biochem. J* 313, 17-29.
6. Babior, B. M., Kipnes, R.S., Curnutte, J.T., . (1973) Biological defense mechanisms. The production by leucocytes of superoxide, a potential bactericidal agent, *J. Clin. Invest.* 52, 741-744.
7. Roos, D., van Bruggen, R., Meischl, C. (2003) Oxidative killing of microbes by neutrophils, *Microb. Infect.* 5, 1307-1315.
8. Test, S. T., Weiss, S.J. (1986) The generation of utilization of chlorinated oxidants by human neutrophils, *Advances in Free Radical Biology & Medicine* 2, 91-116.

9. Prutz, W. A. (1996) Hypochlorous acid interactions with thiols, nucleotides, DNA, and other biological substrates, *Arch. Biochem. Biophys.* 332, 110-120.
10. Pattison, D. I., Davies, M.J. (2001) Absolute rate constants for the reaction of hypochlorous acid with protein side-chains and peptide bonds, *Chem. Res. Toxicol.* 14, 1453-1464.
11. Folkes, L. K., Candeias, L.P., Wardman, P. (1995) Kinetics and mechanisms of hypochlorous acid reactions, *Arch. Biochem. Biophys.* 323, 120-126.
12. Peskin, A. V., Winterbourn, C.C. (2001) Kinetics of the reactions of hypochlorous acid and amino acid chloramines with thiols, methionine and ascorbate, *Free Radical Biol. Med.* 30, 572-579.
13. Peskin, A. V., Winterbourn, C.C. (2003) Histamine chloramine reactivity with thiol compounds, ascorbate, and methionine and with intracellular glutathione, *Free Radical Biol. Med.* 35, 1252-1260.
14. Peskin, A. V., Winterbourn, C.C. (2006) Taurine chloramine is more selective than hypochlorous acid at targeting critical cysteines and inactivating creatine kinase and glyceraldehyde-3-phosphate dehydrogenase, *Free Radical Biol. Med.* 40, 45-53.
15. Marcinkiewicz, J. (1997) Neutrophil chloramines: missing links between innate and acquired immunity *Immunol. Today* 18, 577-580.
16. Tauber, A. I. (2003) Metchnikoff and the phagocytosis theory, *Nature Rev.* 4, 897-901.

17. Hiddessen, A. L., Sulchek, T.A., Shen, N., Thomas, C., Woo, Y., Blanchette, C.D. (2009) Decoupling internalization, acidification and phagosomal-endosomal/lysosomal fusion during phagocytosis of InIA coated beads in epithelial cells, *PLoS One* 4, 1-13.
18. Babior, B. M., Lambeth, J.D., Nauseef, W. (2002) The neutrophil NADPH oxidase, *Arch. Biochem. Biophys.* 397, 342-344.
19. Quinn, M. T., Gauss, K.A. (2004) Structure and regulation of the neutrophil respiratory burst oxidase: comparison with nonphagocyte oxidases, *J. Leukocyte Biol.* 76, 760-781.
20. Hancock, J. T., Desikan, R., Neill, S.J. (2001) Role of reactive oxygen species in cell signalling pathways, *Biochem. Soc. Trans.* 29, 345-350.
21. Dedon, P. C., Tannenbaum, S.R. (2004) Reactive nitrogen species in the chemical biology of inflammation, *Arch. Biochem. Biophys.* 423, 12-22.
22. Shackelford, R. E., Kaufmann, K.W., Paules, R.S. (2000) Oxidative stress and cell cycle checkpoint function, *Free Radical Biol. Med.* 28, 1387-1404.
23. Saran, M., Michael, C., Bors, W. (1990) Reaction of NO with O_2^- : Implications for the action of endothelium-derived relaxing factor (EDRF), *Free Radic. Res. Commun.* 10, 221-226.
24. Koppenol, W. H., Moreno, J.J., Pryor, W.A., Ischiropoulos, H., Beckman, J.S. (1992) Peroxynitrite, a cloaked oxidant formed by nitric oxide and superoxide *Chem. Res. Toxicol.* 5, 834-842.
25. Huie, R. E., Padmaja, S. (1993) The reaction of NO with superoxide *Free Radic. Res. Commun.* 18, 195-199.

26. Ashby, M. T., Nagy, P. (2006) On the kinetics and mechanism of the reaction of cysteine and hydrogen peroxide in aqueous solution, *J. Pharm. Sci.* 95, 15-18.
27. Fenton, H. J. H. (1894) Oxidation of tartaric acid in the presence of iron, *J. Chem. Soc.* 65, 899-910.
28. Grisham, M. B., Conner, E.M. (1996) Inflammation, free radicals, and antioxidants, *Nutrition* 12, 274-277.
29. Cohen, M. S., Britigan, B.E., Hassett, D.J., Rosen, G.M. (1988) Do human neutrophils form hydroxyl radical? Evaluation of an unresolved controversy, *Free Radical Biol. Med.* 5, 81-88.
30. Winterbourn, C. C., Kettle, A.J. (1994) Superoxide-dependent hydroxylation by myeloperoxidase, *J. Biol. Chem.* 269, 17146-17151.
31. Tauber, A. I., Babior, B.M. (1977) Evidence for hydroxyl radical production by human neutrophils, *J. Clin. Invest.* 60, 374-379.
32. Weiss, S. J., Rustagi, P.K., LoBuglio, A.F. (1978) Human granulocyte generation of hydroxyl radical, *J. Exp. Med.* 147, 316-323.
33. Rosen, H., Klebanoff, S.J. (1979) Hydroxyl radical generation by polymorphonuclear leukocytes measured by electron spin resonance spectroscopy, *J. Clin. Invest.* 64, 1725-1729.
34. Weiss, S. J., LoBuglio, A.F. (1982) Phagocyte-generated oxygen metabolites and cellular injury, *Lab. Invest.* 47, 5-18.
35. Ashby, M. T. (2008) Inorganic chemistry of defensive peroxidases in the human oral cavity, *J. Dent. Res.* 87, 901-915.

36. Weiss, S. J., Klein, R., Slivka, A., Wei, M. (1982) Chlorination of taurine by human-neutrophils is evidence for hypochlorous acid generation, *J. Clin. Invest.* 70, 598–607.
37. Foote, C. S., Goyne, T.E., Lehrer, R.I. (1983) Assessment of chlorination by human-neutrophils, *Nature* 301, 715-716.
38. Slungaard, A., Mahoney, J.R. (1991) Thiocyanate is the major substrate for eosinophil peroxidase in physiologic fluids. Implications for cytotoxicity, *J. Biol. Chem.* 266, 4903-4910
39. vanDalen, C. J., Whitehouse, M. W., Winterbourn, C. C., Kettle, A. J. (1997) Thiocyanate and chloride as competing substrates for myeloperoxidase, *Biochem. J* 327, 487-492.
40. Thomas, E. L., Fishman, M. (1986) Oxidation of chloride and thiocyanate by isolated leukocytes, *J. Biol. Chem.* 261, 9694-9702.
41. Winterbourn, C. C. (1985) Comparative reactivities of various biological compounds with myeloperoxidase-hydrogen peroxide-chloride, and similarly of the oxidant to hypochlorite *Biochim. Biophys. Acta* 840, 204-210.
42. Pattison, D. I., Davies, M.J., Hawkins, C.L. (2003) Hypochlorous acid mediated oxidation of lipid components and antioxidants present in low density lipoproteins: absolute rate constants, product analysis and computational modeling, *Chem. Res. Toxicol.* 16, 439-449.

43. Peskin, A. V., Winterbourn, C.C., Midwinter, R.G., Harwood, D.T. (2005) Chlorine transfer between glycine, taurine and histamine: reaction rates and impact on cellular reactivity *Free Radical Biol. Med.* 38, 397-405.
44. Pattison, D. I., Davies, M.J. (2005) Kinetic analysis of the role of histidine chloramines in hypochlorous acid mediated protein oxidation, *Biochemistry* 44, 7378-7387.
45. Pattison, D. I., Davies, M.J. (2006) Evidence for rapid inter- and intramolecular chlorine transfer reactions of histamine and carnosine chloramines: implications for the prevention of hypochlorous-acid - mediated damage, *Biochemistry* 45, 8152-8162.
46. Prutz, W. A. (1999) Consecutive halogen transfer between various functional groups induced by reaction of hypohalous acids: NADH oxidation by halogenated amide groups, *Arch. Biochem. Biophys.* 371, 107-114.
47. Prutz, W. A. (1998) Interactions of hypochlorous acid with pyrimidine nucleotides, and secondary reactions of chlorinated pyrimidines with GSH, NADH and other substrates, *Arch. Biochem. Biophys.* 349, 183-191.
48. winterbourn, C. C., Stacey, M.M., Peskin, A.V., Vissers, M.C. (2009) Chloramines and hypochlorous acid oxidize erythrocyte peroxiredoxin 2, *Free Radical Biol. Med.* 47, 1468-1476.
49. Hawkins, C. L., Davies, M.J. (2005) Inactivation of protease inhibitors and lysozyme by hypochlorous acid: role of side-chain oxidation and protein

- unfolding in loss of biological function, *Chem. Res. Toxicol.* 18, 1600-1610.
50. Nagl, M., Gottardi, W. (2010) N-chlorotaurine, a natural anticeptic with outstanding tolerability, *J. Antimicrob. Chemother.* 65, 399-409.
 51. Hawkins, C. L., Davies, M.J. (1999) Hypochlorite-induced oxidation of proteins in plasma: Formation of chloramines and nitrogen-centred radicals and their role in protein fragmentation, *Biochem. J* 340, 539-548.
 52. Das, D., De, P.K., Banerjee, R.K. (1995) Thiocyanate, a plausible physiological electron-donor of gastric peroxidase, *Biochem. J* 305, 59-64.
 53. Ihalin, R., Loimaranta, V., Tenovuo, J. (2006) Origin, structure and biological activities of peroxidases in human saliva, *Arch. Biochem. Biophys.* 445, 261-268.
 54. Wang, Z., Nicholis, S.J., Rodriguez, E.R., Kummu, O., Horkko, S., Barnard, J., Reynolds, W.F., Topol, E.J., DiDonato, J.A., Hazen, S.L. (2007) Protein carbamylation links inflammation, smoking, uremia and atherogenesis, *Nat. Med.* 13, 1176-1184.
 55. Galanti, L. M. (1997) Specificity of salivary thiocyanate as marker of cigarette smoking is not affected by alimentary sources *Clin. Chem.* 43.
 56. Foss, O. P., Lund-Larsen, P.G. (1986) Serum thiocyanate and smoking: interpretation of serum thiocyanate levels observed in a large health study, *Scand. J. Clin. Lab. Invest.* 46, 245-251.

57. Ashby, M. T., Carlson, A.C., Scott, M.J. (2004) Redox buffering of hypochlorous acid by thiocyanate in physiologic fluids, *J. Am. Chem. Soc.* 126, 15976-15977.
58. Ashby, M. T., Nagy, P., Beal, J.L. (2006) Thiocyanate is an efficient endogeneous scavenger of the phagocytic killing agent hypobromous acid, *Chem. Res. Toxicol.* 19, 587-593.
59. Pullar, J. M., Vissers, M.C., Winterbourn, C.C. (2000) Living with a killer: the effects of hypochlorous acid on mammalian cells, *Int. Union Biochem. Mol. Biol.* 50, 259-266.
60. Fahey, R. C., Brown, W. C., Adams, W. B., Worsham, M. B. (1978) Occurrence of glutathione in bacteria, *J. Bacteriol.* 133.
61. Arlandson, M., Decker, T., Roongta, V.A., Bonilla, L., Mayo, K.H., MacPherson, J.C., Hazen, S.L., Slungaard, A. (2001) Eosinophil peroxidase oxidation of thiocyanate. Characterization of major reaction products and a potential sulfhydryl-targeted cytotoxicity system, *J. Biol. Chem.* 276, 215-224.
62. Hawkins, C. L., Pattison, D.I., Davies, M.J., Stanley, N.R. (2008) Tryptophan residues are targets in hypothiocyanous-acid mediated protein oxidation, *Biochem. J* 416, 441-452.
63. Smirnova, G. V., Oktyabrsky, O. N. (2005) Glutathione in bacteria, *Biochemistry* 70, 1199-1211.
64. Meister, A. (1988) Glutathione metabolism and its selective modification, *J. Biol. Chem.* 263, 17205-17208.

65. Meldrum, N. U., Tarr, H.L. (1935) The reduction of glutathione by the Warburg-Christian system, *Biochem. J* 29, 108-115.
66. Asnis, R. E. (1955) A glutathione reductase from *Escherichia coli* *J. Biol. Chem.* 213, 77-85.
67. Ulusu, N. N., Tandogan, B. (2007) Purification and kinetic properties of glutathione reductase from bovine liver, *Mol. Cell. Biochem.* 303, 45-51.
68. Bashir, A., Perham, R.N., Scrutton, N.S., Berry, A. (1995) Altering kinetic mechanism and enzyme stability by mutagenesis of the dimer interface of glutathione reductase, *Biochem. J* 312, 527-533.
69. Carlberg, I., Mannervik, B. (1981) Purification and characterization of glutathione reductase from calf liver. An improved procedure for affinity chromatography on 2', 5'-ADP-Sepharose 4B, *Anal. Biochem.* 116, 531–536.
70. Lopez-Barea, J., Lee, C.Y. (1979) Mouse-liver glutathione reductase. Purification, kinetics, and regulation, *Eur. J. Biochem.* 98, 487-499.
71. De Lamotte, F., Vianey-Liaud, N., Duviau, M.P., Kobrehel, K. (2000) Glutathione reductase in wheat grain.1.Isolation and characterization, *J. Agric. Food. Chem.* 48, 4978-4983.
72. Bruchez, M. P., Waggoner, A.S., Berget, P.B., Woolford, C.A., Szent-Gyorgyi, C., Schwarz, U., Dyba, M., Sieber, J.J., Yan, Q., Fitzpatrick, J.A.J. (2009) STED nanoscopy in living cells using fluorogen activating proteins, *Bioconjugate Chem.* 20, 1843-1847.

73. de Silva, A. P., Gunaratne, H.Q.N., Gunnlaugsson, T., Huxley, A.J.M., McCoy, C.P., Rademacher, J.T., Rice, T.E. (1997) Signaling recognition events with fluorescent sensors and switches, *Chem. Rev.* *97*, 1515-1566.
74. Rurack, K., Resch-Genger, U. (2002) Rigidization, preorientation and electronic decoupling—the ‘magic triangle’ for the design of highly efficient fluorescent sensors and switches, *Chem. Soc. Rev.* *31*, 116-127.
75. Callan, J. F., de Silva, A.P., Magri, D.C. (2005) Luminescent sensors and switches in the early 21st century, *Tetrahedron* *61*, 8551-8588.
76. Taki, M., Iyoshi, S., Ojida, A., Hamachi, I., Yamamoto, Y. (2010) development of highly sensitive fluorescent probes for detection of intracellular copper (I) in living systems, *J. Am. Chem. Soc.* *132*, 5938-5939.
77. Peng, X., Du, J., Fan, J., Wang, J., Wu, Y., Zhao, J., Sun, S., Xu, T. (2007) A selective fluorescent sensor for Imaging Cd²⁺ in Living Cells, *J. Am. Chem. Soc.* *129*, 1500-1501.
78. Taki, M., Iyoshi, S., Ojida, A., Hamachi, I., Yamamoto, Y., Desaki, M., Hirayama, T. (2008) Fluorescence imaging of intracellular cadmium using a dual-excitation ratiometric chemosensor, *J. Am. Chem. Soc.* *130*, 12564-12565.
79. Cheng, T., Xu, Y., Zhang, S., Zhu, W., Qian, X., Duan, L. (2008) A highly sensitive and selective off-on fluorescent sensor for cadmium in aqueous solution and living cell, *J. Am. Chem. Soc.* *130*, 16160-16161.

80. Tong, A., Xiang, Y. (2006) A new rhodamine-based chemosensor exhibiting selective FeIII-amplified fluorescence, *Org. Lett* 8, 1549-1552.
81. Johnson, I. (1998) Fluorescent probes for living cells, *Histochem. J.* 30, 123-140.
82. Chang, M. C., Pralle, A., Isacoff, E.Y., Chang, C.J. (2004) A selective, cell-permeable optical probe for hydrogen peroxide in living cells, *J. Am. Chem. Soc.* 126, 15392-15393.
83. Chang, C. J., Srikun, D., Miller, E.W., Domaille, D.W. (2008) An ICT-based approach to ratiometric fluorescence imaging of hydrogen peroxide produced in living cells, *J. Am. Chem. Soc.* 130, 4596-4597.
84. Chang, C. J., Dickinson, B.C., Huynh, C. (2010) A Palette of fluorescent probes with varying emission colors for imaging hydrogen peroxide signaling in living cells, *J. Am. Chem. Soc.* 132, 5906-5915.
85. Nagano, T., Kojima, H., Urano, Y., Kenmoku, S. (2007) Development of a highly specific rhodamine-based fluorescence probe for hypochlorous acid and its application to real-time imaging of phagocytosis, *J. Am. Chem. Soc.* 129, 7313-7318.
86. Hilderbrand, S. A., Weissleder, R., McCarthy, J., Aikawa, E., Figueiredo, J., Waterman, P., Wildgruber, M., Nahrendorf, M., Panizzi, P. (2009) Oxazine conjugated nanoparticle detects in vivo hypochlorous acid and peroxynitrite generation, *J. Am. Chem. Soc.* 131, 15739-15744.
87. Libby, P., Shepherd, J., Hilderbrand, S.A., Waterman, P., Heinecke, J.W., Weissleder, R. (2007) A fluorescent probe for the detection of

- myeloperoxidase activity in atherosclerosis-associated macrophages, *Chem. Biol.* *14*, 1221-1231.
88. Yang, D., Sun, Z.N., Liu, F.Q., Chen, Y., Tam, P.K.H. (2008) A highly specific BODIPY-based fluorescent probe for the detection of hypochlorous acid, *Org. Lett* *10*, 2171-2174.
89. Ma, H., Wang, K., Shi, W., Wang, S., Wang X., Chen, X. (2008) A highly selective and sensitive fluorescence probe for the hypochlorite anion, *Chem. Eur. J.* *14*, 4719-4724.
90. Tae, J., Shin, I., Cho, J.C., Yang, Y.K. (2009) A rhodamine-hydroxamic acid-based fluorescent probe for hypochlorous acid and its applications to biological imagings, *Org. Lett* *11*, 859-861.
91. Calvo, P., Crueiras, J., Rios, A., Rios, M.A. (2007) Nucleophilic substitution reactions of N-chloramines: evidence for a change in mechanism with increasing nucleophile reactivity, *J. Org. Chem.* *72*, 3171-3178.
92. Ashby, M. T., Xulu, B.A. (2010) Small molecular, macromolecular and cellular chloramines react with thiocyanate to give the human defense factor hypothiocyanite, *Biochemistry* *49*, 2068-2074.
93. Coker, M. S. A., Hu, W., Senthilmohan S.T., Kettle, A.J. (2008) Pathways for the decay of organic dichloramines and liberation of antimicrobial chloramines gases, *Chem. Res. Toxicol.* *21*, 2334-2343.

CHAPTER 2: EXPERIMENTAL METHODS

2.1 Reagents. All chemicals were A.C.S certified grade or better. Water was doubly distilled in glass and was used for all aqueous solutions. All reagents were purchased from Sigma-Aldrich (St. Louis, MO) unless otherwise indicated. The phosphate buffer solution was prepared from $\text{NaH}_2\text{PO}_4 \cdot \text{H}_2\text{O}$ (99%) and Na_2HPO_4 (99%) purchased from Mallinckrodt, the ionic strength was adjusted with NaCl (99%). Unless otherwise stated, all solutions were prepared using 0.1 M phosphate buffer at pH 7.4 ($I = 1.0$). Sodium hydroxide (98%), sodium thiocyanate (99%), taurine (98%), hydrogen peroxide (30 wt % in H_2O), ascorbic acid (99%), L-cysteine (98%), glutathione (98%), methionine (98%), dithiothreol (98%), N-acetyl cysteine (98%), S-methyl cysteine (98%), S-methyl glutathione (97%), N-acetyl lysine (99%), Ubiquitin (98%) and bovine lactoperoxidase were all used as received from Sigma-Aldrich.

The tetrasodium salt of β -nicotinamide adenine dinucleotide phosphate (NADPH, reduced form) and the glutathione reductase from baker's yeast (as a suspension in 3.6 M $(\text{NH}_4)_2\text{SO}_4$ at pH 7.0, containing 0.1 mM dithiothreitol) were obtained from Sigma-Aldrich. The enzyme was stored at $T = 4^\circ\text{C}$, and NADPH was stored at $T = -20^\circ\text{C}$ until needed. The concentration of the stock NADPH solutions were spectrophotometrically determined in phosphate + EDTA buffer at pH 7.4 using $\epsilon(\text{NADPH})_{340\text{nm}} = 6.22 \text{ mM}^{-1}\text{cm}^{-1}$ (1-3).

2.2. Sample preparation

2.2.1 Hypochlorite (OCl^-) .Stock solutions of OCl^- were prepared by sparging Cl_2 into a 0.3 M solution of NaOH. Solutions of NaOH, mostly free of CO_2 contamination, were quantified by titration with a standardized HCl solution using phenolphthalein as an indicator. The sparging was stopped when the $[\text{OCl}^-]$ achieved approximately 100 mM (pH 12), as determined spectrophotometrically ($\epsilon(\text{OCl}^-)_{292\text{nm}} = 350 \text{ M}^{-1}\text{cm}^{-1}$) (4-5).

2.2.2 Taurine chloramine (TauCl). A 2.5 mM stock solution of TauCl solution, free of dichloramine (TauCl_2) and excess taurine (Tau), was prepared by adding 5.0 mM OCl^- in 0.10 M NaOH dropwise to 5.0 mM Tau in 0.10 M NaOH while vortexing (6). The formation of TauCl was confirmed by observation of the characteristic absorbance spectrum ($\epsilon_{252\text{nm}} = 429 \text{ M}^{-1}\text{cm}^{-1}$) (6). Solutions of TauCl in 0.10 M phosphate buffer were prepared from the stock solution by adjusting the pH to 7.4 using a 10 mM solution of HCl.

2.2.3 Reaction of TauCl with SCN^- and quantification of OSCN^- . Solutions of OSCN^- were prepared by addition of 5 mL TauCl (100 μM) to 5 mL SCN^- (100, 200, and 500 μM) while vortexing over a period of ~ 1 min. The samples were transferred to 10 mL plastic syringes, the solutions were injected into the 1 m fiber optic cell, and the UV-vis spectra were recorded.

2.2.4 Taurine dichloramine (TauCl₂). A 2.5 mM stock solution of TauCl₂ solution, free of chlorotaurine (TauCl) and excess taurine (Tau), was prepared by adding 5.0 mM Tau in 0.10 M phosphate buffer to 10 mM OCl⁻ in 0.10 M phosphate buffer dropwise while vortexing at pH 5.5 (6). The formation of TauCl₂ was confirmed by observation of the characteristic absorbance spectrum ($\epsilon_{300\text{nm}} = 370 \text{ M}^{-1}\text{cm}^{-1}$) (6). There was no evidence of a shoulder at 252 nm, indicating that there was no detectable TauCl present ($\epsilon_{252\text{nm}} = 429 \text{ M}^{-1}\text{cm}^{-1}$) (6). Solutions of TauCl₂ in 0.10 M phosphate buffer were prepared from the stock solution by adjusting the pH to 7.4 using a 10 mM solution of NaOH.

2.2.5 Synthesis of 5-thio-2-nitrobenzoic acid (TNB). TNB was synthesized by the reduction of DTNB with NaBH₄. To a DTNB solution (3.96 g, 10mmol) in 20 mL THF was added NaBH₄ (0.76 g, 20 mmol) at 0 °C. The reaction mixture was stirred at room temperature for 2 h. To the mixture was then added 20 mL of 6 N HCl at 0 °C. After the removal of THF under vacuum, Et₂O (20 mL) and water (20 mL) were added to the residue, and the organic phase was extracted with Et₂O three times. The combined organic solution was washed with brine and dried over MgSO₄. After filtration and the removal of the solvents, crude TNB was obtained in quantitative yield (>99% purity).

2.2.6 Hypothiocyanite (OSCN⁻). Fresh solutions of OSCN⁻ were prepared enzymatically using LPO-catalyzed oxidation of SCN⁻ with H₂O₂. LPO (~ 0.1 μM) was incubated with SCN⁻ (5 mM) and the reaction was initiated by the addition of

H₂O₂ (1 mM) in phosphate buffer (pH 7.4, 0.1 M) at room temperature. The concentration of OSCN⁻ stock solution was quantified by absorbance at $\epsilon_{376\text{nm}} = 25.6 \text{ M}^{-1} \text{ cm}^{-1}$ (7). The OSCN⁻ samples were used with 1 h (i.e. about half-life of OSCN⁻) after preparation due to their low stability. This method typically produced ~ 1 mM OSCN⁻.

2.2.7 Ubiquitin chloramines (Ub*Cl). Quantitative oxidation of ubiquitin Met-1 to a sulfone (Ub*) was accomplished with performic acid using a literature procedure (8). The performic acid was prepared by mixing 0.50 mL of 30 % hydrogen peroxide with 9.5 mL of 99% formic (HCOOH) acid and allowing the mixture to stand for 2 h at room temperature. Before use, this freshly-prepared performic acid (10 ml) was pre-cooled to 0 °C (ca. 1 mL of methanol was added to the reagent to prevent freezing). Ub (3.0 mg) was dissolved in the performic acid (3.0 mL), the mixture was allowed to stand for 4 h at 20 °C, and cold HBr (2.0 ml of 48%) was added to destroy the excess performic acid. The volatiles were removed using a rotary evaporator at 37°C, and the residue was re-dissolved in 0.10 M phosphate buffer at pH 7.4. Oxidized ubiquitin (25 µM Ub*, as determined by the absorption at 280 nm) was treated with OCl⁻ (250 µM) for various amounts of time (0-2 hours) in 0.1 M phosphate buffer at pH 7.4. The resulting chloramines (Ub*Cl) were quantified with 5-thio-2-nitrobenzoic acid ($\epsilon_{412\text{nm}} = 14,150 \text{ M}^{-1} \text{ cm}^{-1}$) (9-10). Ub*Cl was incubated with TNB for 3 min before the UV-vis measurements were made. Based on the TNB analysis, 33-41% (n = 3) of the original HOCl oxidizing equivalents were recovered from Ub*Cl.

2.2.8 Reaction of Ub*Cl with SCN⁻ and quantification of OSCN⁻. Equal volumes (5 mL) of 6.8 μM Ub*Cl with 0.50 mM SCN⁻ were mixed. After 20 min, the Ub*Cl/SCN⁻ mixture was reacted with TNB (59 μM) in a stopped-flow spectrophotometer with 1:1 mixing in single-mixing mode. The rate constant observed ($3.73 \pm 0.01 \times 10^5 \text{ M}^{-1}\text{s}^{-1}$) is consistent with the value that was independently measured for the reaction of TNB with authentic samples of OSCN⁻. The absorption change (ΔAbs) was constant with the recovery of 80 % of the redox equivalents that were measured for Ub*Cl using TNB.

2.2.9 Chlorination of *E. coli* and quantification of oxidizing equivalents.

Cultures of *E. coli* (MG1655) were grown from frozen stocks to their terminal density in 15 h at 37 °C in Luria-Bertani medium using a shaking water bath. A portion of the culture (40 ml) was centrifuged (10 min at 5000 *g* and 5 °C), washed twice with 0.1 M phosphate buffer (2 x 4 ml), and the resulting cell pellet was re-suspended in phosphate buffer (4 mL) to give a cell density of ca. 10^9 cells/ml ($\text{OD}_{600} = 0.76$). The cell suspension was treated with OCl⁻ (1 mM after dilution) for 5 hours. After incubation, the chlorinated cells were centrifuged (10 min at 5000 *g* and 5 °C), the supernatant was removed, and the cells were re-suspended in 0.1 M phosphate buffer (4 ml). This washing procedure was repeated three times. Following the final resuspension, the oxidizing equivalence (i.e., “chlorine cover”) was determined by treating the chlorinated cells with TNB in 0.10 M phosphate buffer for 12 min. Approximately 423 μM of 2-electron oxidizing equivalents (42 % of the OCl⁻) were recovered.

2.2.10 Reaction of chlorinated MG1655 with SCN^- and quantification of OSCN^- . Equal volumes (5 ml) of chlorinated *E. coli* (10^7 cells/ml, 6 μM of 2-electron oxidizing equivalents) and SCN^- (2.5 mM) were mixed. After 12 min., the cell suspension was filtered through a 0.2 μm polyamide filter. The supernatant was reacted with TNB (61 μM) in a stopped-flow spectrophotometer with 1:1 mixing in single-mixing mode. Quantification of OSCN^- was computed from ΔAbs at 412 nm within the timeframe of reaction of OSCN^- .

2.2.11 Synthesis of the Rhodamine derivative 1. The rhodamine derivative 1 was prepared from rhodamine 6G in three steps using the procedure described by Tae et al (11). Sodium hydroxide (1.69 M) was added to a 0.08 M solution of rhodamine 6G in ethanol and stirring the mixture for 2 h under reflux conditions. After 2 h, 15 mL of distilled water were added and the solution was cooled to room temperature. The resulting precipitate was filtered and dried at 70 $^{\circ}\text{C}$ for 30 min to give 400 mg (85%) of rhodamine 19. In the second step, phosphorus oxychloride (0.26 mL) was added dropwise over 2 min to a 0.096 M solution of rhodamine 19 in dichloromethane. The solution was refluxed for 3 h. The mixture was then cooled and evaporated *in vacuo* to give a crude rhodamine acid chloride. The crude product was not purified but dissolved dichloromethane (10 mL). The solution of the crude product was reacted with hydroxylamine hydrochloride (150 mg) and triethylamine (0.3 mL). The reaction mixture was stirred for 6 h at room temperature and extracted with dichloromethane (20 mL x 3). The organic layer was collected and dried over anhydrous MgSO_4 . Concentrating the mixture under vacuum, yielded a crude product which was

purified by column chromatography (hexane/ethyl acetate = 2:1 to 1:1). The result was 150 mg of a pink solid of the rhodamine derivative **1**.

2.2.12 Assay for the Glutathione reductase (GOR) reduction of GSSG. The activity of glutathione reductase was assayed using a published procedure (12). The depletion of NADPH was followed at $\lambda = 340$ nm with added EDTA (0.5 mM). Conditions for a typical assay solution (control): $[\text{GSSG}]_0 = 1$ mM, $[\text{NADPH}]_0 = 0.1$ mM, $[\text{GOR}] = 0.025$ U/mL, $[\text{phosphate buffer}] = 0.1$ M, pH 7.4 and $T = 25$ °C. The reaction was initiated by the addition of GSSG. Unit definition: One unit will reduce 1.0 μmol of oxidized glutathione per min at pH 7.4 at 25 °C. The inactivation of GOR was achieved by incubation with 40 μM HOCl for 20 min and with iP for an additional 20 min before the GOR assay. The reactivation of GOR was done by incubating HOCl-modified GOR with 160 μM SCN^- for 20 min before the GOR assay.

2.3 Instrumentation and data analysis

2.3.1 UV/Visible spectroscopy. Electronic spectra were measured using a HP 8452A diode array spectrophotometer and quartz cells with calibrated 1 cm path lengths. For the identification of OSCN^- ($\lambda_{\text{max}} = 376$ nm, $\epsilon = 26.5$ $\text{M}^{-1}\text{cm}^{-1}$) (7) as a product of the reaction of TauCl with SCN^- , we collected the UV-vis spectra using an Ocean Optics UBC2000 CCD spectrometer equipped with a 1 meter WPI fiber optic cell and an ATS D 1000 CE UV light source.

2.3.2 Fluorescence spectroscopy. Fluorescence spectra were recorded using a Shimadzu RF-5301 PC spectrofluorometer. The slit width was 2.5 nm for both excitation and emission and the photomultiplier voltage was 700 V. To reduce the fluctuation in the excitation intensity during measurement, the lamp was kept on for 1 h prior to the experiment. All fluorescence spectra were measured with an excitation wavelength of 500 nm.

2.3.3 pH measurements. The $[H^+]$ of the buffered solutions was determined with an Orion Ion Analyzer EA920 using a Ag/AgCl combination pH electrode.

2.3.4 Stopped-flow studies. Kinetic measurements were made using a Bio-Logic SFM-400/Q mixer and a MOS-450 spectrophotometer equipped with a Xe arc lamp and a PMT detector. All monochromatic traces for the reaction of chloramines with TNB were collected at $\lambda_{max} = 412$ nm using a 1 cm optical path length. Single-mixing mode was used for all the stopped-flow experiments. The pseudo-second-order rate constants were obtained by nonlinear least-squares fits of the data with KaleidaGraph 3.6 (Synergy Software). All stopped-flow kinetic traces represent the average of at least nine mixing cycles.

2.3.5 Confocal microscopy and flow-cytometry. The cells were imaged with an Olympus FLUOVIEW (FV500) microscope which is configured on an Olympus BX-61 motorized research microscope. The system has laser lines in the green (488 nm), red (543 nm), far-red (633 nm) spectrum. The microscope is

configured for phase contrast and differential interference contrast (DIC) in addition to fluorescence. Images were analyzed with confocal assistant software (LaserSharp computer software).

The extent of apoptosis and necrosis was quantified using the Annexin V-FITC Apoptosis Detection Kit (eBioscience, USA). Briefly, A549 cells treated with HOCl and SCN⁻ (according to the protocol in Table 2.1) were harvested by scrapping and re-suspended binding buffer (10 mM Hepes, pH 7.4; 140 mM NaCl and 2.5 mM CaCl₂). The cells were then doubly-stained with Annexin V-FITC and propidium iodide prior to quantification. Cell fluorescence was read with a Becton Dickinson LSR II flow-cytometer (housed at OMRF, OKC) and a Beckman Coulter Elite ESP flow-cytometer (housed in the department chemistry and biochemistry, University of Oklahoma).

2.3.6 Cell assay and Protocol. A549 human lung carcinoma cells (American Type Culture Collection, Manassas, VA) were cultured in RPMI 1640 medium supplemented with 10% FBS, 50 unit/mL of penicillin and 50 µg/mL of streptomycin at 37 °C in a 5 % CO₂ humidified incubator. They were seeded in T-25 flasks. After three days, the cells approached confluence and to keep them proliferating, they were subcultured. This included the removal of the old medium, followed by washing with phosphate buffer. The cells were then detached by the addition of 1 mL 0.25% trypsin/EDTA solution and gently tapping the sides of the flask. Once the cells were detached, they were then mixed with

fresh medium to form a cell suspension. The cell suspension was further diluted (1:10) with fresh medium and stored in the incubator at 37 °C. For the confocal experiments, A549 cells were subcultured in 4-well plates 24 hours prior to the experiment at a density of 10^4 cells per mL. After 24 hours, the cells were treated with SCN⁻, OSCN⁻ and/or HOCl according to the protocol below (Table 2.1). The protocol was adopted in order to ensure that all samples including the controls were handled the same way:

Table 2.1: Protocol adopted for treatment of A549 cells (controls and experiments)

1	2	3	5	5	6	7
HOCl	SCN⁻	HOCl + SCN⁻	SCN⁻ + HOCl	OSCN⁻	Buffer	No treatment
Remove medium	Remove medium	Remove medium	Remove medium	Remove medium	Remove medium	Remove medium
Add 800 µl (50 mM HOCl)	Add 800 µl (50 mM SCN)	Add 800 µl (50 mM HOCl)	Add 400 µl (100 mM SCN)	Add 800 µl (50 mM OSCN)	Add 800 µl (medium)	Add 400 µl (Dye)
Incubate 20 min at 37 °C	Incubate 20 min at 37 °C	Incubate 20 min at 37 °C	Add 400 µl (100 mM HOCl)	Incubate 20 min at 37 °C	Incubate 20 min at 37 °C	Incubate 10 min at 37 °C
Remove medium	Remove medium	Remove medium	Incubate 20 min at 37 °C	Remove medium	Remove medium	Imaging
Wash (PBS)	Wash (PBS)	Wash (PBS)	Remove medium	Wash (PBS)	Wash (PBS)	-
Add 800 µl (medium)	Add 800 µl (medium)	Add 800 µl (500 mM SCN)	Wash (PBS)	Add 800 µl (medium)	Add 800 µl (medium)	-
Incubate 20 min at 37 °C	Incubate 20 min at 37 °C	Incubate 20 min at 37 °C	Add 800 µl (medium)	Incubate 20 min at 37 °C	Incubate 20 min at 37 °C	-
Remove medium	Remove medium	Remove medium	Incubate 20 min at 37 °C	Remove medium	Remove medium	-
Wash (PBS)	Wash (PBS)	Wash (PBS)	Remove medium	Wash (PBS)	Wash (PBS)	-
Add 400 µl (Dye)	Add 400 µl (Dye)	Add 400 µl (Dye)	Wash (PBS)	Add 400 µl (Dye)	Add 400 µl (Dye)	-
Incubate 10 min at 37 °C	Incubate 10 min at 37 °C	Incubate 10 min at 37 °C	Add 400 µl (Dye)	Incubate 10 min at 37 °C	Incubate 10 min at 37 °C	-
Imaging	Imaging	Imaging	Incubate 10 min at 37 °C	Imaging	Imaging	-
-	-	-	Imaging	-	-	-

2.4 References

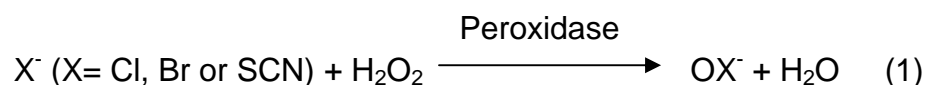
1. Carlberg, I., Mannervic, B. (1985) Glutathione reductase, *Method Enzymol.* 113, 485-490.
2. Dringen, R., Gutterer, J.M. (2002) Glutathione reductase from bovine brain, *Method Enzymol.* 348, 281-288.
3. Ashby, M. T., Nagy, P. (2007) Kinetics and mechanism of the oxidation of the glutathione dimer by hypochlorous acid and catalytic reduction of the chloroamine product by glutathione reductase, *Chemical research in toxicology* 20, 79-87.
4. Pattison, D. I., Davies, M.J., Hawkins, C.L. (2007) Hypochlorous acid-mediated protein oxidation: how important are chloramine transfer reactions and protein tertiary structure?, *Biochemistry* 46, 9853-9864.
5. Kettle, A. J., Winterbourn, C.C. (1994) Assays for the chlorination activity of myeloperoxidase, *Method Enzymol.* 233, 502-512.
6. Thomas, E. L., Grisham, M. B., and Jefferson, M. M. (1986) Preparation and characterization of chloramines, *Method Enzymol.* 132, 569-585.
7. Nagy, P., Alguindigue, S. S., Ashby, M. T. (2006) Lactoperoxidase-catalyzed oxidation of thiocyanate by hydrogen peroxide: a reinvestigation of hypothiocyanite by nuclear magnetic resonance and optical spectroscopy, *Biochemistry* 45, 12610-12616.
8. Simpson, R. J. (2003) *Proteins and proteomics: A laboratory manual* New York: Cold Spring Harbor.

9. Eyer, P., Worek, F., Kiderlen, D., Sinko, G., Stuglin, A., Simeon-Rudolf, V., Reiner, E. (2003) Molar absorption coefficients for the reduced ellman reagent: Reassessment, *Anal. Biochem.* 312, 224-227.
10. Riddles, P. W., Blakeley, R.L., Zerner, B. (1979) Ellmans reagent-5'5'-Dithiobis(2-nitrobenzoic acid)-Re-examination, *Anal. Biochem.* 94, 75-81.
11. Tae, J., Yang, Y., Cho, H.J., Lee, J., Shin, I. (2009) A rhodamine-hydroxamic acid-based fluorescent probe for hypochlorous acid and its applications to biological imagings, *Org. Lett.* 11, 859-861.
12. Smith, I. K., Vierheller, T. L., and Thorne, C. A. (1988) Assay of glutathione reductase in crude tissue homogenates using 5,5'dithiobis-(2-nitrobenzoic acid), *Anal. Biochem.* 175, 408-413.

CHAPTER 3: SMALL MOLECULAR, MACROMOLECULAR AND CELLULAR CHLORAMINES REACT WITH THIOCYANATE TO GIVE THE HUMAN DEFENSE FACTOR HYPOTHIOCYANITE

3.1 Introduction

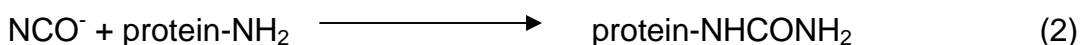
This chapter describes the reactions of thiocyanate (SCN^-) with chloramines of free amino acid (taurine), low molecular protein (ubiquitin) and cellular (*E. coli*). The main question we sought to answer was whether chloramines are capable of oxidizing SCN^- to OSCN^- at physiological conditions pH 7.4. Peroxidase enzymes (including myeloperoxidase (MPO), eosinophil peroxidase (EP), lactoperoxidase (1) and salivary peroxidase (SP)) play an important role in human defense mechanisms (2-3). They catalyze the oxidation of halides (Cl^- and Br^-) and pseudohalide (SCN^-) by hydrogen peroxide to produce HOCl, HOBr and HOSCN respectively which are implicated in human health and disease (2, 4-7).



The hypohalides HOCl, HOBr and HOSCN have pKa values of 7.6; 8.5 and 5.3 respectively (8), which means that at physiological pH conditions (pH = 7.4) they exist as mixtures of both the acid (i.e. HOX) and anion (OX^-) forms. HOCl and HOBr are powerful oxidizing agents that are responsible for the killing of invading pathogens (9-13). However, it has been hypothesized that the over production of

these oxidants can initiate host tissue damage and this has been detected in a wide range of inflammatory diseases including atherosclerosis, kidney disease, asthma and cystic fibrosis (9-10, 12-13). It has been reported that at physiological halide ion concentrations (100-140 mM Cl⁻, 20-100 μM Br⁻ and ≤ 120 μM SCN⁻) approximately 50% of the H₂O₂ consumed by MPO oxidizes SCN⁻ with most of the remaining H₂O₂ (45%) being used to oxidize Cl⁻ (14-16).

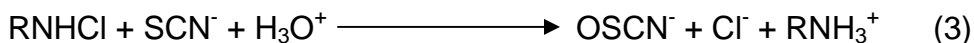
While many studies have focused on HOCl and HOBr, the role of SCN⁻-derived oxidants (e.g. OSCN⁻) in human health and disease remains poorly understood (11-13). This is due in part to the lack of specific biomarkers for SCN⁻-mediated damage and challenges associated with the characterization and quantification of OSCN⁻. Recently, the importance of SCN⁻-derived oxidants was demonstrated by the detection of elevated levels of carbamylated proteins in atherosclerotic plaques (17).



This was attributed to the reaction of the amino groups with OCN⁻, a minor product generated by the peroxidase system. In addition to the peroxidase-catalyzed system, OSCN⁻ can also be produced cleanly by the non-catalytic reaction of HOCl and HOBr with SCN⁻ (18-19). A study that sought to reconcile conflicting reports in literature regarding the spectra of OSCN⁻ reported that it has a unique UV absorption spectra ($\lambda_{\text{max}} = 376 \text{ nm}$, $\epsilon = 26.5 \text{ M}^{-1}\text{cm}^{-1}$) (20). To date,

some of the known methods for the production of OSCN⁻ include the peroxidase-catalyzed oxidation of SCN⁻ by H₂O₂ at pH 7 (Eq. 1); the hydrolysis of (SCN)₂ at pH 13 and the oxidation of SCN⁻ by OX⁻ (X = Cl and Br) at pH 13 (20).

In the present study, we demonstrate another method for the production of OSCN⁻ through the oxidation of SCN⁻ by chloramines (free small molecule, protein-bound and cellular).



This method has potential biological implications since a recent study has suggested that in human plasma like environment, HOCl would preferentially react with proteins thereby producing protein chloramines as one of the significant initial products (12). The chloramines ultimately initiate secondary damage as they hydrolyse to aldehydes and radical intermediates or transfer of the chlorine to other substrates (eq. 5). It is conceivable that a small molecule such as SCN⁻, especially in environments where it is present in high concentrations (e.g. oral cavity and plasma of smokers), will be among the primary targets of these protein-bound chloramines. We propose that the reaction of SCN⁻ with chloramines repairs some of the damage inflicted on proteins by HOCl.

3.2 Results and discussion

3.2.1 Reaction of small molecular chloramines with thiocyanate

In a recent publication, Calvo, *et al.* (23) studied the nucleophilic substitution reactions of N-chloramines. The study involved the mechanism of the reaction of taurine chloramine (TauCl) with thiocyanate (SCN^-). While they succeeded in showing that the reaction was slow around physiological pH conditions ($128.6 \pm 0.1 \text{ M}^{-1}\text{s}^{-1}$ at pH 7.4) they however were unable to identify the reaction product(s). They concluded that the product was possibly unstable chlorine thiocyanate (ClSCN) which rapidly decomposes to form thiocyanogen (SCN_2). Based on previous studies that were published by our laboratory in which it was observed that the reactions of the electrophilic halogenating agents (HOCl and HOBr) with SCN^- at high pH conditions (18-19) produced hypothiocyanite (OSCN^-), we wondered whether TauCl reacted with SCN^- to give the same product?

Since OSCN^- is already known to have a unique spectroscopic signature ($\lambda_{\text{max}} = 376 \text{ nm}$, $\epsilon = 26.5 \text{ M}^{-1}\text{cm}^{-1}$) (20), we employed the UV-vis technique to identify the product of TauCl with SCN^- . The additional advantage of this approach was that no interference from TauCl ($\lambda_{\text{max}} = 252 \text{ nm}$, $\epsilon = 429 \text{ M}^{-1}\text{cm}^{-1}$) was expected. The main challenge however was the fact that OSCN^- has a small molar extinction coefficient. To resolve this issue we used two approaches, first we employed a spectrophotometric cell with a long (effectively 1 meter) pathlength which enabled us to use low (physiologically relevant) concentrations of TauCl and SCN^- $[\text{TauCl}]_0 = 50 \text{ }\mu\text{M}$ and $50 \leq [\text{SCN}]_0 \leq 250 \text{ }\mu\text{M}$ (Figure 3.1). The range of

[SCN⁻] we used is comparable to the normal reference values in human physiological fluids (33.5 ± 25.4 and 111.2 ± 92.1 μM in plasma, and 542 ± 406 and 1655 ± 841 μM in saliva, for smokers and non-smokers, respectively) (24). Similar results to those of Figure 3.1 were obtained for $[\text{TauCl}]_0 = 80$ μM and $0.5 \leq [\text{SCN}]_0 \leq 5$ mM, with chemical yields of OSCN⁻ of 27-100% (Figure 3.2). In both cases we successfully confirmed our suspicion that TauCl was capable of oxidizing SCN⁻ to OSCN⁻.

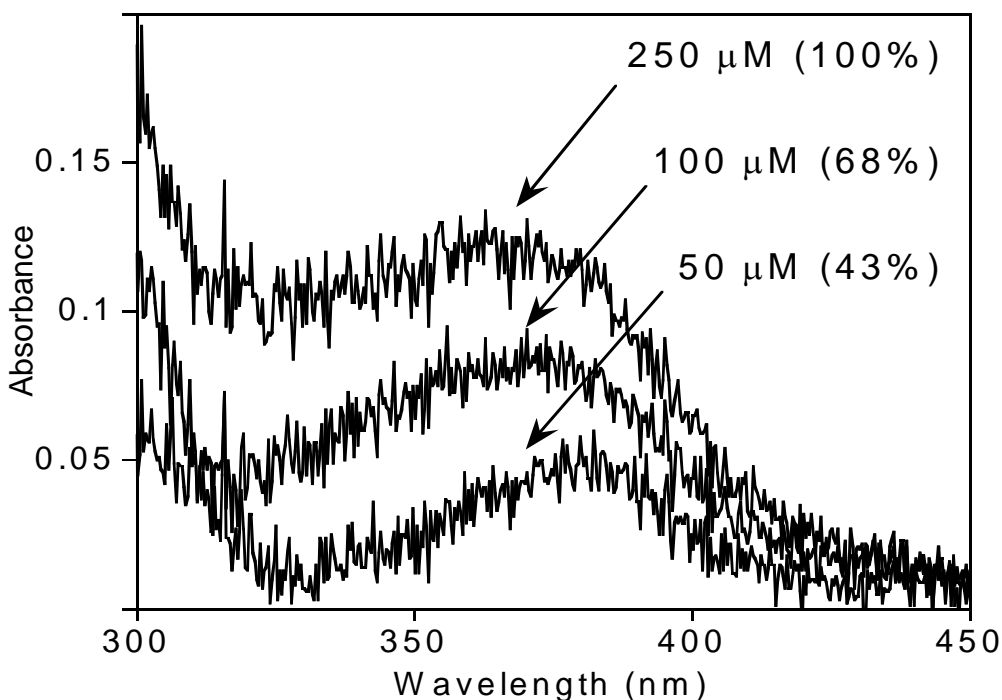


Figure 3.1. UV-vis spectra obtained for the reactions of TauCl (50 μM) with SCN⁻ (50-250 μM) in phosphate buffer (100 mM, pH 7.4) at 20 °C. The spectra were recorded with a 1 meter fiber optic cell. The chemical yield of OSCN⁻ is indicated versus [SCN⁻]₀.

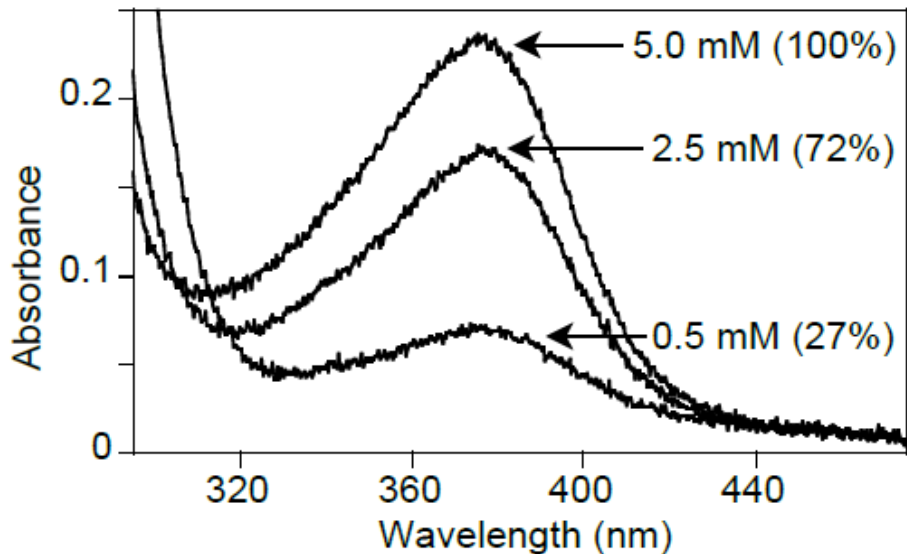


Figure 3.2. UV-vis spectra obtained for the reactions of TauCl (80 μM) with SCN^- (0.5-5.0 mM) in phosphate buffer (100 mM, pH 7.4) at 20 $^\circ\text{C}$. The spectra were recorded with a 1 meter fiber optic cell. The chemical yield of OSCN^- is indicated versus $[\text{SCN}^-]_0$.

The second approach we took to identify the product of TauCl with SCN^- was to use a 10 cm pathlength spectrophotometric cell which allowed us to use high concentrations of the reactants (SCN^- and TauCl $[\text{SCN}^-] = 10$ mM and $[\text{TauCl}]_0 = 0.25, 0.50, 1.0, \text{ and } 2.0$ mM (Figure 3.3)). The main concern with this approach was that it has been reported previously that the presence of excess SCN^- accelerates the decomposition of OSCN^- (25). In his study, Thomas (25) observed that at high concentration (0.1-1 M) SCN^- , the decomposition of OSCN^- (generated by an enzyme system $\text{LPO} + \text{SCN}^- + \text{H}_2\text{O}_2$) was instantaneous. At intermediate concentrations (1-10 mM SCN^-), the decomposition appeared to be first order with respect to $[\text{OSCN}^-]$. At low concentration (0.2-1 mM SCN^-), the

decomposition was second order with respect to $[\text{OSCN}^-]$. It was observed that by keeping the concentration of SCN^- constant (10 mM) and increasing the chloramine concentration $0.25 \leq [\text{TauCl}]_0 \leq 2.0$ mM the yield of OSCN^- appears to be first-order (Figure 3.3).

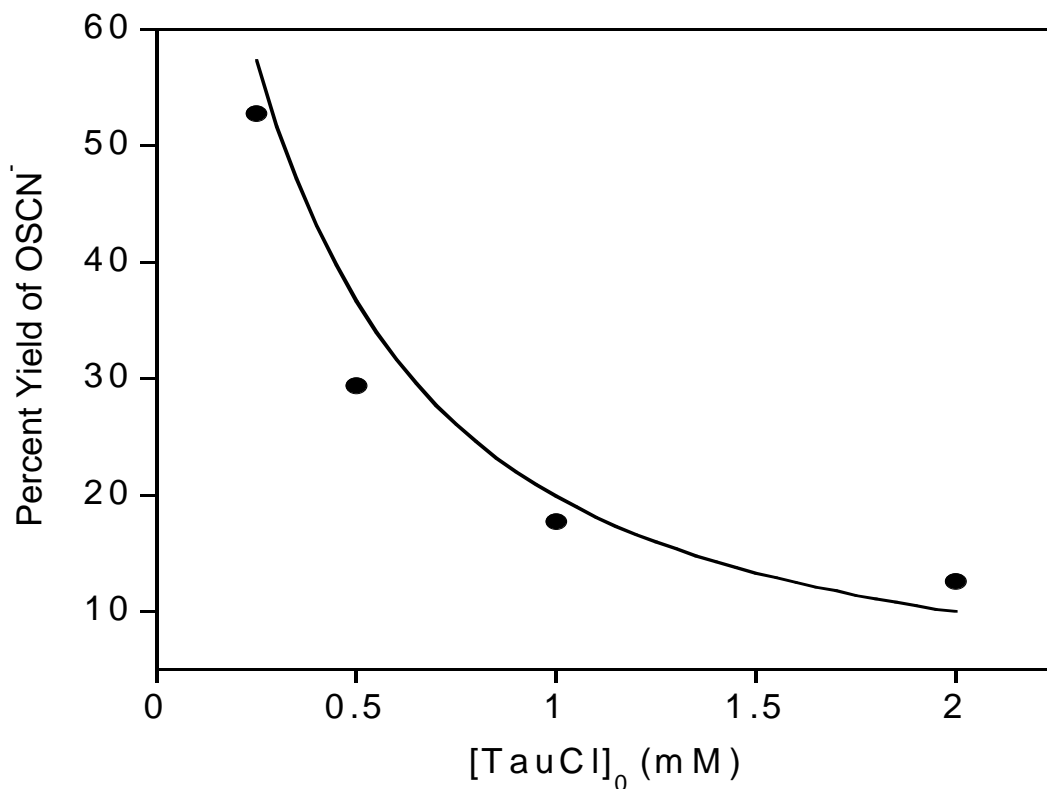
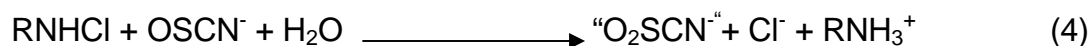


Figure 3.3. Chemical yield of OSCN^- for $[\text{SCN}] = 10$ mM and $[\text{TauCl}]_0 = 0.25$, 0.50, 1.0, and 2.0 mM in phosphate buffer (100 mM, pH 7.4) at 20 °C.

The observed inverse relationship between the yield of OSCN^- upon the $[\text{TauCl}]_0$ indicate that OSCN^- is capable of further reaction with TauCl resulting in over-oxidized products (18-19).



The kinetics of the reaction of OSCN^- with TauCl at pH 7.4 was briefly investigated. One of the challenges we encountered was that in all the existing methods for OSCN^- preparation, excess SCN^- (a competing reductant for TauCl) is required. We chose to synthesize OSCN^- using the LPO-catalyzed system since it is a more efficient method for preparing high (mM) concentrations of OSCN^- that are relatively free of excess SCN^- and over-oxidation products (20). The LPO-catalyzed oxidation of 5.0 mM SCN^- by 5.0 mM H_2O_2 produced 3.5 mM OSCN^- . No attempts were made to destroy unreacted H_2O_2 that remained after catalysis by the addition of catalase because we did not know the effects of catalase on the TauCl (26). Also the possible reaction of H_2O_2 with SCN^- was ignored because it is known that the uncatalyzed reaction is very slow (27-28). Figure 3.4 illustrates the reaction of equimolar concentrations of TauCl and OSCN^- (mixed second-order conditions). The reaction was monitored at two wavelengths, 252 nm (filled circles, λ_{max} for TauCl , $\epsilon = 429 \text{ M}^{-1}\text{cm}^{-1}$) and 376 nm (open circles, λ_{max} for OSCN^- , $\epsilon = 26.5 \text{ M}^{-1}\text{cm}^{-1}$).

The observed absorption change at 252 nm ($\Delta \text{Abs}(\text{obs}) = 0.38 \text{ AU}$) was comparable to the change expected for the consumption of 0.74 mM TauCl ($\Delta \text{Abs}(\text{calc}) = 0.38 \text{ AU}$). The observed absorption change at 376 nm ($\Delta \text{Abs}(\text{obs}) = 0.008 \text{ AU}$) was about half that expected for the consumption of 0.74 mM OSCN⁻ ($\Delta \text{Abs}(\text{calc}) = 0.019 \text{ AU}$). The apparent discrepancy between the expected and the observed change in absorbance is possibly due to some reaction products. In order to fit the kinetic data to a mixed second-order rate equation (Figure 3.4, solid lines), we assumed that the absorption changes were due to the consumption of 0.74 mM of both TauCl and OSCN⁻. Given the order-of-magnitude difference in absorptivities of TauCl and OSCN⁻, the data at 252 nm are more precise than the data at 376 nm. The data show that TauCl reacts much faster with OSCN⁻ ($2.8 \times 10^3 \text{ M}^{-1} \text{ s}^{-1}$) than with SCN⁻ ($128.6 \text{ M}^{-1} \text{ s}^{-1}$). We note that the reaction is more complicated and possibly involves a lot of intermediates; as such a detailed mechanistic study is necessary for a better understanding of the overall redox cascade.

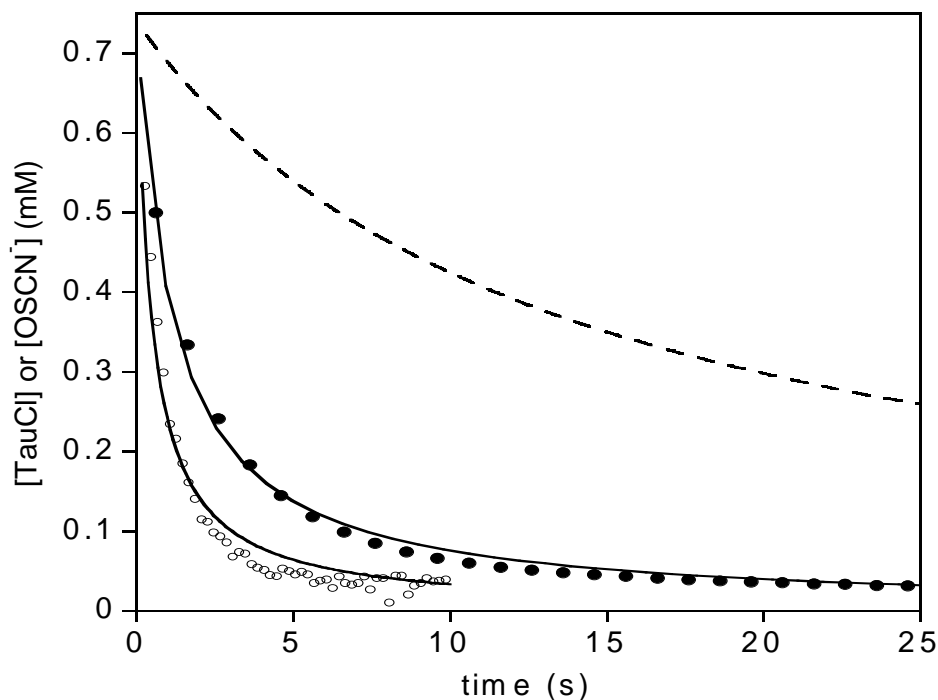


Figure 3.4. Concentrations determined at 252 nm (solid circles, λ_{\max} for TauCl) and 376 nm (open circles, λ_{\max} for OSCN⁻) versus time for the reaction of [TauCl]₀ = 0.74 mM and [OSCN⁻]₀ = 0.74 mM in phosphate buffer (100 mM, pH 7.4) at 20 °C. The OSCN⁻ was prepared by the LPO-catalyzed oxidation of 5 mM SCN⁻ by 5 mM H₂O₂ to give a 3.5 mM stock solution of OSCN⁻ (determined spectrophotometrically). The solid lines are imperfect nonlinear least-squares fit of the experimental data (for clarity, 1% and 10% shown for TauCl and OSCN⁻, respectively) using a mixed second-order rate equation $k = (1.182 \pm 0.002) \times 10^3$ and $(2.84 \pm 0.03) \times 10^3 \text{ M}^{-1} \text{ s}^{-1}$ at 276 and 376 nm, respectively). The dashed line is the expected absorption change for a second-order absorption decay for $k = 128.6 \pm 0.1 \text{ M}^{-1} \text{ s}^{-1}$ (the independently measured rate constant for the reaction of TauCl and SCN⁻ under the same reaction conditions).

3.2.2 Reaction of protein chloramines with thiocyanate

It was not possible to identify products of the reaction of protein derived chloramines with SCN^- by following changes in the UV-vis at 376 nm (i.e. OSCN^-) due to its low molar absorptivity compared to the protein. To address this limitation, we employed a kinetic approach taking advantage of the fact that thiols are preferred targets of OSCN^- with rate constants ranging between $10^3 - 10^6 \text{ M}^{-1}\text{s}^{-1}$ reported (8). We selected 5-thio-2-nitrobenzoic acid (TNB) as a model compound for thiols because of its high molar absorptivity ($\epsilon_{412} = 14,150 \text{ M}^{-1}\text{cm}^{-1}$) which allowed us to follow the reaction at low (μM) concentrations. TNB was used both to quantify the concentration of protein chloramines and also to measure the rate constant of the reaction of chloramines with OSCN^- . Before investigating the reaction of SCN^- with protein chloramines, OSCN^- was independently synthesized using the enzyme system ($\text{LPO} + \text{SCN}^- + \text{H}_2\text{O}_2$) (20) and the reaction of TauCl with SCN^- (which was shown in section 2.3.1 to produce OSCN^-). The kinetic measurements in each case (Figure 3.5 – 3.6) for the reaction of OSCN^- with TNB, resulted in a second-order rate constant of $10^5 \text{ M}^{-1}\text{s}^{-1}$.

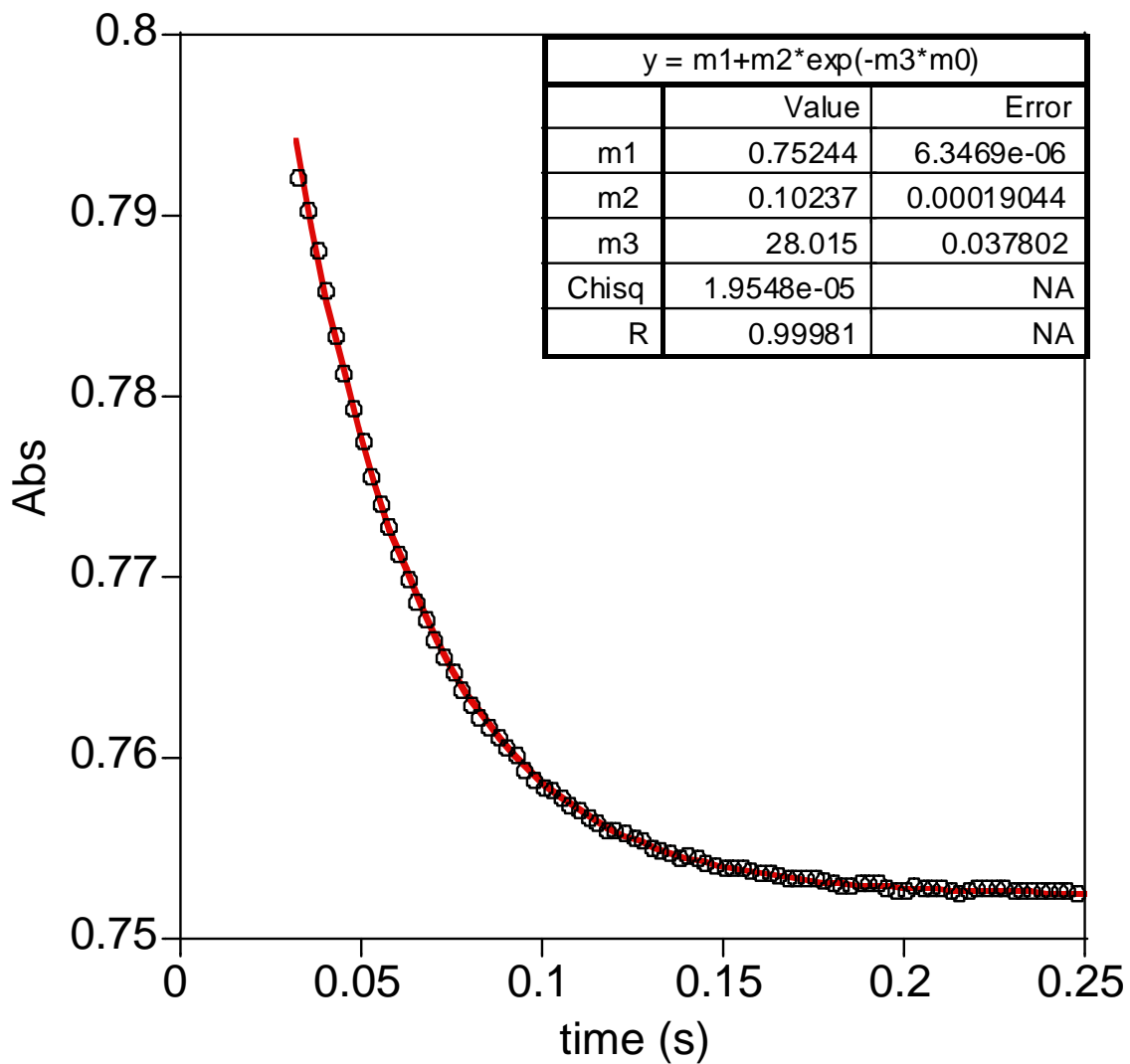


Figure 3.5. Observed absorbance decrease at 412 nm for the reaction of OSCN^- (4 μM , produced by the LPO-catalyzed oxidation of SCN^- by H_2O_2) with TNB (56 μM) at pH 7.4 and $I = 1.0 \text{ M}$. A first-order fit (red) and 20% of the data (black circles) are illustrated.

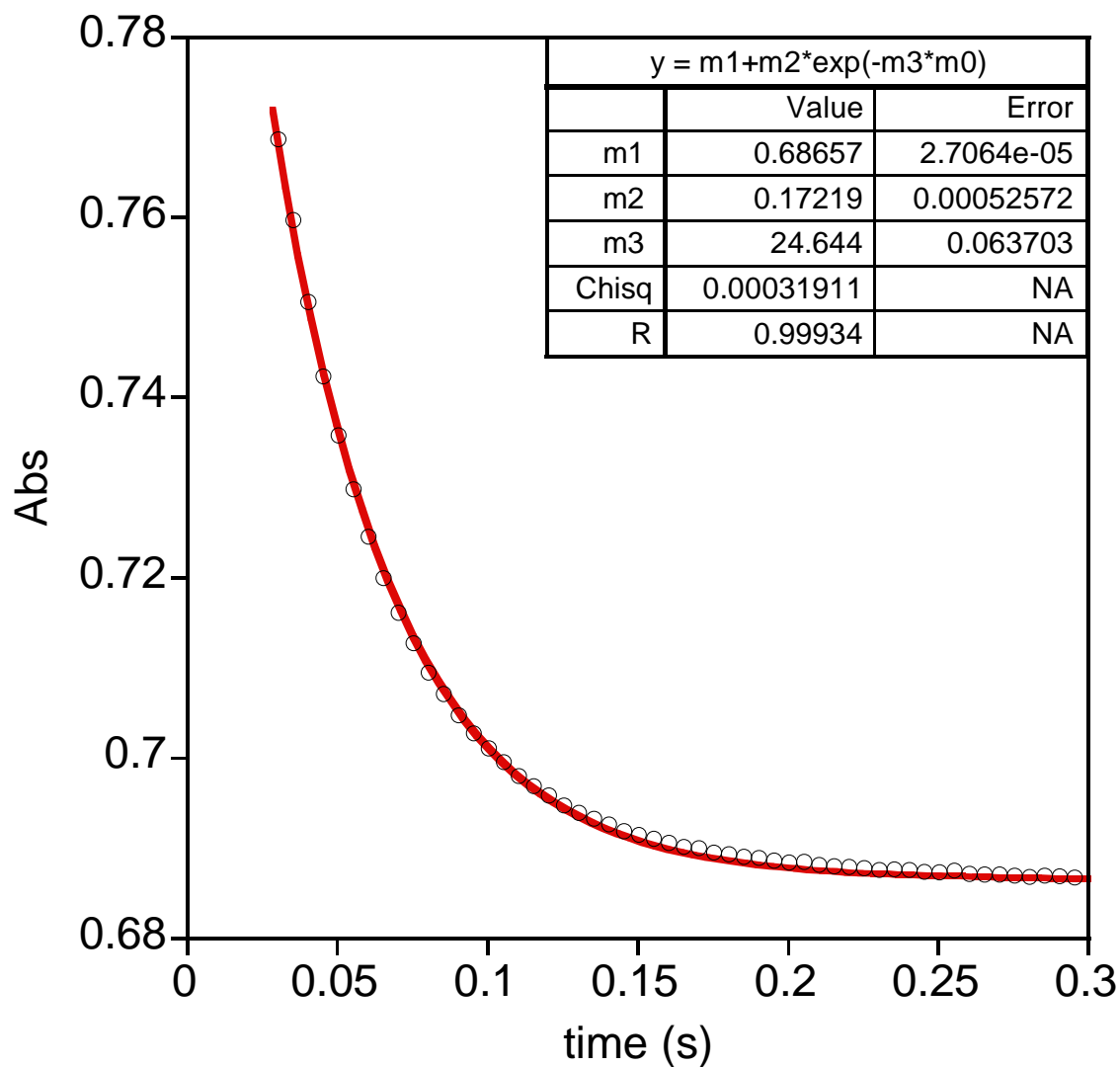


Figure 3.6. Observed absorbance decrease at 412 nm for the reaction of OSCN^- (5.5 μM , produced by the uncatalyzed oxidation of SCN^- by TauCl) with TNB (56 μM) at pH 7.4 and $I = 1.0 \text{ M}$. A first-order fit (red) and 10% of the data (black circles) are illustrated.

Ubiquitin (Ub) a small protein (8.5 KDa) found in cells of plants and animals (including humans) where it's used mainly to label damaged or old proteins earmarked for degradation was chosen for the protein chloramines investigation (29). It is a very stable protein that can withstand extreme temperatures and pH conditions (30-31). Its selection for our investigation was based purely on the fact that it has no thiols, only one methionine and loaded in amino groups (seven lysines). Since methionine (Met) reacts much faster with HOCl ($3.8 \times 10^7 \text{ M}^{-1}\text{s}^{-1}$) than any of the other groups (36), we decided that it would be best to block the methionine before mixing the protein with HOCl. This undertaking was important for two reasons including the reduction of the non-recoverable oxidizing equivalence and also the prevention of the subsequent competitive reaction of chloramines with Met (a reaction that has recently been shown to produce a reactive dehydromethionine derivative) (31). A procedure involving the use of performic acid was employed to block the N-terminal methionine by oxidizing it to a sulfone (hereafter Ub*) (22). After treating Ub* with HOCl for various amounts of time the amount of protein chloramines (Ub*Cl) was quantified by TNB analysis. We found that the yield of the recoverable oxidizing equivalence (Ub*Cl) varied between 33-41% (based upon the amount of HOCl). This yield is consistent with the 45% recovery reported by Davies and Hawkins for lysozyme chloramines. The rest of the HOCl oxidizing equivalence is lost through the oxidation of other protein side chains such as tyrosine and the decomposition of the protein chloramines. In the case of lysozyme chloramines, Davies and Hawkins observed that about 50% of the protein chloramines decomposed in ca

30 min (32-33). We measured the rate constant for the reaction of Ub*Cl with TNB and found that the kinetics were biphasic with pseudo-second order rate constants of ca. 10^3 and $10^3 \text{ M}^{-1}\text{s}^{-1}$ (Figure 3.7) which are comparable with $1.38 \pm 0.08 \times 10^4 \text{ M}^{-1}\text{s}^{-1}$ for TauCl with TNB (Figure 3.8). To assess whether OSCN⁻ was formed by the reaction of protein chloramines with SCN⁻, Ub*Cl was reacted with excess SCN⁻ followed by the reaction of the mixture with TNB. A rate constant of $3.73 \pm 0.01 \times 10^5 \text{ M}^{-1}\text{s}^{-1}$ which is similar to the one independently measured for authentic OSCN⁻ with TNB was measured (Figure 3.9).

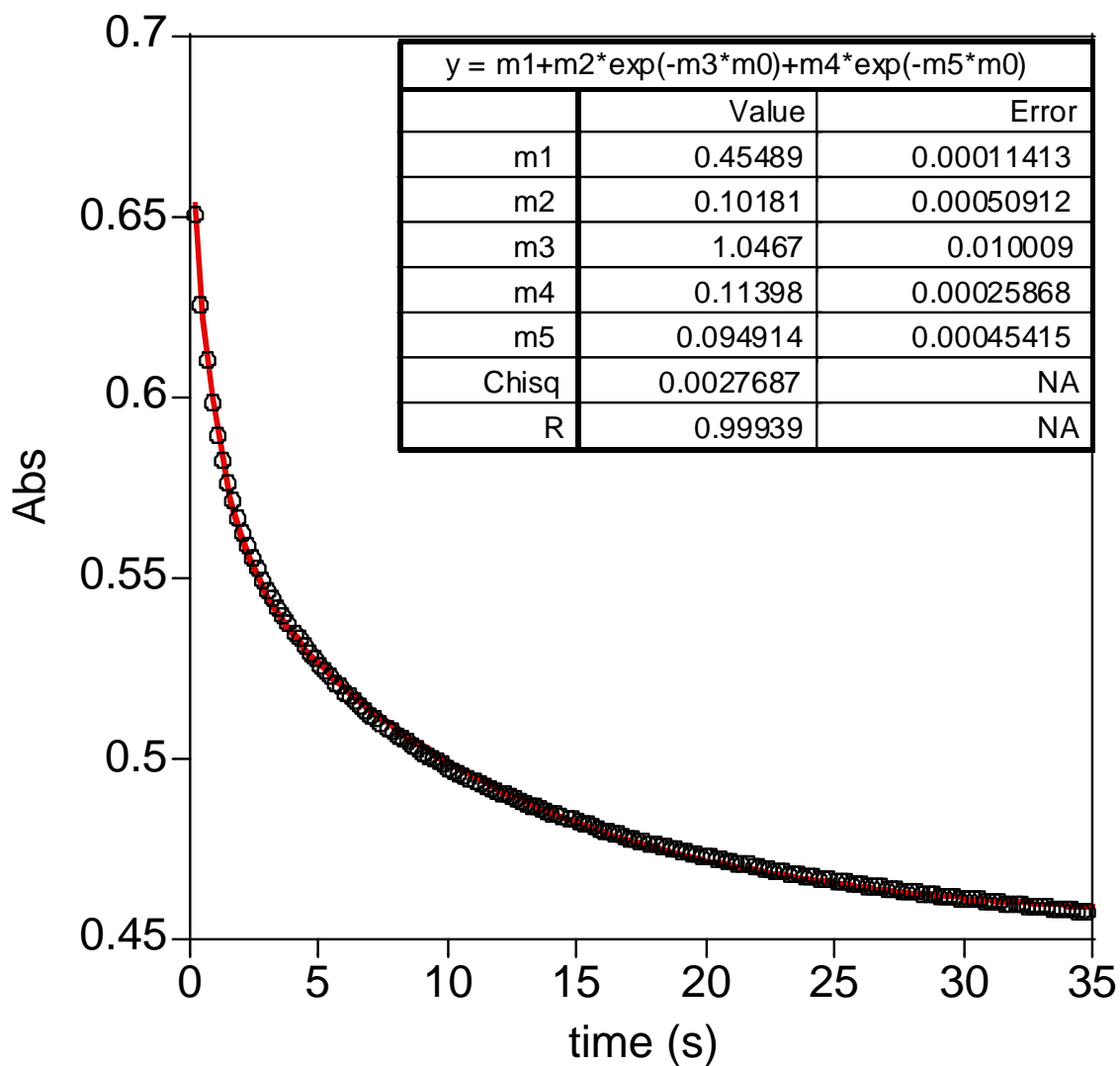


Figure 3.7. Observed biexponential (decrease-decrease) absorbance decrease at 412 nm for the reaction of Ub*Cl (6 μ M, based upon the amount of HOCl used) with TNB (68 μ M) at pH 7.4 and I = 1.0 M. A biexponential fit (red) and 10% of the data (black circles) are illustrated.

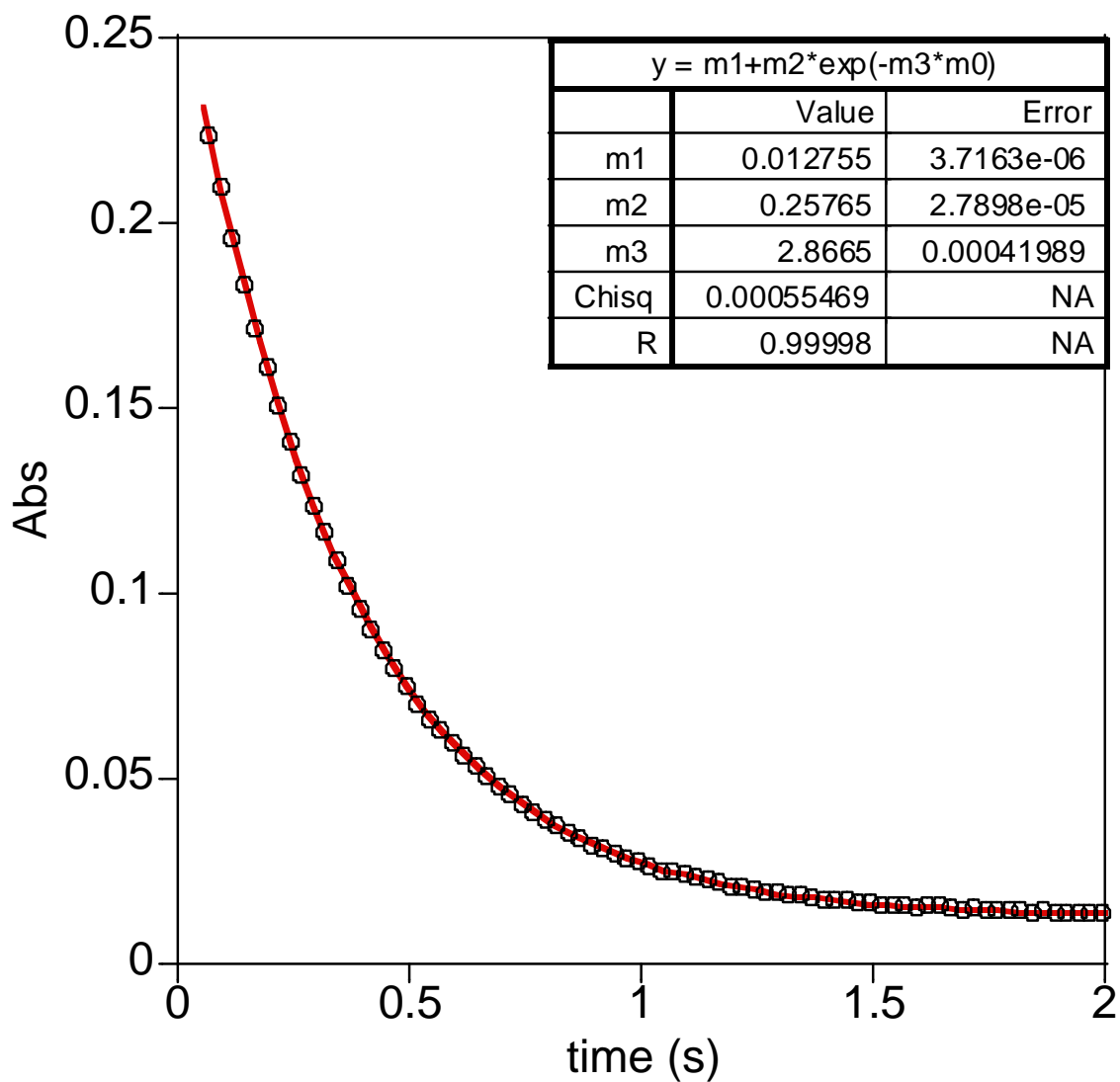


Figure 3.8. Observed absorbance decrease at 412 nm for the reaction of TauCl (208 μM) with TNB (16 μM) at pH 7.4 and $I = 1.0 \text{ M}$. A first-order fit (red) and 2% of the data (black circles) are illustrated.

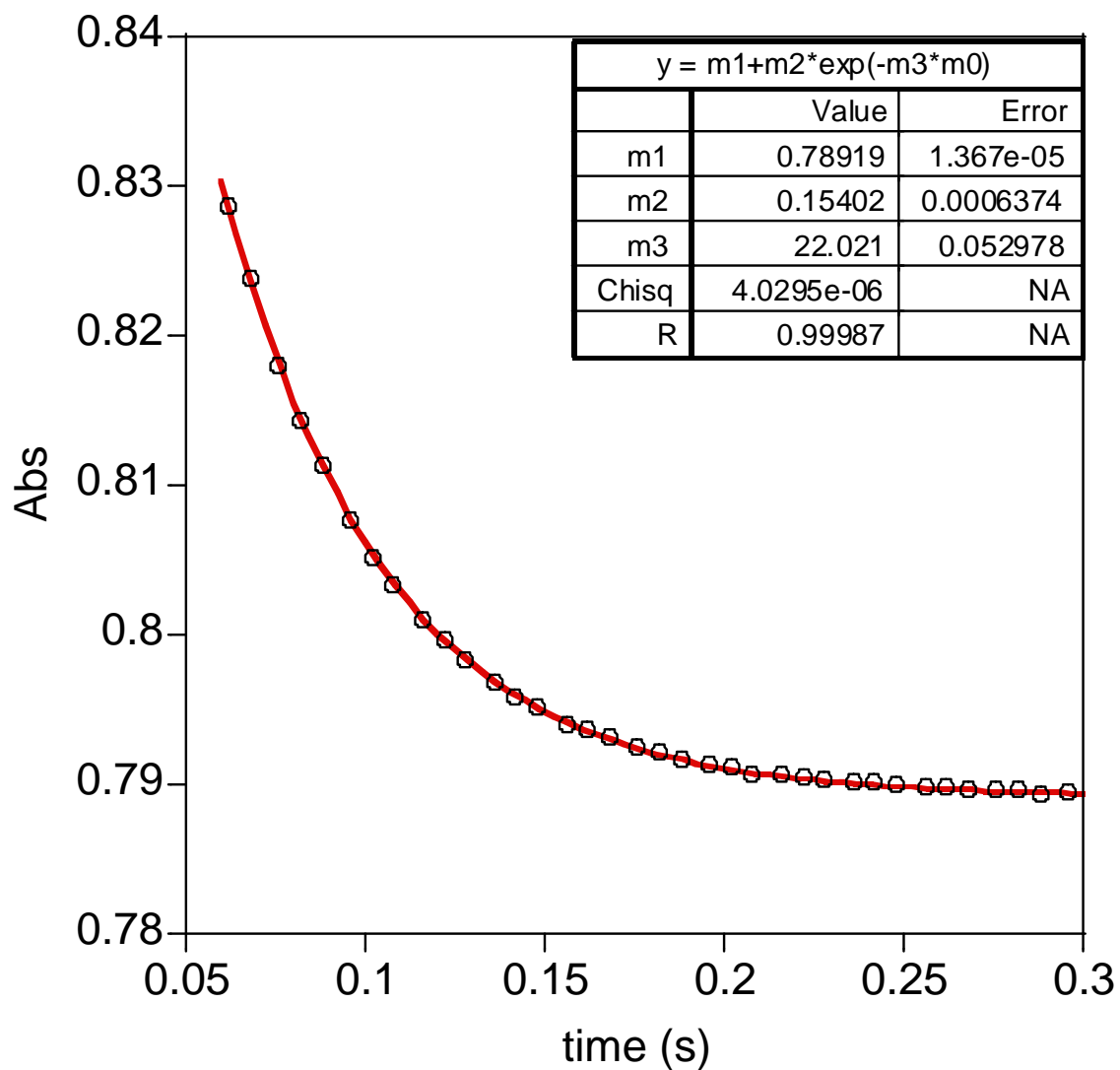


Figure 3.9. Observed absorbance decrease at 412 nm for the reaction of Ub*Cl (6.75 μ M) with SCN⁻ (0.5 mM) for 20 minutes, followed by reaction with TNB (58.66 μ M) at pH 7.4 and I = 1.0 M. A first-order fit (red) and 10% of the data (black circles) are illustrated.

3.2.3 Reaction of cellular chloramines with thiocyanate

The investigation was extended to include cellular-derived chloramines using *E. coli* (MG1655) as a model bacteria. Chlorination of bacteria to kill them is one of the mechanisms used by human leucocytes *in vivo* (34). The chlorinating agents used include HOCl produced by the enzyme system (MPO+Cl⁻+H₂O₂) and chloramines (e.g. TauCl). The chlorination of the bacterial surfaces was achieved by incubating 10⁹ cell/ml *E. coli* (MG1655) with 1 mM HOCl for 5 h in phosphate buffer at physiological pH conditions. After incubation, the chlorinated cells were washed and centrifuged with phosphate buffer to remove any unreacted HOCl. TNB assay was then used to quantify the generated chloramines on the surface of the cells and 42% of the oxidizing equivalence (based on the initial concentration of HOCl) was recovered. Previously some authors (21) have suggested that the reaction of chloramines with TNB is usually complete during mixing time, however it was reported recently (34) that a contact time of at least 8 min was necessary for the reaction of chlorinated bacteria with TNB. We conducted a few trial experiments by allowing between 5-15 min waiting period after mixing the chloramines with TNB. We found that approximately 12 min contact time was optimal for the reaction of cellular chloramines with TNB under the conditions of our experiments. In measuring the rate constant(s) for the reaction of chlorinated cells with TNB, we observed biphasic kinetic trace, possibly indicating the reaction of different chloramines with TNB (Figure 3.10). The chlorinated cells were then treated with 2.5 mM SCN⁻ and filtered through a 0.2 μm polyamide filter. The supernatant was reacted with TNB and 71% of the

oxidizing equivalence was recovered. The rate constant of the oxidant in the supernatant with TNB was measured and found to be $9.40 \pm 0.01 \times 10^5 \text{ M}^{-1}\text{s}^{-1}$ (Figure 3.11) a value consistent with the presence of OSCN^- .

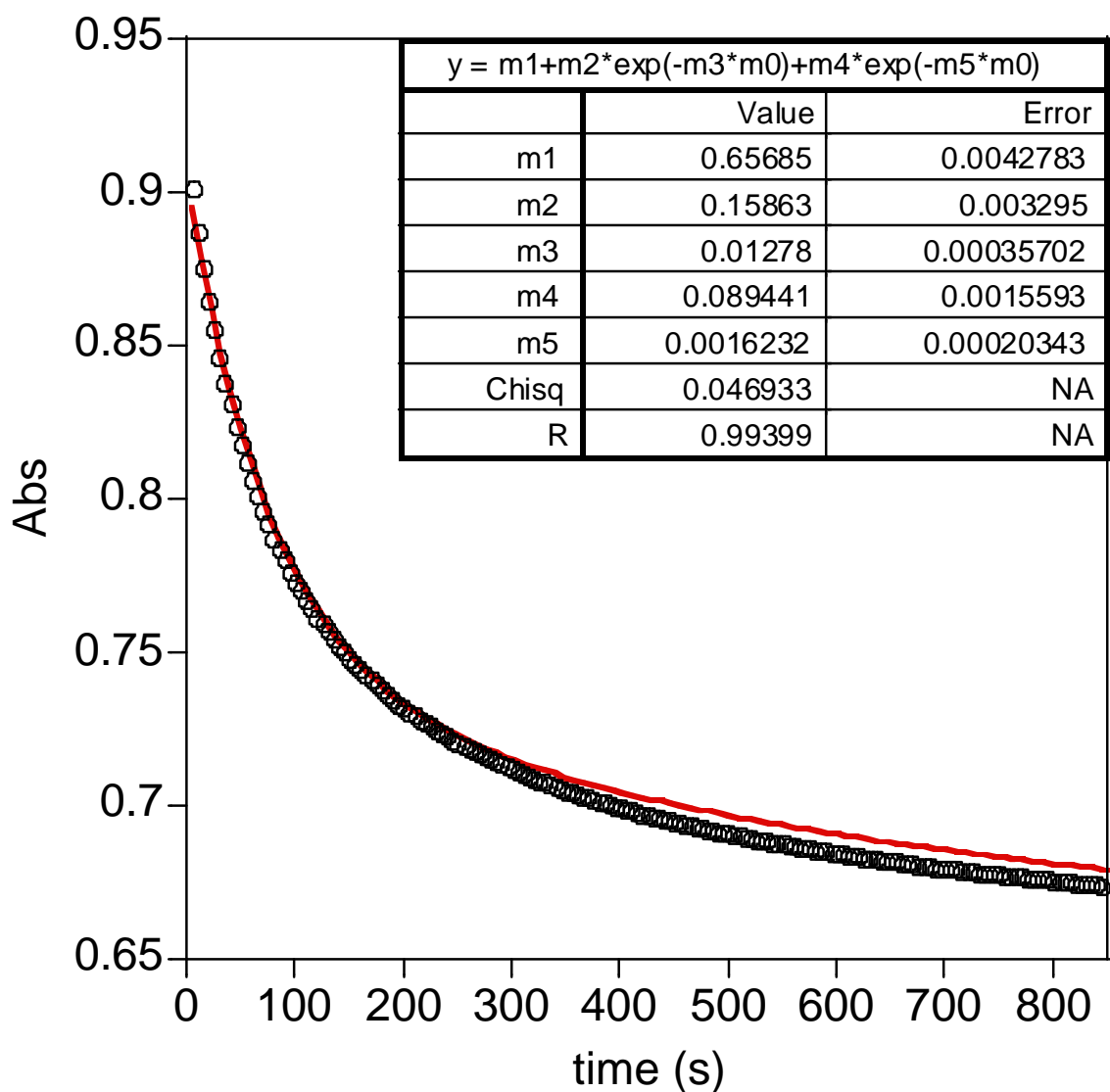


Figure 3.10. Absorbance decrease at 412 nm for the reaction of chlorinated *E. coli* (6 μM , based upon the HOCl used) with TNB (60.8 μM) at pH 7.4 and $I = 1.0 \text{ M}$. A biexponential fit (red) and 10% of the data (black circles) are illustrated. The kinetics are apparently multi-phasic.

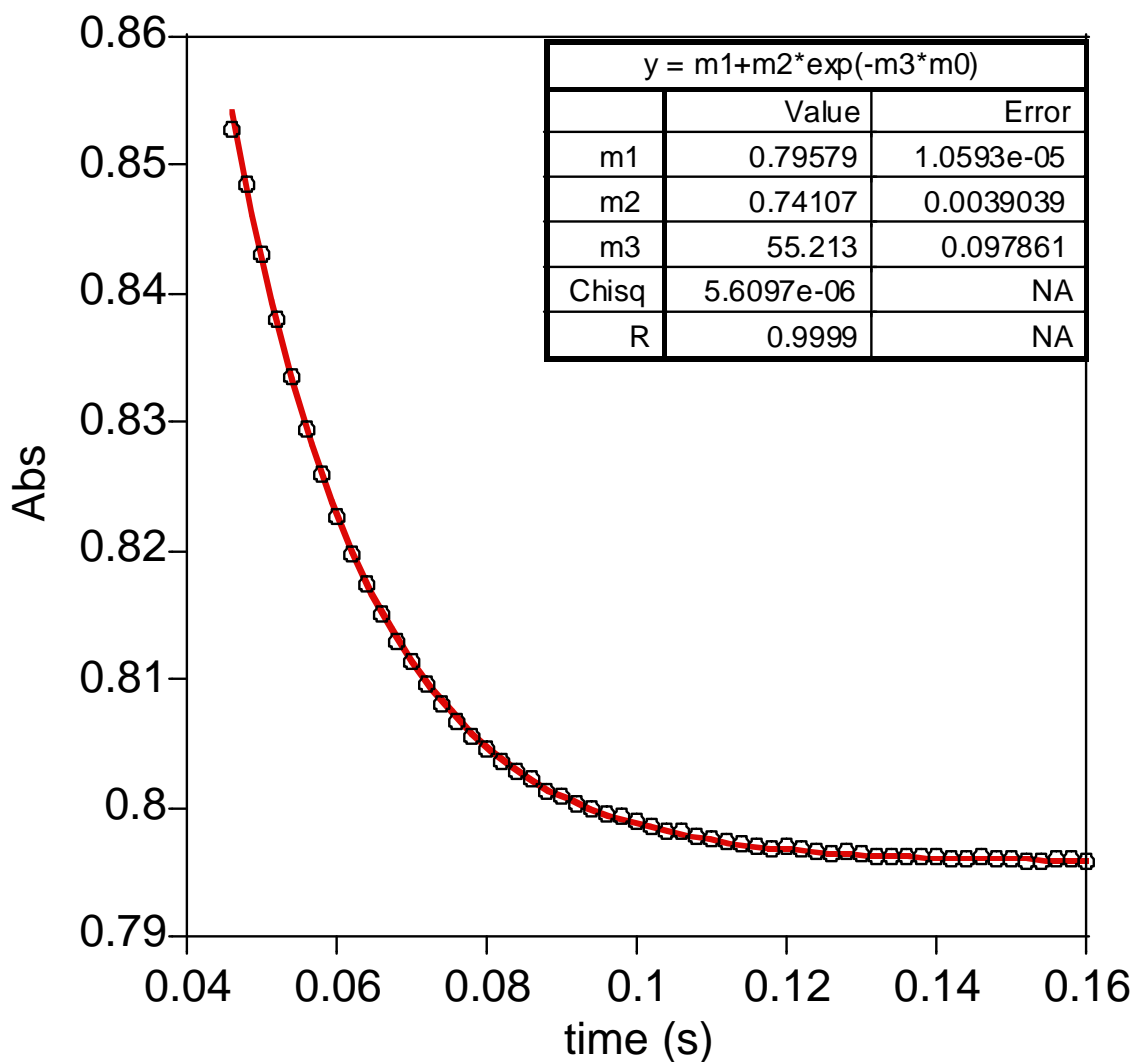


Figure 3.11. Observed absorbance decrease at 412 nm for the reaction of chlorinated *E. coli* (6 μM , based upon the HOCl used) with SCN^- (2.5 mM) for 12 minutes, followed by reaction with TNB (58.66 μM) at pH 7.4 and $I = 1.0 \text{ M}$. A first-order fit (red) and 50% of the data (black circles) are illustrated.

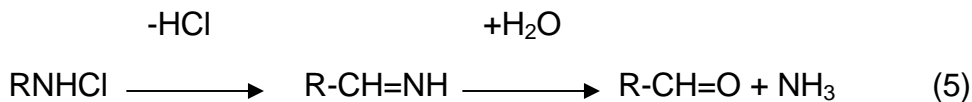
3.2.4 Possible biological significance of the reduction of chloramines by SCN⁻ and OSCN⁻

The formation of HOCl in human blood plasma has been a subject of a number of studies (5, 34-36). The investigations have focused on quantifying the consumption of known primary targets of HOCl such as thiols, antioxidants and amines. Efforts have also been made to identify and quantify the decomposition products of chloramines (products of HOCl reaction with amines) such as oxo-aldehydes and radical intermediates (37-39). The question that remained unanswered was, given the number possible HOCl targets in a complex biological environment such as plasma, which are the major primary targets? To shed some light on this matter, Pattison, *et al.* has developed a mathematical model which can be used to predict the fate of HOCl in plasma (12). The model included plasma proteins (albumin), free amino acids, antioxidant (ascorbate) and SCN⁻.

The model predicts that proteins are the major targets consuming about 94% of HOCl which results in 5% yield of protein chloramines. This is in contrast with the suggestion by some studies that free amino acid chloramines are the major products of HOCl oxidation in plasma (37, 39). Perhaps one of the most important conclusions of the kinetic model was that chloramines formed on cell surfaces are significant, thus future studies should consider the role of protein-bound chloramines in mediating oxidative damage. The data also indicates that antioxidants have a low efficacy to prevent HOCl-mediated plasma damage.

Depending upon the individuals smoking habits, the model predicted that about 2-8% of HOCl is consumed by SCN^- to form OSCN^- . The kinetic model however suffers from some limitations. These include the use of experimental rate constants for small molecules despite the evidence that proteins were a major target of HOCl, not making distinctions between intermolecular reactions involving two small molecules, a small molecule and a protein, or between two proteins. The reactions involving two proteins relative to the other reaction pathways are presumably kinetically disfavored.

The redox cascade that begins with HOCl produces chemically inert products (e.g. chlorotyrosine and methionine sulfoxide) and also reactive intermediates (e.g. free and protein-bound chloramines and OSCN^-). Chloramines are the major species resulting from HOCl-attack on proteins in biological fluids such as plasma (12). The formation of protein-bound chloramines can result in irreversible alterations to protein structure and function (33). The mechanism proposed for this type of modification result in the formation of an aldehyde (33).



The present study suggests that the reaction of chloramines with SCN^- to produce OSCN^- may be important biologically as the rate constant of $129 \text{ M}^{-1}\text{s}^{-1}$ is comparable to that of the best nucleophiles such as cysteine ($200\text{-}900 \text{ M}^{-1}\text{s}^{-1}$) and

methionine ($40\text{-}300\text{ M}^{-1}\text{s}^{-1}$) at pH 7.4. This reaction ensures that no permanent alterations of protein amino groups occur. On the other hand, the formation of OSCN^- is potentially harmful as it preferentially targets thiols. Recently, it has been suggested that the selective targeting of thiols by OSCN^- may play a major role in inflammation-induced oxidative damage (40). We found that OSCN^- reacts with chloramines much faster than SCN^- , possibly producing the over-oxidized product(s). These over-oxidized products presumably hydrolyze to give inert products. Between the repair of the damage caused by HOCl (through the formation of chloramines) and the potential subsequent attack on the thiol groups by OSCN^- , the biological implication of the reaction of chloramines with SCN^- in human health/disease remains unclear.

3.3 Conclusions

The present study demonstrates that chloramines (i.e. major secondary products of HOCl -mediated attack on proteins) are capable of oxidizing SCN^- to OSCN^- (a human defense factor). This reaction is important because it suggests that *in vivo* SCN^- potentially repairs some of the HOCl inflicted damage on the proteins. The implication of the OSCN^- formation on human health/disease remains unclear since OSCN^- itself oxidizes thiols more efficiently than either HOCl or HOBr . Evidence showing that OSCN^- may play a critical role in the health of individuals with elevated levels of SCN^- arising from cigarette smoking has been provided (17). Surprisingly, this study also reports that OSCN^- reacts with a chloramine (TauCl) much faster than SCN^- , a reaction which we suspect

produces the over-oxidized product(s). These over-oxidized products presumably hydrolyze to give inert products.

3.4 References

1. Hoyano, Y., Bacon, V., Summons, R.E., Pereira, W.E., Halpern, B., Duffield, A.M. (1973) Chlorination studies .4. reaction of aqueous hypochlorous acid with pyrimidine and purine bases, *Biochem. Biophys. Res. Commun.* 53, 1195-1199.
2. Pattison, D. I., Davies, M.J. (2006) Reactions of myeloperoxidase-derived oxidants with biological substrates: Gaining chemical insight into human inflammatory diseases, *Curr. Med. Chem.* 13, 3271-3290.
3. Davies, M. J., Hawkins, C. L., Pattison, D. I., and Rees, M. D. (2008) Mammalian heme peroxidases: From molecular mechanisms to health implications, *Antioxid. Redox Signaling* 10, 1119-1234.
4. Mainemare, A., Megarbane, B., Soueidan, A., Daniel, A., Chapple, I. L. C. (2004) Hypochlorous acid and taurine-N-monochloramine in periodontal diseases, *J. Dent. Res.* 83, 823-831.
5. Venglarik, C. J., Giron-Calle, J., Wigley, A. F., Malle, E., Watanabe, N., Forman, H. J. (2003) Hypochlorous acid alters bronchial epithelial cell membrane properties and prevention by extracellular glutathione, *J. Appl. Physiol.* 95, 2444-2452.
6. Kruidenier, L., Kuiper, I., Lamers, C. B. H. W., Verspaget, H. W. (2003) Intestinal oxidative damage in inflammatory bowel disease: semi-quantification, localization, and association with mucosal antioxidants, *J. Pathol.* 201, 28-36.

7. Krasowska, A., Konat, G. W. (2004) Vulnerability of brain tissue to inflammatory oxidant, hypochlorous acid, *Brain Res.* 997, 176-184.
8. Skaff, O., Pattison, D. I., Davies, M. J. (2009) Hypothiocyanous acid reactivity with low-molecular-mass and protein thiols: absolute rate constants and assessment of biological relevance *Biochem. J.* 422, 111-117.
9. Weiss, S. J., Test, S.T., Eckmann, C.M., Roos, D., Regiani, S. (1986) Brominating oxidants generated by human eosinophils, *Science* 234, 200-203.
10. Hawkins, C. L., Davies, M.J. (2005) The role of reactive N-bromo species and radical intermediates in hypobromous acid-induced protein oxidation, *Free Radical Biol. Med.* 39, 900-912.
11. Pattison, D. I., Davies, M.J. (2004) Kinetic analysis of the reactions of hypobromous acid with protein components: implications for cellular damage and use of 3-bromotyrosine as a marker of oxidative stress, *Biochemistry* 43, 4799-4809.
12. Pattison, D. I., Hawkins, C.L., Davies, M.J. (2009) What are the plasma targets of the oxidant hypochlorous acid? a kinetic modeling approach., *Chem. Res. Toxicol.* 22, 807-817.
13. Thomas, E. L., Bozeman., P. M., Jefferson, M. M., King, C. C. (1995) Oxidation of bromide by the human leukocyte enzymes myeloperoxidase and eosinophil peroxidase: formation of bromamines, *Journal of Biological Chemistry*, 270, 2906-2913.

14. Thomas, E. L., Fishman, M. (1986) Oxidation of chloride and thiocyanate by isolated leukocytes, *J. Biol. Chem.* 261, 9694-9702.
15. vanDalen, C. J., Whitehouse, M. W., Winterbourn, C. C., Kettle, A. J. (1997) Thiocyanate and chloride as competing substrates for myeloperoxidase, *Biochem. J.* 327, 487-492.
16. Slungaard, A., Mahoney, J.R. (1991) Thiocyanate is the major substrate for eosinophil peroxidase in physiologic fluids. Implications for cytotoxicity, *J. Biol. Chem.* 266, 4903-4910
17. Wang, Z., Nicholls, S.J., Stephen, J.; Rodriguez, E.R., Kummu, O., Horkko, S., Barnard, J., Reynolds, W.F., Topol, E.J., DiDonato, J.A., Hazen, S. L. (2007) Protein carbamylation links inflammation, smoking, uremia and atherogenesis, *Nat. Med.* 13, 1176-1184.
18. Ashby, M. T., Carlson, A.C., Scott, M.J. (2004) Redox buffering of hypochlorous acid by thiocyanate in physiologic fluids, *J. Am. Chem. Soc.* 126, 15976-15977.
19. Nagy, P., Beal, J. L., Ashby, M. T. (2006) Thiocyanate is an efficient endogenous scavenger of the phagocytic killing agent hypobromous acid, *Chem. Res. Toxicol.* 19, 587-593
20. Nagy, P., Alguindigue, S. S., Ashby, M. T. (2006) Lactoperoxidase-catalyzed oxidation of thiocyanate by hydrogen peroxide: a reinvestigation of hypothiocyanite by nuclear magnetic resonance and optical spectroscopy, *Biochemistry* 45, 12610-12616.

21. Calvo, P., Crugeiras, J., Rios, A., Rios, M.A. (2007) Nucleophilic substitution reactions of N-chloramines: evidence for a change in mechanism with increasing nucleophile reactivity, *J. Org. Chem.* 72, 3171-3178.
22. Tsuge, K., Kataoka, M., Seto, Y. (2000) Cyanide and thiocyanate levels in blood and saliva of healthy adult volunteers, *J. Health Sci.* 46, 343-350.
23. Thomas, E. L. (1981) Lactoperoxidase-catalyzed oxidation of thiocyanate: equilibria between oxidized forms of thiocyanate, *Biochemistry* 30, 3273-3280.
24. Maskino, T., Fridovich, I. (1988) NADPH mediates the inactivation of bovine liver catalase by monochloroamine., *Arch. Biochem. Biophys.* 265, 279-285.
25. Wilson, I. R., and Harris, G. M. (1960) The oxidation of thiocyanate ion by hydrogen peroxide. I. The pH-independent reaction, *J. Am. Chem. Soc.* 82, 4515-4517.
26. Wilson, I. R., and Harris, G. M. (1961) The oxidation of thiocyanate ion by hydrogen peroxide .II. The acid-catalyzed reaction, *J. Am. Chem. Soc.* 83, 286-289.
27. Schmitt, H. P. (2006) Protein ubiquitination, degradation and the proteasome in neuro-degenerative disorders: No clear evidence for a significant pathogenetic role of proteasome failure in Alzheimer disease and related disorders, *Med. Hypotheses* 67, 311-317.

28. Ramage, R., Green, J., Muir, T.W., Ogunjobi, O.M., Love, S., Shaw, K. (1994) Synthetic, structural and biological studies of the ubiquitin system: the total chemical synthesis of ubiquitin., *Biochem. J.* 299, 151-158.
29. Ibarra-Molero, B., Loladze, V.V., Makhatadze, G.I., Sanchez-Ruiz, J.M. (1999) Thermal versus guanidine-induced unfolding of ubiquitin. an analysis in terms of the contributions from charge–charge interactions to protein stability, *Biochemistry* 38, 8138-8149.
30. Pattison, D. I., Davies, M.J. (2001) Absolute rate constants for the reaction of hypochlorous acid with protein side chains and peptide bonds, *Chem. Res. Toxicol.* 14, 1453-1464.
31. Ashby, M. T., Beal, J.L., Foster, S.B. (2009) Hypochlorous acid reacts with the N-terminal methionines of proteins to give dehydromethionine, a potential biomarker for neutrophil-induced oxidative stress, *Biochemistry* 48, 11142–11148.
32. Simpson, R. J. (2003) *Proteins and proteomics: A laboratory manual*, New York: Cold Spring Harbor
33. Hawkins, C. L., Davies, M.J. (2005) Inactivation of protease inhibitors and lysozyme by hypochlorous acid: role of side-chain oxidation and protein unfolding in loss of biological function, *Chem. Res. Toxicol.* 18, 1600-1610.
34. Gottardi, W., Nagl, M. (2005) Chlorine covers on living bacteria: the initial step in antimicrobial action of active chlorine compounds., *J. Antimicrob. Chemother.* 55, 475-482.

35. Thomas, E. L., Grisham, M. B., and Jefferson, M. M. (1986) Preparation and characterization of chloramines, *Methods Enzymol.* 132, 569-585.
36. Hawkins, C. L., Pattison, D.I., Davies, M.J. (2003) Hypochlorite-induced oxidation of amino acids, peptides and proteins, *Amino Acids* 25, 259-274.
37. Pattison, D. I., Hawkins, C. L., Davies, M. J. (2007) Hypochlorous acid-mediated protein oxidation: how important are chloramine transfer reactions and protein tertiary structure?, *Biochemistry* 46, 9853–9864.
38. Hazen, S. L., d'Avignon, A., Anderson, M. A., Hsu, F. F., Heinecke, J. W. (1998) Human neutrophils employ the myeloperoxidase-hydrogen peroxide-chloride system to oxidise alpha-amino-acids to a family of reactive aldehydes: mechanistic studies identifying labile intermediates along the reaction pathway, *J. Biol. Chem.* 273, 4997-5005.
39. Hawkins, C. L., Davies, M. J. (1999) Hypochlorite-induced oxidation of proteins in plasma: Formation of chloramines and nitrogen-centred radicals and their role in protein fragmentation, *Biochem. J.* 340, 539–548.
40. Hazen, S. L., Hsu, F. F., d'Avignon, A., Heinecke, J. W. (1998) Human neutrophils employ myeloperoxidase to convert alpha-amino acids to a battery of reactive aldehydes: A pathway for aldehyde generation at sites of inflammation, *Biochemistry* 37, 6864-6873.
41. Hawkins, C. L., Pattison, D.I., Stanley, N.R., Davies, M.J. (2008) Tryptophan residues are targets in hypothiocyanous acid-mediated protein oxidation *Biochem. J.* 416, 441-452.

CHAPTER 4: FORMATION OF STABLE ORGANIC DICHLORAMINES AND THEIR REACTIVITIES TOWARDS THIOLS AND OTHER ANTIOXIDANTS

4.1 Introduction

Hypochlorous acid (HOCl) is believed to be the main killing agent used by neutrophils during phagocytosis to eliminate invading bacteria (1). Proteins are the primary targets of HOCl due to their high concentrations (2-4). The rate constants for the reaction of HOCl with sulfur-containing side chains at pH 7.4 (e.g. cysteine ($k = 3.0 \times 10^7 \text{ M}^{-1}\text{s}^{-1}$) and methionine ($k = 3.8 \times 10^7 \text{ M}^{-1}\text{s}^{-1}$)) and for amino groups (e.g. lysine and histidine) ranges between $k > 10^3 - 10^5 \text{ M}^{-1}\text{s}^{-1}$ (5). Chloramines, the intermediates of the reaction of HOCl with amines retain the oxidizing ability of HOCl (6-10). Depending on the conditions, the reaction of HOCl with the amines produces monochloramines (RNHCl) and/or dichloramines (RNCl₂).

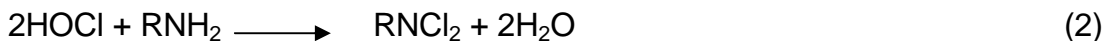
It has been more than 40 years since it was first discovered that oxidants, including chloramines play an important role in the human defense system (11-12). Chloramines have since been recognized both for their ability to kill bacteria and also to regulate the inflammatory response. In 1930, the dichloramine of glycine was reported as efficient in the killing of *Bacillus anthracis* spores (13). To date, there have been a number of published studies describing the antibacterial and antifungal activities of chloramines (14-20). It wasn't until the

1990s that it was discovered that at sub-lethal levels, monochloramines down-regulated proinflammatory chemokines, cytokines and enzymes (21-24).

Taurine (2-aminoethanesulfonic acid, $\text{H}_2\text{NCH}_2\text{CH}_2\text{SO}_3\text{H}$) is abundant in mammalian tissue with concentrations of 22 mM in neutrophils and 26 mM in leukocytes (25). In neutrophils, taurine forms about 50% of the amino acid pool (26). Among its various physiological functions, it is believed to be a scavenger for HOCl produced by the myeloperoxidase- $\text{H}_2\text{O}_2\text{-Cl}^-$ system (25). N-chlorotaurine (TauCl) is the main product of the reaction of taurine with HOCl under physiological conditions. TauCl is milder, long-lived and more selective oxidant than HOCl and thus its formation is a mechanism by which cellular components are protected against an indiscriminant, more powerful oxidant i.e. HOCl (27). Due to its unique characteristics (including its high concentration and superior stability), TauCl is considered a good representative of monochloramines (28-29).



In addition to monochloramines, dichloramines (e.g. N-dichlorotaurine, TauCl_2) can be formed. Two pathways for formation of dichloramines are oxidation of taurine by excess HOCl and disproportionation of TauCl. In the presence of excess amounts of HOCl (HOCl:amine ratio ≥ 2), the reaction produces quantitative amounts of N-dichloramines at $5.0 \leq \text{pH} \leq 8$ (5, 30-31).

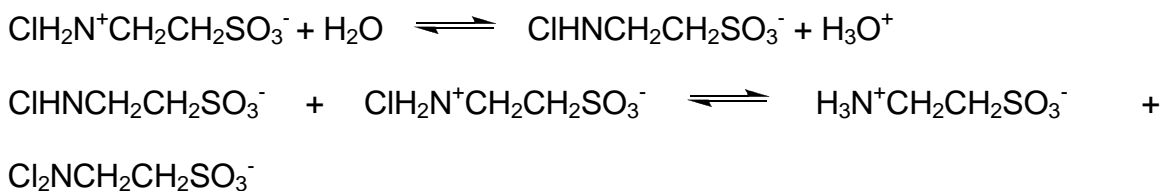


Under acidic (pH < 6.0) conditions monochloramines disproportionate to dichloramines.



Zgliczynski et al. were the first investigators of TauCl that noticed its tendency to disproportionate to TauCl₂ and taurine (32). A detailed kinetic study for the reversible disproportionation reaction of TauCl was later conducted by Antelo et al. (5). Prior studies by several authors on disproportionation reactions have proposed a 2 step mechanism (Scheme 1), including the protonation of TauCl in a pre-equilibrium step followed by the reaction of the protonated chloramine with an unprotonated form to give the corresponding TauCl₂ and taurine (33-35).

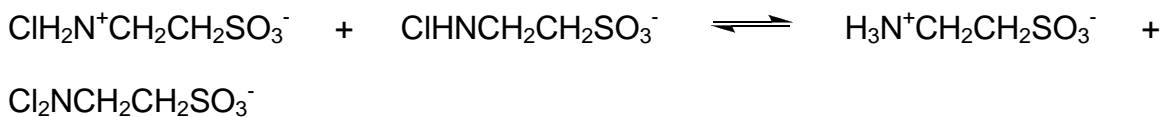
Scheme 1



Antelo et al. proposed that contrary to prior reports, the disproportionation of TauCl occurs by a concerted mechanism in which the proton and chlorine transfer takes place simultaneously in the transition state (Scheme 2) (5). This

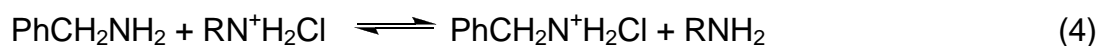
conclusion was reached after observing that the reaction of protonated TauCl₂ with TauCl was subject to general base catalysis. This observation indicates that the mechanism is stepwise and involves a fast equilibrium reaction to give the protonated TauCl₂ intermediate, followed by a slow proton transfer to the medium. However, Antelo et al. argued that since protonated TauCl₂ is extremely acidic with a pK_a of approximately -10 (5), its deprotonation in aqueous solutions would be diffusion-controlled. This implies that the proposed TauCl₂ intermediate is too unstable to have a significant lifetime in aqueous solutions which supports a concerted mechanism in which deprotonation of a neutral chloramine molecule occurs simultaneously with chlorine transfer.

Scheme 2



It was reported that the second-order rate constant for disproportionation was $1.51 \times 10^2 \text{ M}^{-1}\text{s}^{-1}$ pH 7.4 and equilibrium constant was $1.10 \times 10^6 \text{ M}^{-1}$ pH 1.8 - 9. Following a successful synthesis of pure crystalline sodium salt of N-chlorotaurine (ClHNCH₂CH₂SO₃Na), Gottardi and Nagl investigated its chemical properties including disproportionation (36). A new equilibrium constant for the disproportionation reaction of $4.50 \times 10^6 \text{ M}^{-1}$ at pH < 7 was reported. The rate constants for the reaction of N-chlorotaurine with nucleophiles (e.g. thiols) have been reported (1, 37), however the kinetic information involving dichloramines is

missing. Without measuring the actual rate constants, Thomas et al. (38) observed that RNCl_2 reacted rapidly with thiols and Gottardi and Nagl were surprised to observe that RNCl_2 was less efficient at chlorinating other amines compared to RNHCl (39). The observed lower potency of RNCl_2 was attributed to mechanistic effects. The reactive species for the reaction of RNHCl with RNH_2 is $\text{RN}^+\text{H}_2\text{Cl}$ (39).



In the case of RNCl_2 , the authors believe that the presence of the two chlorine atoms on the same nitrogen, creates a high enough partial positive charge on the nitrogen thus negating the need to form the protonated reactive species $\text{RN}^+\text{Cl}_2\text{H}$. In a recent publication, Coker et al. investigated the stability and bactericidal activity of dichloramines likely to be formed within the phagosome (40). It was found that most were unstable (except those of lysine and taurine) and decomposed to give cytotoxic inorganic monochloramine (NH_2Cl) and dichloramine (NHCl_2). It was then proposed that this is probably one of the mechanisms by which HOCl kills ingested bacteria. The inorganic chloramines are lipophilic and thus can diffuse easily from the neutrophil and damage the host tissue. However, the study did not discuss the fate of the stable dichloramines (dichlorotaurine and dichlorolysine), but speculated that they eventually decompose via metal-catalyzed reactions to form radicals.

4.2 Results and discussion

4.2.1 The chemical stability of dichloramines

The stability of various small peptide dichloramines were investigated recently by Coker et al. (40). The compounds that were investigated include alanine, aspartate, glutamate, glycine, N- α -acetyl lysine and taurine. By monitoring changes in the UV maxima of dichloramines around 300 nm they were able to measure the half-lives for the decomposition of these dichloramines (Table 4.1).

Table 4.1: Stabilities of monochloramines and dichloramines at pH 7.4

<i>Amine</i>	<i>TauCl₂</i> <i>half-life(min)</i>	<i>TauCl</i> <i>half-</i> <i>life(min)</i>
Alanine	61	<0.3
Aspartate	14	<0.3
Glutamate	38	<0.3
Glycine	>> 120	14
Lysine	>>120	>>120
Taurine	>>120	>>120

The stabilities of chloramines were determined by monitoring changes in their UV absorption spectrum recorded every minute. In each case, 1 mM chloramine in PBS at pH 7.4 was used and the half-lives ($t_{1/2}$) were estimated from their decay curves. No rate law was proposed for the decomposition data.

We confirmed their observation in this study by monitoring the stability of dichlorotaurine (TauCl₂) at pH 7.4. No absorbance change at 300 nm (which indicates high stability) was observed over a period of 5 hours. Gottardi and Nagl observed that acidic solutions (pH \leq 5.0) of dichlorotaurine had a half-life of over

30 days (39). The relatively high stability of dichlorotaurine warrants further investigation as to its eventual fate *in vivo*.

4.2.2 Reactions of TauCl₂ with thiols, ascorbate, methionine, and lysine

Gottardi and Nagl were surprised to observe that dichlorotaurine was a poorer trans-halogenating agent than chlorotaurine (39). We investigated its reactivity towards other important biological molecules such as thiols, methionine, ascorbate, and lysine. 5-thio-2-nitrobenzoic acid (TNB) was selected as a model compound for thiols in this study because of its high extinction coefficient ($\epsilon = 14,150 \text{ M}^{-1}\text{cm}^{-1}$ at 412 nm). Much like TNB, ascorbate has a large extinction coefficient ($\epsilon = 14700 \text{ M}^{-1}\text{cm}^{-1}$) at 265 nm. The second-order rate constants for the reaction of TNB and ascorbate with TauCl₂ at various pH conditions were measured directly using the stopped-flow technique by following changes in absorbance at 412 and 256 nm respectively (Figure 4.1 and 4.2). The rate constant obtained at pH 7.4 for the reaction of TauCl₂ with TNB reaction was later used in subsequent competition experiments to determine the rate constant(s) of the other nucleophiles which unlike TNB do not have a strong absorbance. The reaction of excess TauCl₂ with TNB exhibited pseudo-first-order kinetic behavior and the fitting of the data to a single-exponential function allowed for the calculation of pseudo-second-order (pH-dependant) rate constants at pH 7.4) given in Table 4.2. The low pH measurements were included in this work to represent what might happen in the phagosome as the pH drops (41-44).

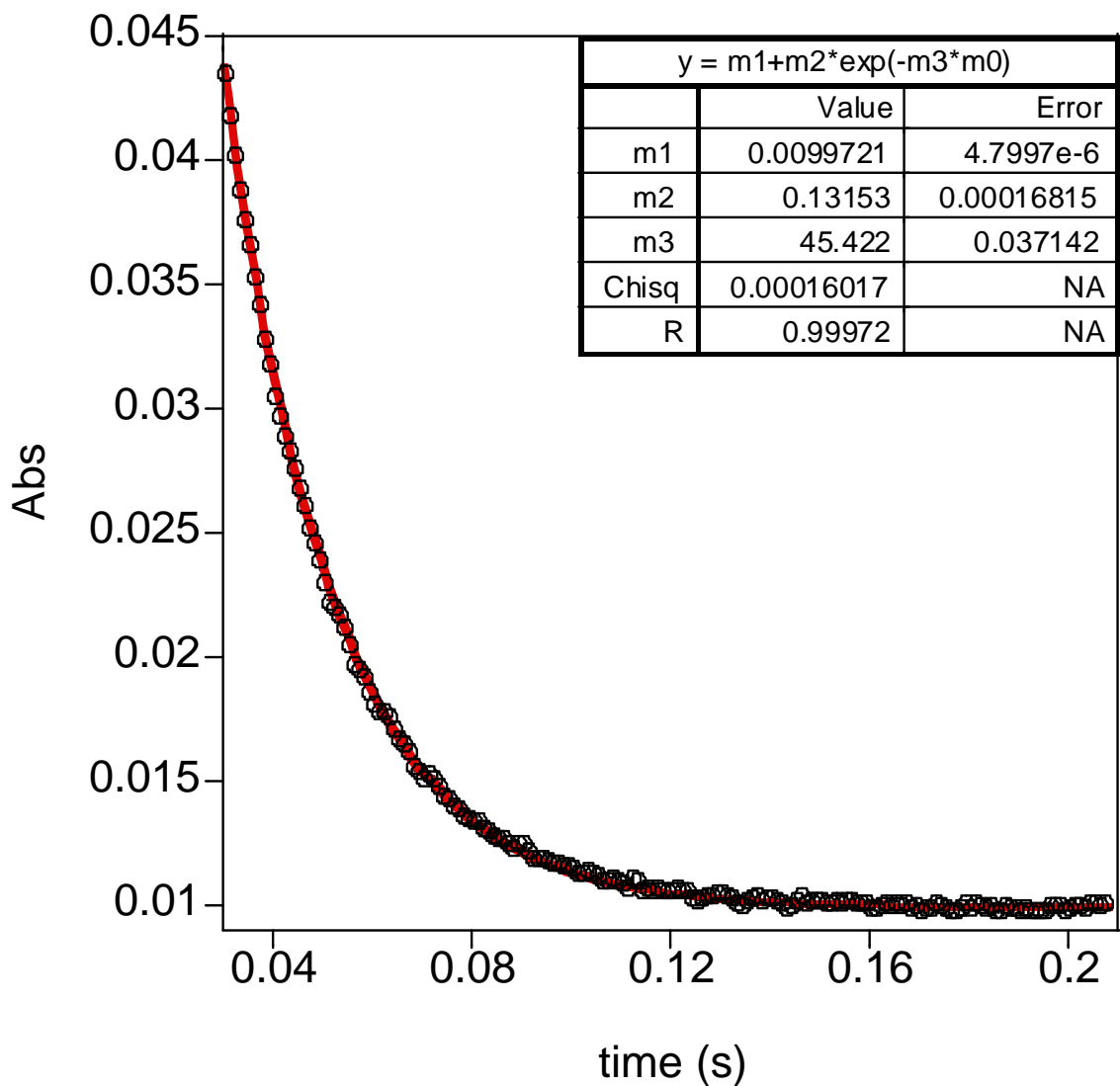


Figure 4.1. Observed absorbance decrease at 412 nm for the reaction of TauCl_2 (40 μM) with TNB (4 μM) at pH 7.4 and $I = 1.0$ M. A first-order fit (red) and 10% of the data (black circles) are illustrated.

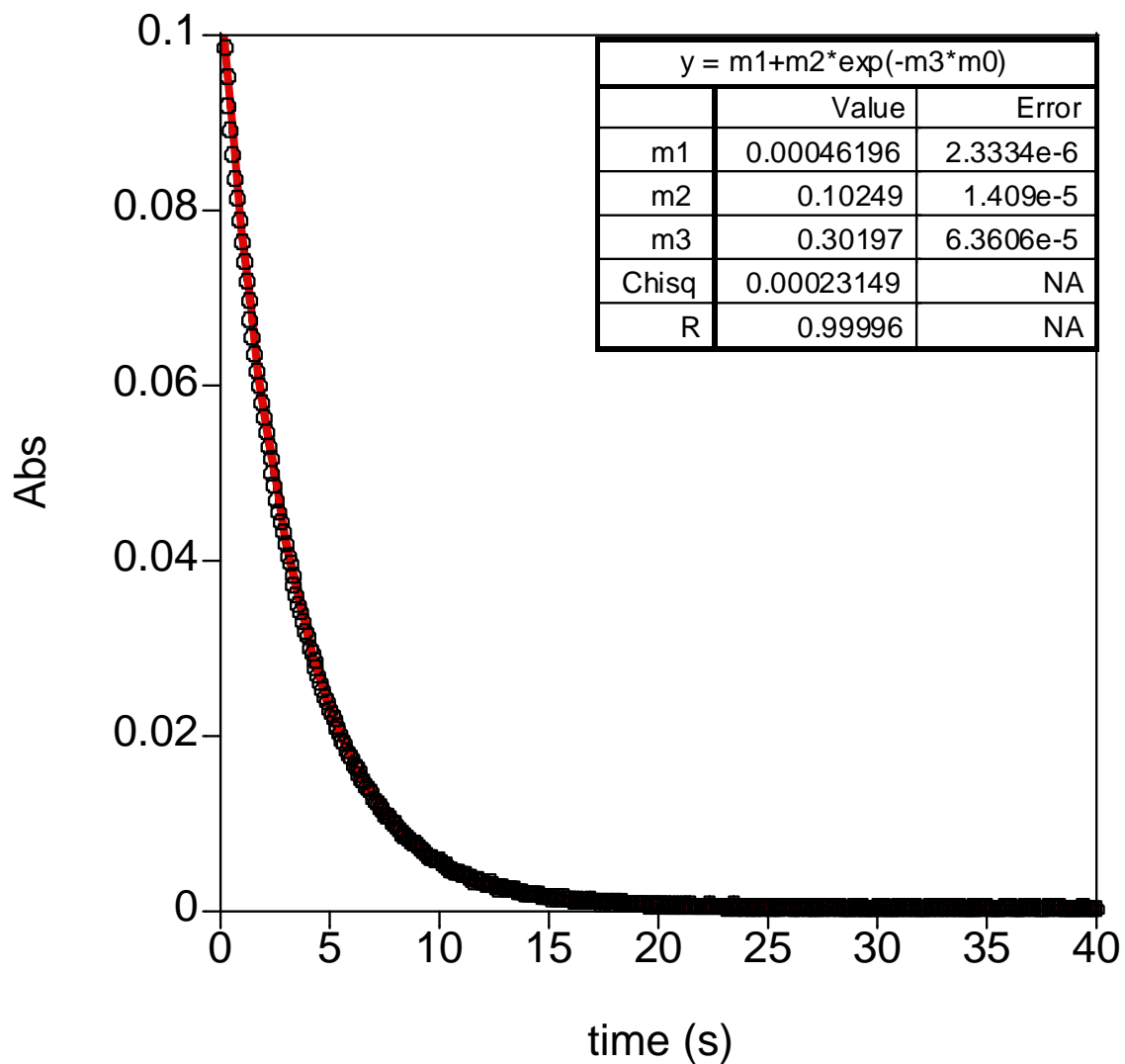


Figure 4.2. Observed absorbance decrease at 265 nm for the reaction of TauCl_2 (200 μM) with ascorbic acid (16 μM) at pH 7.4 and $I = 1.0$ M. A first-order fit (red) and 10% of the data (black circles) are illustrated.

The rate constants for the reaction of TauCl_2 with the other nucleophiles (nu) were estimated by competition kinetics with TNB as a competing substrate. The concentration of each competitive nucleophile was varied while that of TNB was kept constant. At the point where the absorbance of TNB remains constant, the rates of the reaction of TauCl_2 with TNB and the nucleophile are presumed to be the same and thus the following equation was used to determine the rate constant of the nucleophile:

$$k_{(\text{nu})} [\text{nucleophile}] = k_{(\text{TNB})} [\text{TNB}] \quad (5)$$

Knowing the rate constant of TNB allowed for the rate constant(s) of TauCl_2 with the other nucleophiles to be estimated. Not surprising, the amino groups (which are relatively poor nucleophiles) were less reactive than thiols (good nucleophiles). The relatively poor reactivity of TauCl_2 towards methionine compared to thiols was unexpected (Table 4.2).

Table 4.2: Pseudo-second-order rate constants for the reactions of TauCl_2 with thiols, methionine, ascorbate, and lysine at pH 7.4.

<i>Nucleophile</i>	<i>pKa</i>	<i>HOCl</i>	<i>TauCl₂</i>	<i>TauCl</i>
TNB	4.38	-	1.1×10^6	970
Ascorbate	-	-	1.0×10^3	13
Methionine	9.21	3.8×10^7	102	39
N-acetyl lysine	-	5.0×10^3	67	nd
S-methyl glutathione	-	-	164	nd
S-methyl cysteine	-	-	110	nd
N-acetyl cysteine	9.7	-	1.8×10^5	46
Dithiothreol	9.3	-	1.8×10^5	48
Cysteine	8.3	3.0×10^7	1.3×10^6	205
Glutathione	8.7	-	1.3×10^6	115

*nd= not determined

4.2.3 pH dependency of the reaction of TauCl_2 with TNB and ascorbate

The effect of pH on the rates of reaction of ascorbic acid and TNB with TauCl_2 were investigated between pH 5.5 and pH 8.0. In all cases, phosphate buffer was used to control the pH and the concentrations of TNB and ascorbic acid were kept constant at 4 and 16 μM respectively. As can be seen in a sample trace (Figure 4.1 and 4.2), only one reaction was observed under the conditions of excess TauCl_2 . Although the rates of oxidation of both ascorbate and TNB showed a dependency on the pH, differences in terms of the trend were observed. Over the pH 7.5-6.5 range, an inverse relationship between k ($k=k_{\text{obs}}/[\text{TauCl}_2]$) and the pH was observed for the reaction with TNB (Figure 4.3). The kinetic traces are given in Figure 4.4-4.7. These results are not surprising

since the reaction of TNB with chloramines (TauCl and TauCl₂) is believed to proceed via nucleophilic substitution. At pH > 6.5, TNB is expected to be present entirely as the thiolate (pK_a (SH) = 4.38) which is a good nucleophile.

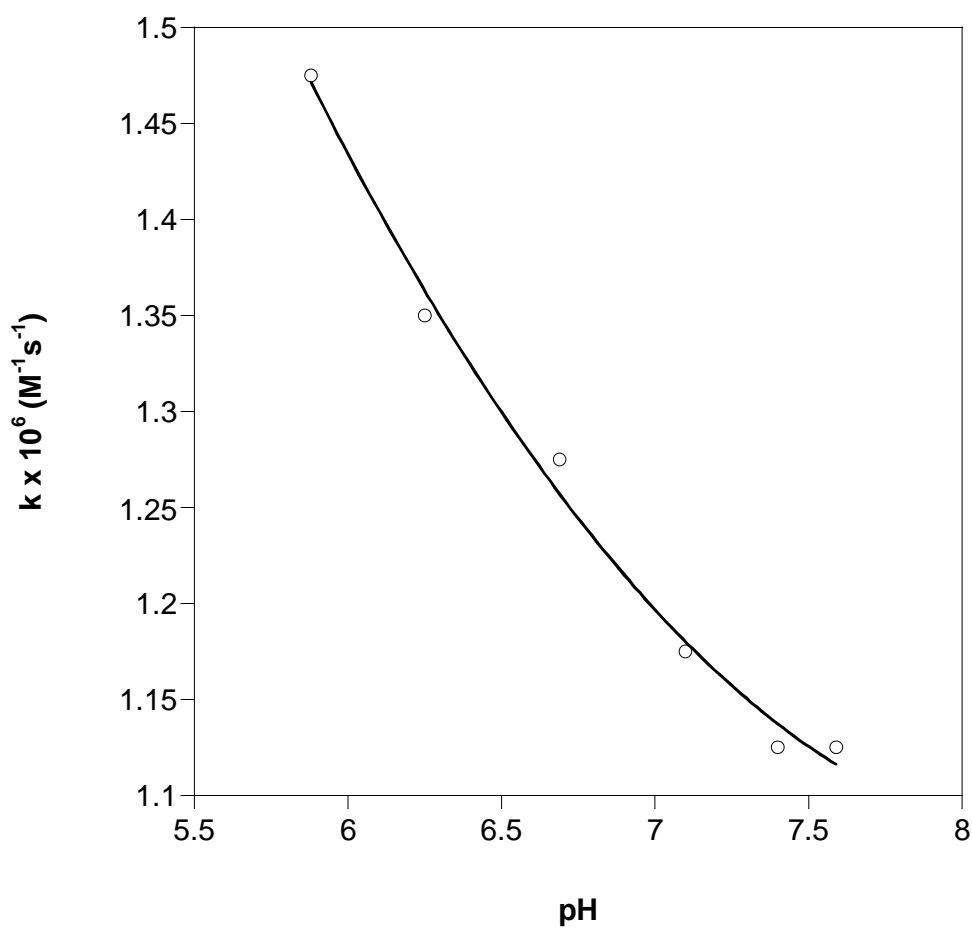


Figure 4.3. pH-rate profile for the reaction of TauCl₂ with TNB

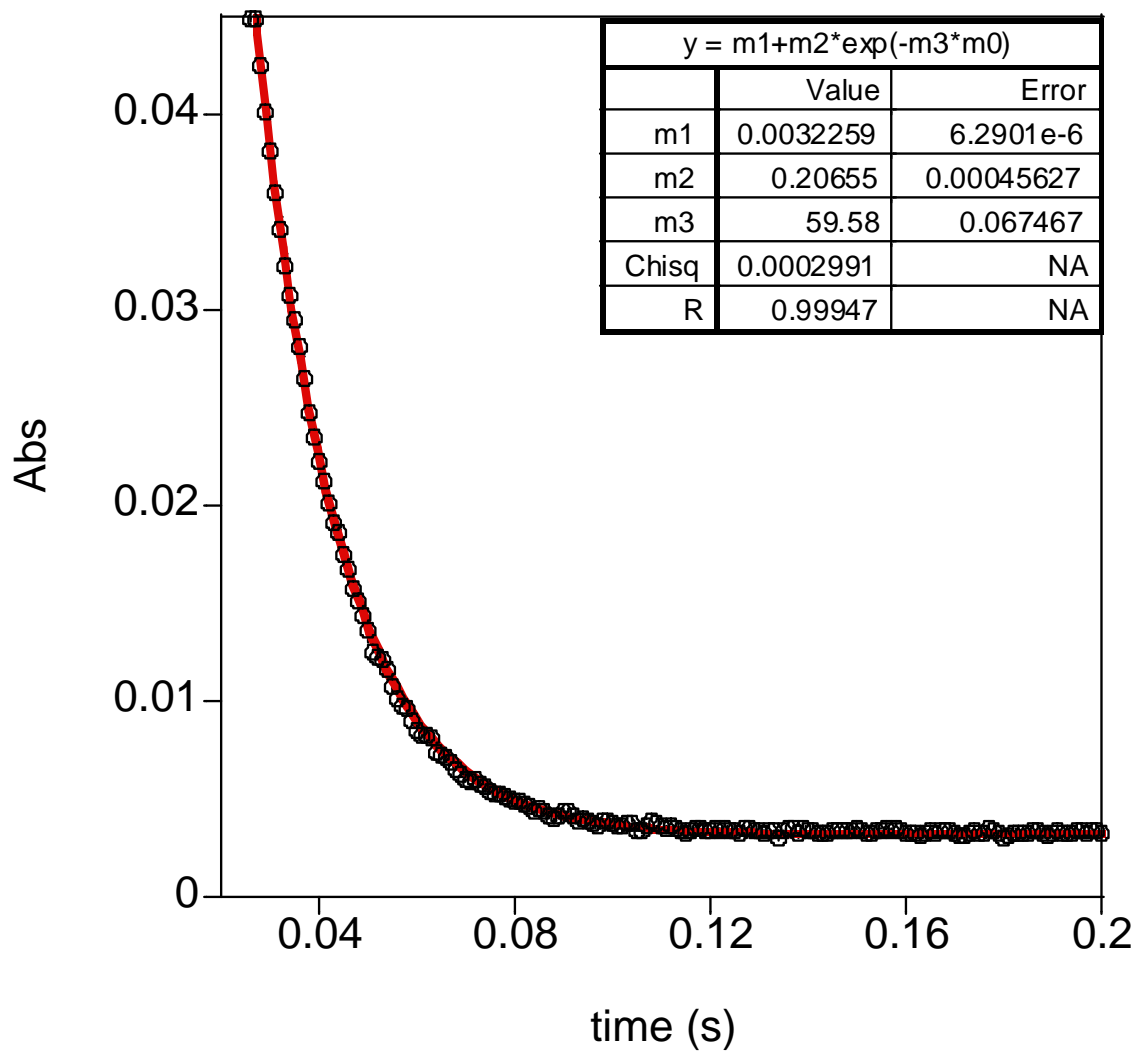


Figure 4.4. Observed absorbance decrease at 412 nm for the reaction of TauCl_2 (40 μM) with TNB (4 μM) at pH 5.9 and $I = 1.0$ M. A first-order fit (red) and 10% of the data (black circles) are illustrated.

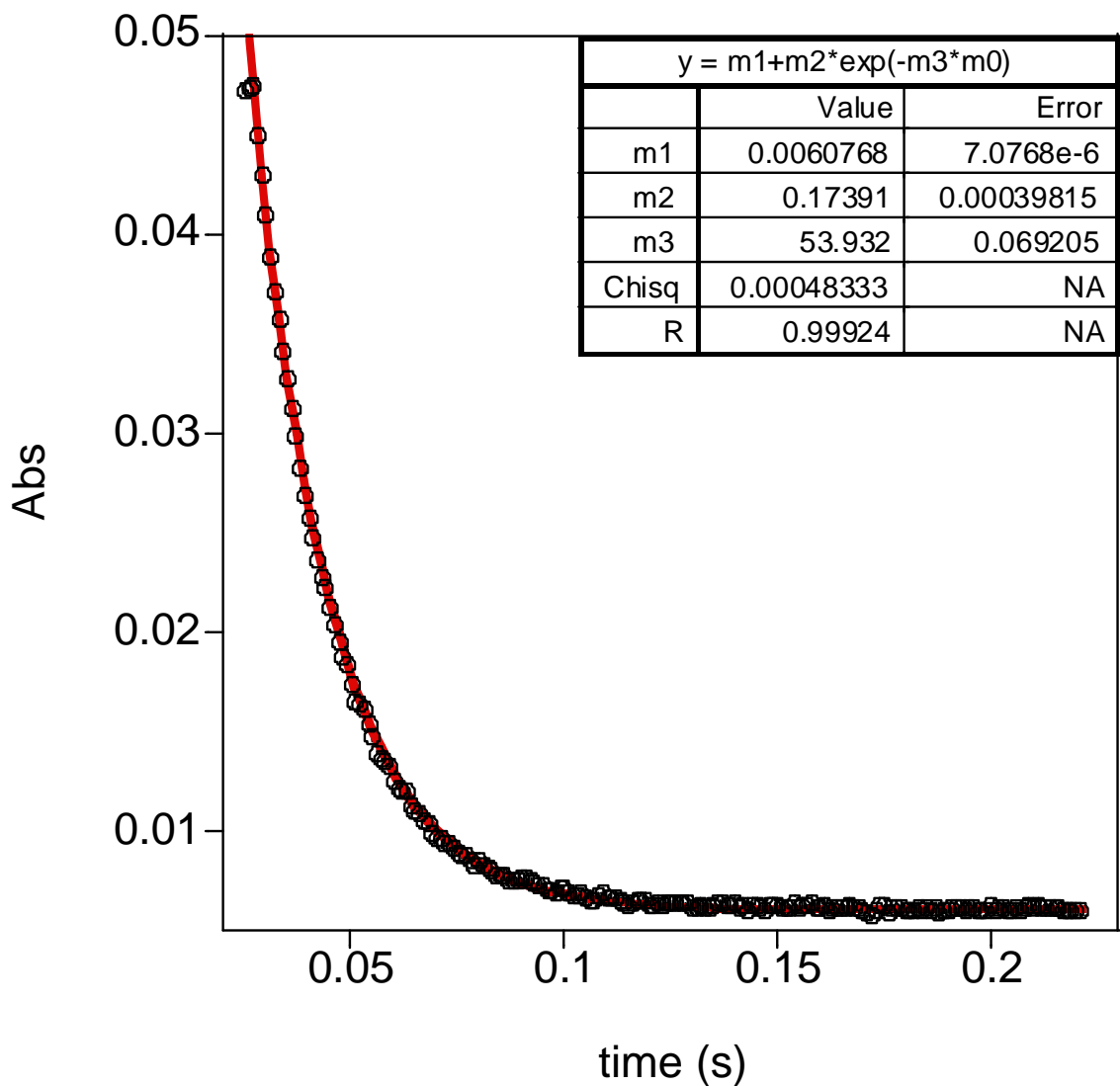


Figure 4.5. Observed absorbance decrease at 412 nm for the reaction of TauCl_2 (40 μM) with TNB (4 μM) at pH 6.2 and $I = 1.0$ M. A first-order fit (red) and 10% of the data (black circles) are illustrated.

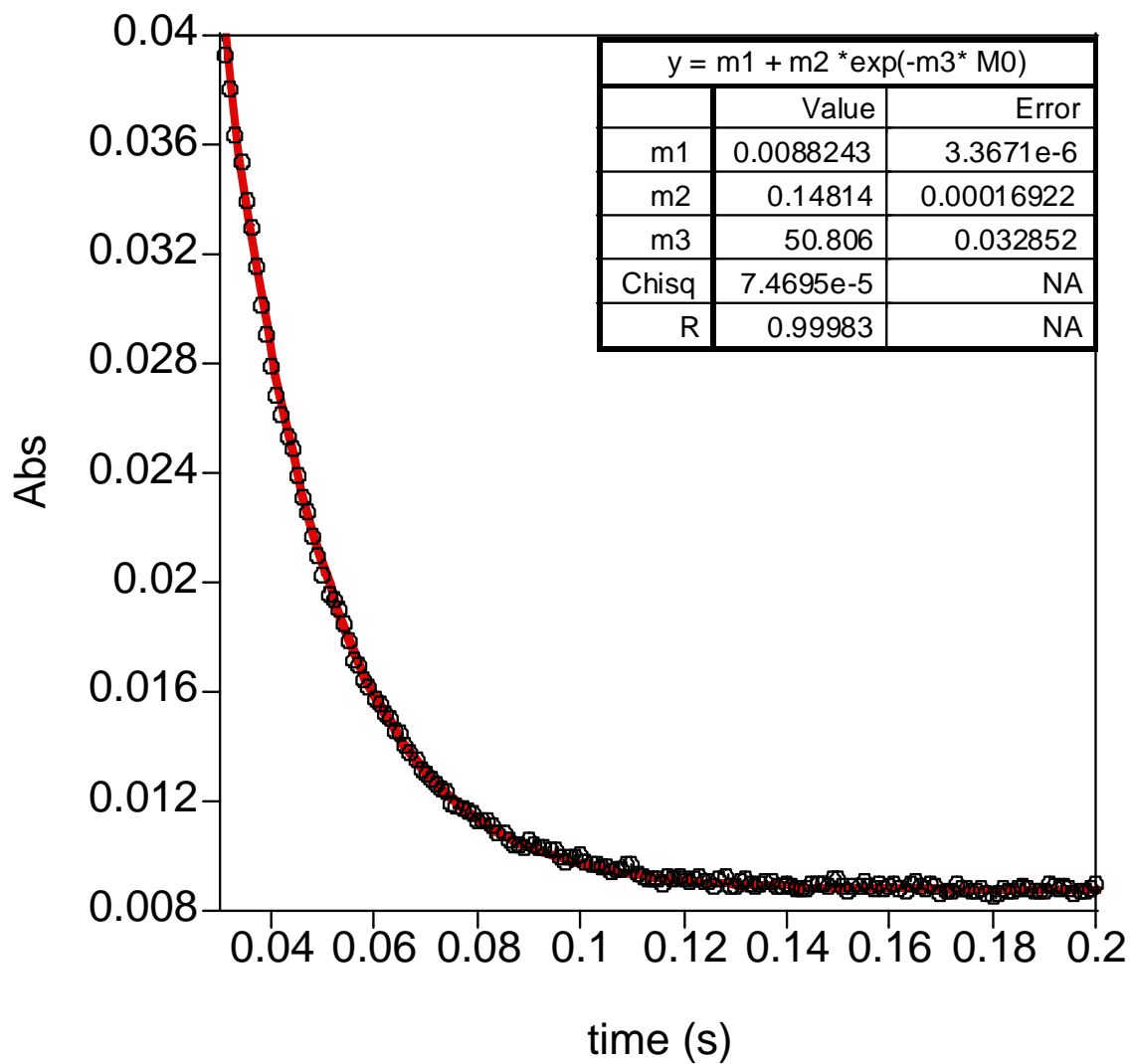


Figure 4.6. Observed absorbance decrease at 412 nm for the reaction of TauCl_2 (40 μM) with TNB (4 μM) at pH 6.7 and $I = 1.0$ M. A first-order fit (red) and 10% of the data (black circles) are illustrated.

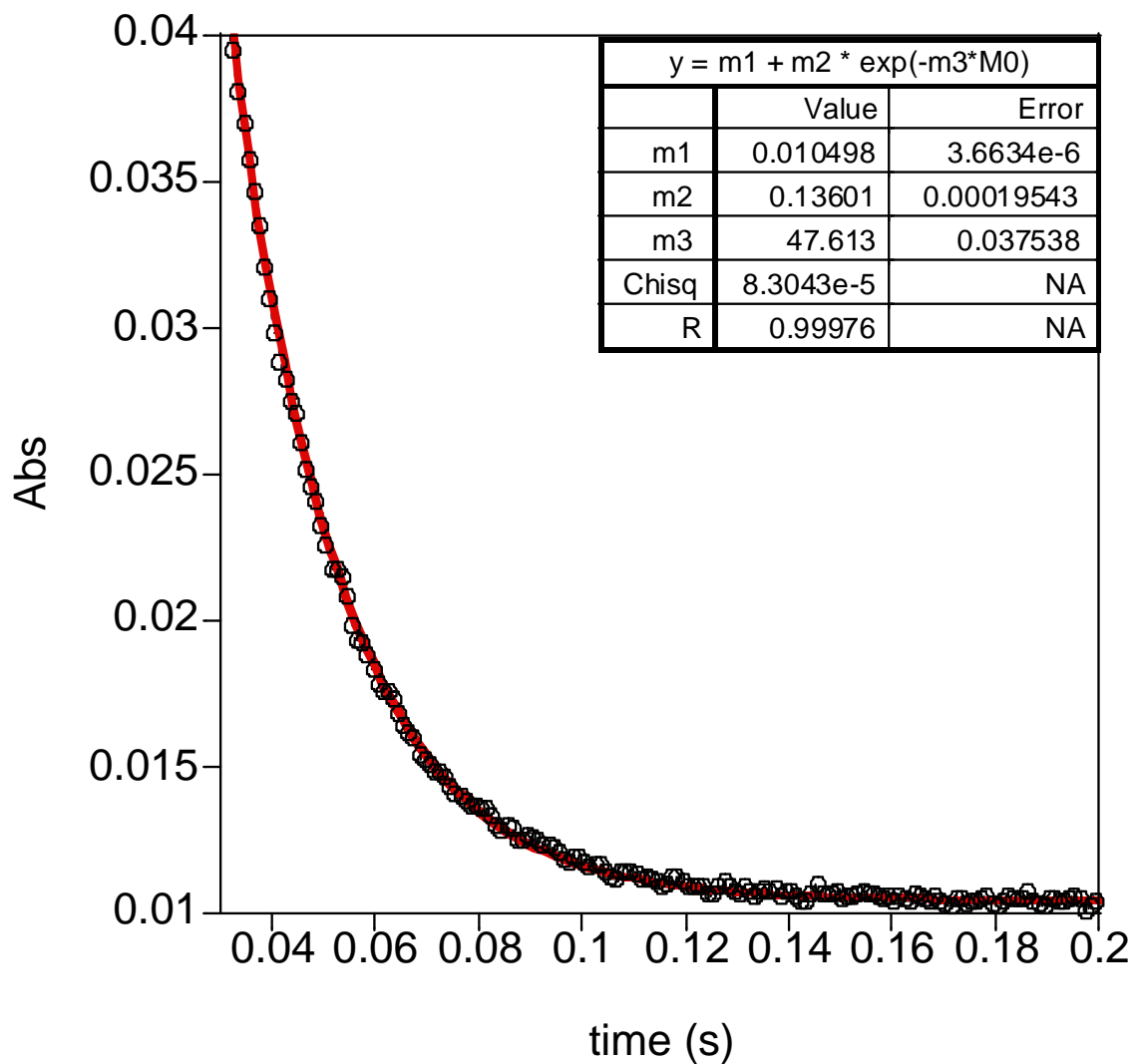


Figure 4.7. Observed absorbance decrease at 412 nm for the reaction of TauCl_2 (40 μM) with TNB (4 μM) at pH 7.1 and $I = 1.0$ M. A first-order fit (red) and 10% of the data (black circles) are illustrated.

Ascorbic acid has two pK_a values of 4.15 and 11.4 (for pK_1 and pK_2 respectively). This means that depending on the pH, there is a maximum of three species that are present as a function of pH including H_2A , HA^- and A^{2-} (equation 6 and 7).



The three species rank as follows $H_2A < HA^- \ll A^{2-}$ in terms of their nucleophilicity. It is reported in the literature that at $pH > 6.0$, HA^- and A^{2-} are the present forms of ascorbic acid. Within the pH range studied, a plot of k ($k=k_{obs}/[TauCl_2]$) vs. pH showed a direct relationship (Figure 4.8). The kinetic traces are given in Figure 4.9-4.12. This is expected since within the pH range of 7.5-6.5, the dominant species is HA^- which reacts with $TauCl_2$.

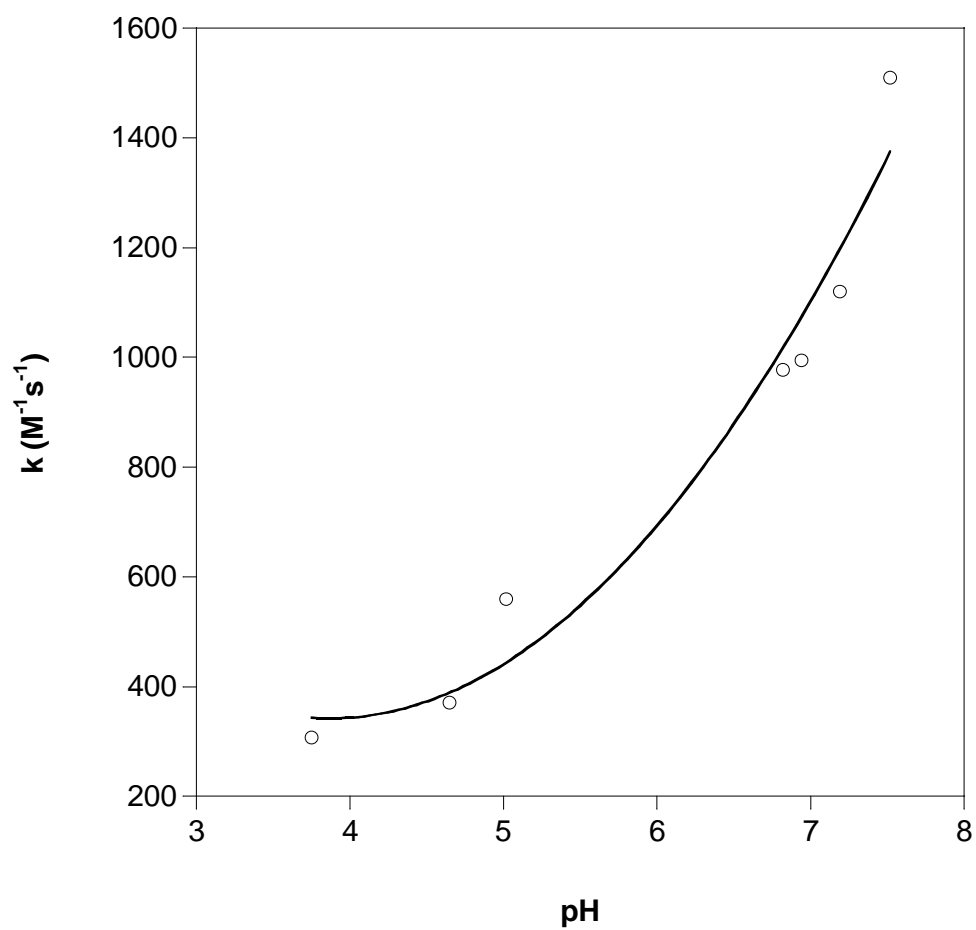


Figure 4.8. pH-rate profile for the reaction of TauCl_2 with ascorbate

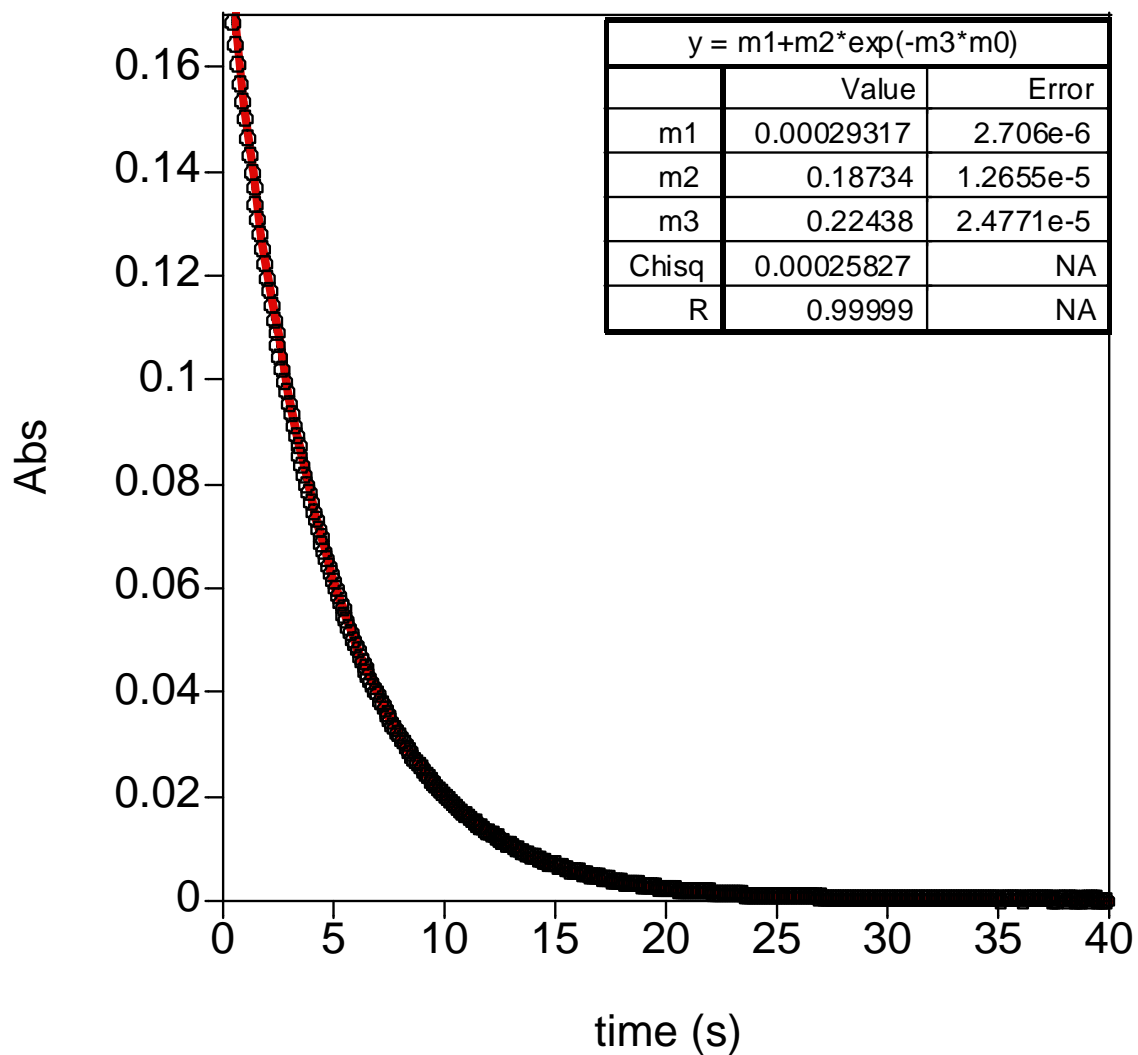


Figure 4.9. Observed absorbance decrease at 265 nm for the reaction of TauCl_2 (200 μM) with ascorbic acid (16 μM) at pH 7.2 and $I = 1.0$ M. A first-order fit (red) and 10% of the data (black circles) are illustrated.

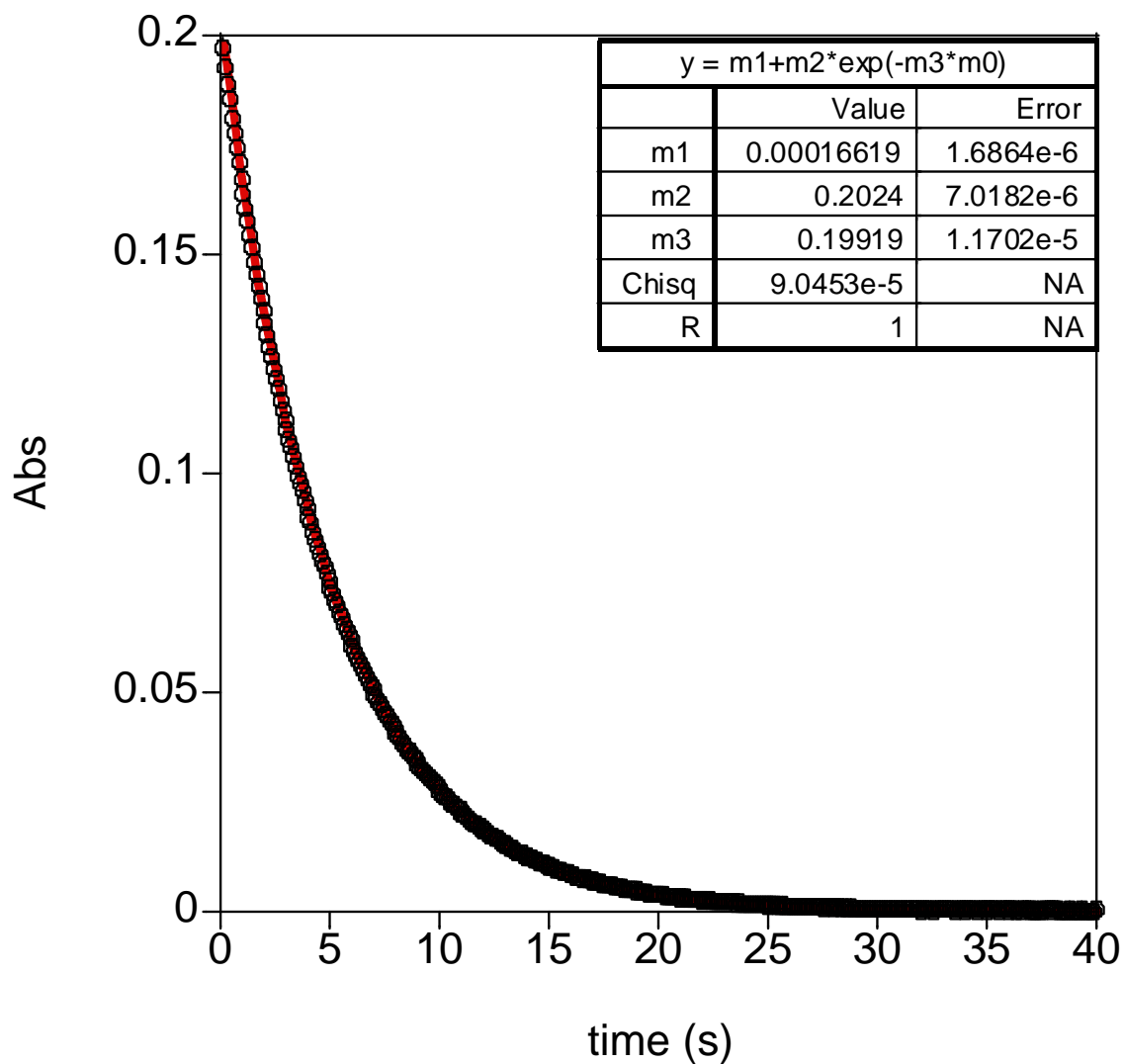


Figure 4.10. Observed absorbance decrease at 265 nm for the reaction of TauCl_2 (200 μM) with ascorbic acid (16 μM) at pH 6.9 and $I = 1.0$ M. A first-order fit (red) and 10% of the data (black circles) are illustrated.

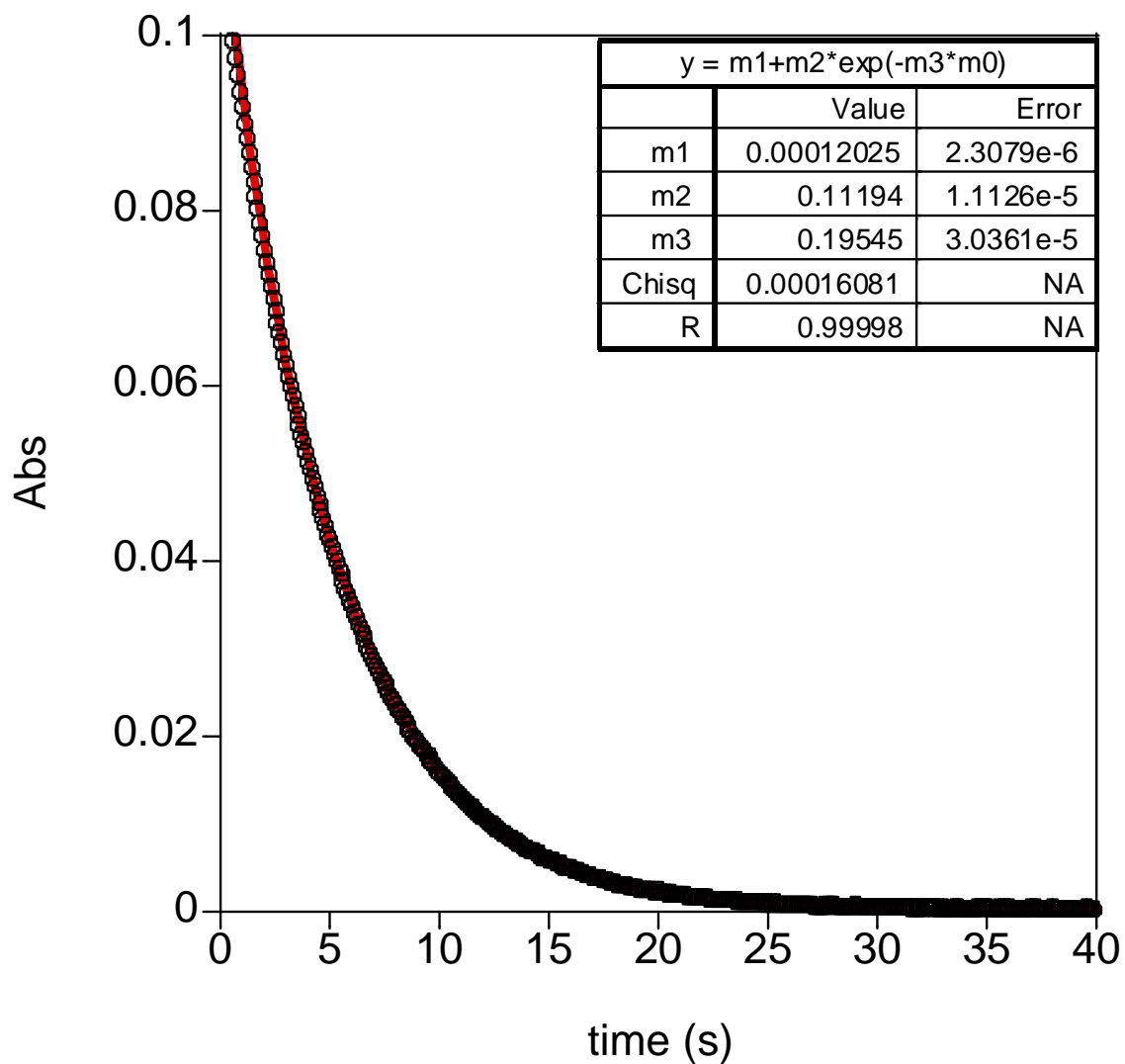


Figure 4.11. Observed absorbance decrease at 265 nm for the reaction of TauCl_2 (200 μM) with ascorbic acid (16 μM) at pH 6.8 and $I = 1.0$ M. A first-order fit (red) and 10% of the data (black circles) are illustrated.

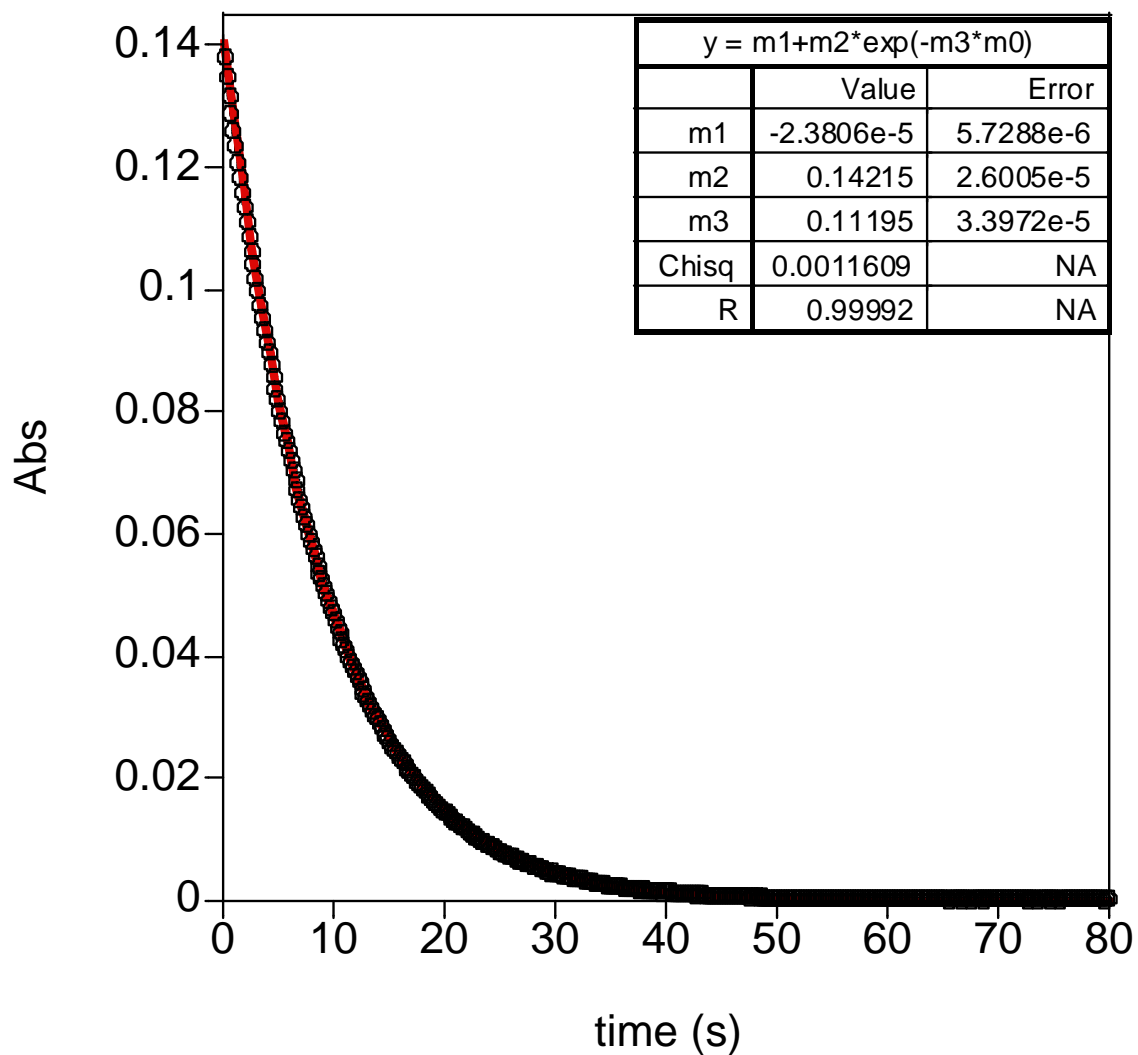


Figure 4.12. Observed absorbance decrease at 265 nm for the reaction of TauCl_2 (200 μM) with ascorbic acid (16 μM) at pH 5.0 and $I = 1.0$ M. A first-order fit (red) and 10% of the data (black circles) are illustrated.

4.2.4 Kinetics of the reaction of TauCl₂ with TNB

4.2.4.1 Concentration dependencies

To determine the rate law for the reaction of TauCl₂ with TNB, the reaction was followed under pseudo first-order conditions. In all cases, the obtained kinetic traces fitted to single exponential equations. Under conditions of excess [TauCl₂] over [TNB], a plot of [TauCl₂] versus k_{obs} exhibits a linear dependency on [TNB] (Figure 4.13). Similarly, a linear relationship was observed between [TNB] and k_{obs} when [TNB] was used in excess over [TauCl₂] (Figure 4.14). Although the linear fits in both cases do not pass through the origin, they do however demonstrate that the reaction is first-order in both reactants. The positive intercept in each plot is characteristic of a reversible reaction, probably indicating the equilibrium mixture of N,N-dichlorotaurine and N-chlorotaurine. The slopes of these linear correlations give the same second-order rate constants of $1.3 \pm 0.01 \times 10^6 \text{ M}^{-1}\text{s}^{-1}$ and $1.2 \pm 0.01 \times 10^6 \text{ M}^{-1}\text{s}^{-1}$ respectively.

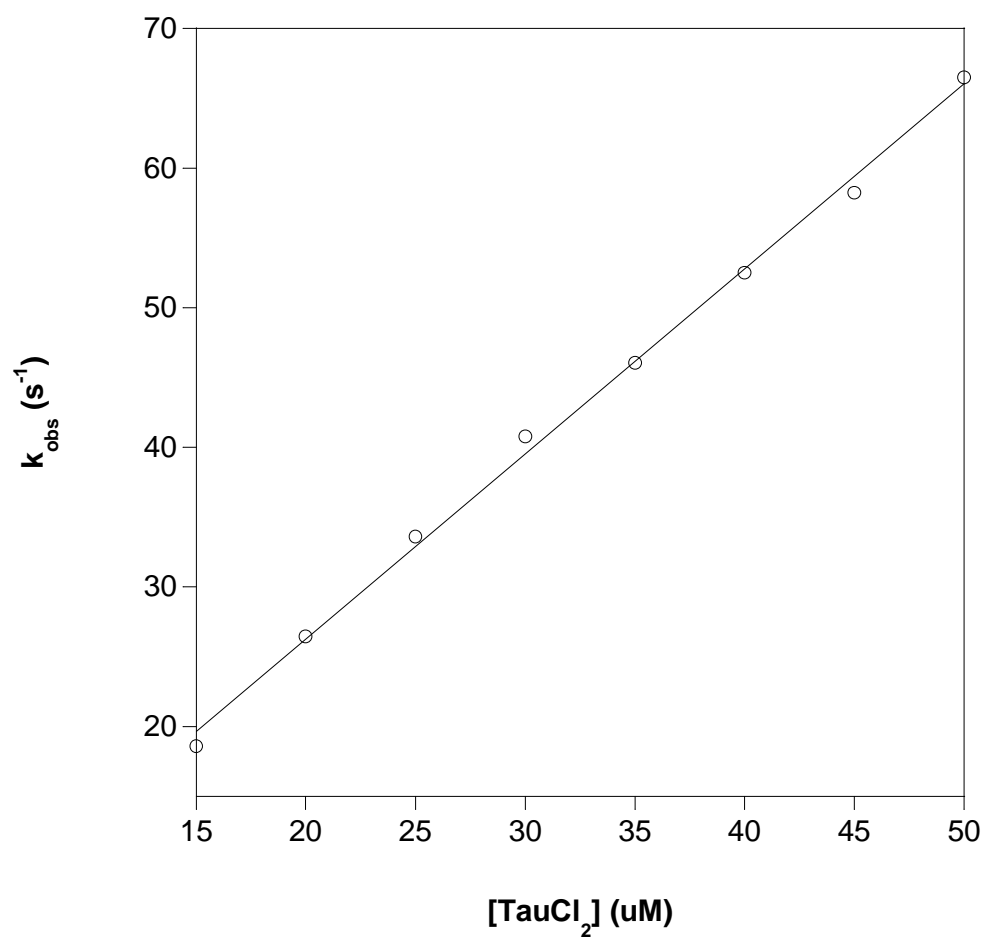


Figure 4.13. [TauCl₂] dependence of the rate law under pseudo-first order conditions.

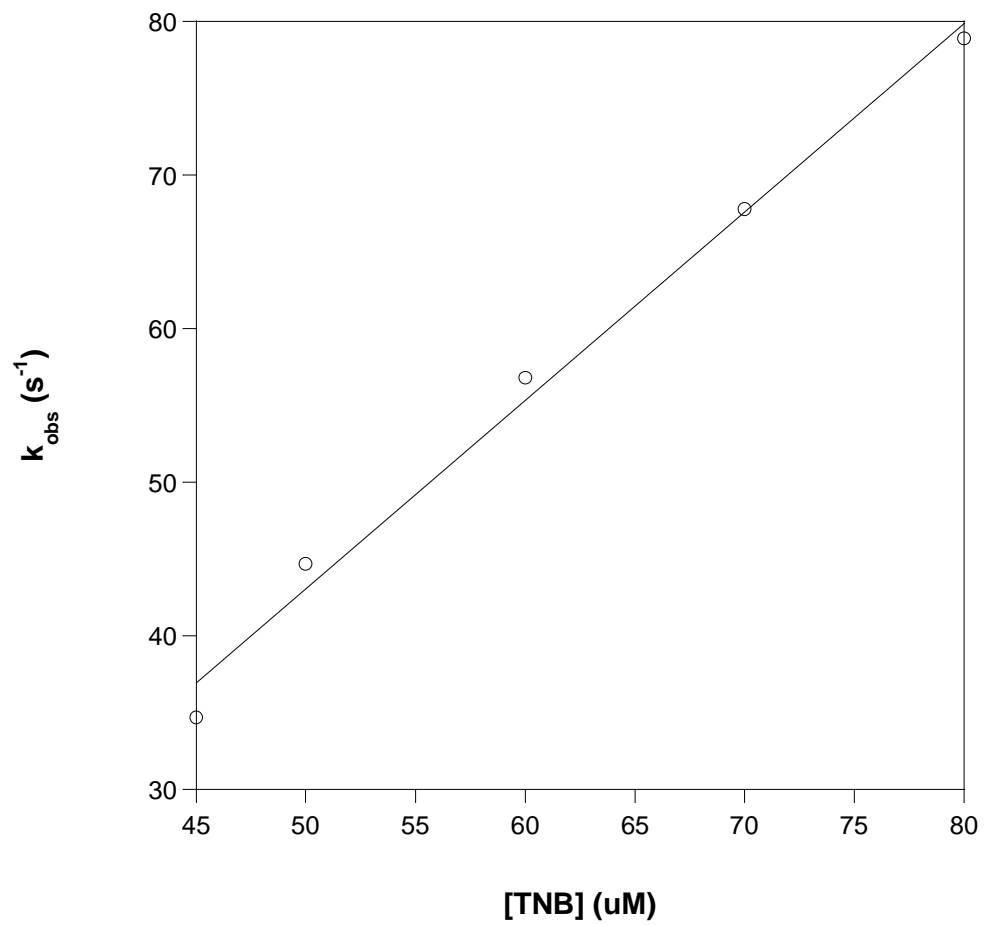


Figure 4.14. [TNB] dependence of the rate law under pseudo-first order conditions.

4.2.4.2 pH dependency

At pH > 5.5, a linear dependency on the $[H^+]$ was observed (Figure 4.15). Under these pH conditions, TNB is a good nucleophile (pK_a (SH) = 4.38) while $TauCl_2$ is a good electrophile. The drop in the rate with increasing pH is probably due to the decomposition of $TauCl_2$ to $TauCl$.

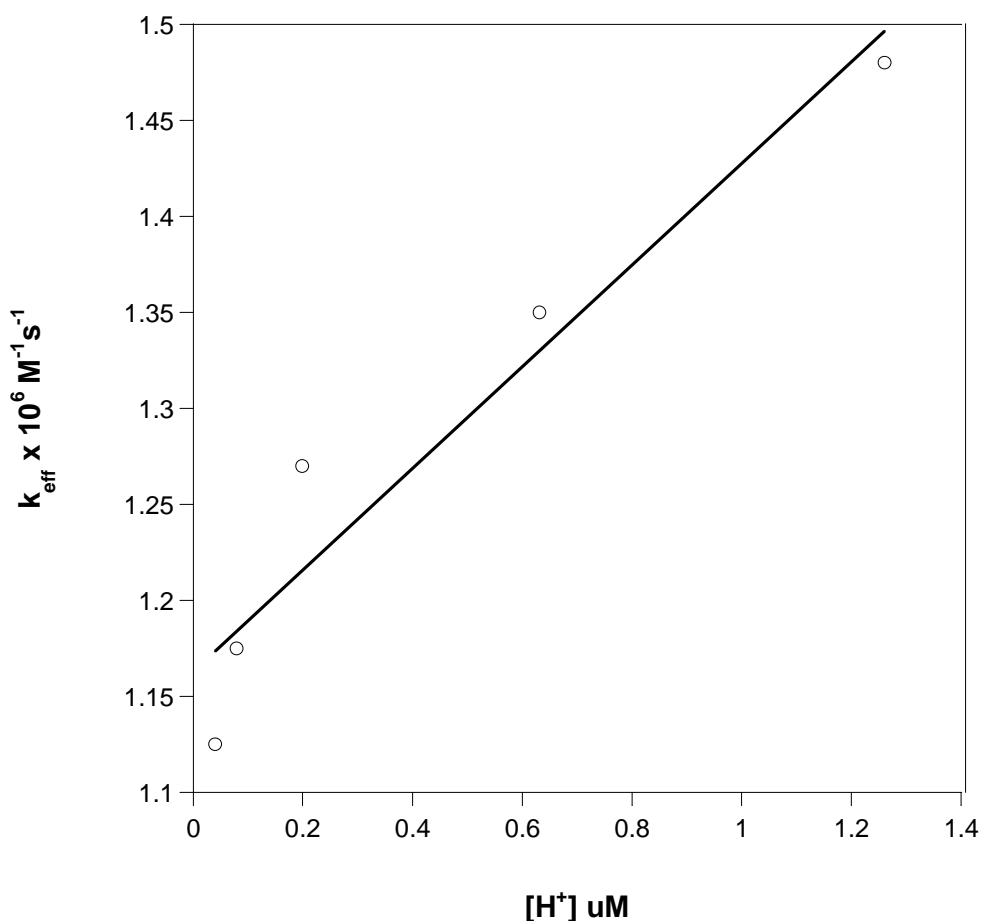
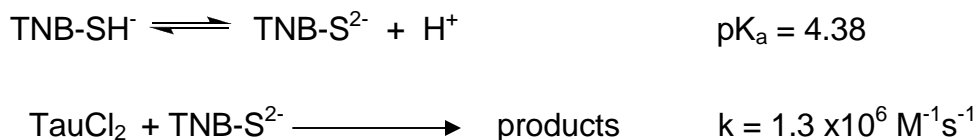


Figure 4.15. Dependence of the observed second-order rate constant k_{eff} ($\text{M}^{-1}\text{s}^{-1}$) for the reaction of $TauCl_2$ with TNB on $[H^+]$ at pH > 5.5

4.2.4.3 Proposed mechanism

Scheme 3: kinetics and mechanism of the oxidation of TNB with TauCl₂



4.2.5 Possible biological significance

We have shown in this study that dichlorotaurine (TauCl₂) is more reactive towards thiols and other biologically important compounds (e.g. ascorbic acid) than chlorotaurine (TauCl) under physiologically-relevant conditions. TauCl₂ reacts approximately 1000 times faster with thiols and about 100 times faster with ascorbate than TauCl at pH 7.4. It is conceivable that under conditions of oxidative stress, both mono- and dichloramines are formed. Surprisingly, unlike HOCl, TauCl₂ despite being more reactive towards thiols was found to be less reactive towards methionine. Evidence for the formation of dichloramines in isolated neutrophil granules that were treated with hydrogen peroxide was shown by Thomas et al. (30). In a recent publication, Gottardi et al. (39) reported that TauCl₂ was significantly more bactericidal than TauCl against gram-negative bacteria *E. coli*, *P. aeruginosa* and *P. mirabilis*.

Due to their hydrophilic nature, it has been suggested that chlorotaurines are restricted to the extracellular milieu which limits its potential cytotoxicity (45). Thomas et al. have shown that upon oxidation, the zwitterion taurine is converted to an organic anion (chlorotaurine and dichlorotaurine) which can be taken up by red blood cells through the anion transport system. After entering the cell, the chloramines react with glutathione (or other reductants) and are reduced back to taurine. When the taurine chloramine uptake exceeds red blood cell glutathione, cytotoxicity ensues (38). Cantin later reported that the respiratory secretions of patients with cystic fibrosis (CF) and other inflammatory disorders have high taurine concentrations (22). The source of the taurine is believed to be the neutrophils which are recruited to the site of inflammation. They showed that chlorotaurines were taken up by lung epithelial cells where TauCl_2 was observed to be most toxic (22). They concluded that taurine plays a role in protecting lung epithelial cells against MPO-derived oxidants such as HOCl through the formation of the less toxic monochlorotaurine. However, the protective effect is significantly decreased in the presence of excess HOCl and in acidic milieu due to the formation of the more reactive TauCl_2 .

It is suggested in the literature that phagocytosis is a highly complex and highly regulated process (44). Although it has been studied extensively, many of the previous studies have neglected to consider the various stages of phagocytosis (44). Broadly, it can be divided into three main processes including internalization, acidification and completion of phagosomal-endosomal fusion

(44). The actual changes in the intraphagosomal pH are still a subject of debate as studies continue to report conflicting results. Earlier studies that employed pH sensitive dyes agreed that the pH of the phagosome dropped significantly but varied on the extent of the pH reduction. It was noted that low pH enhances host defenses as it prevented microbial growth and also increases the activity of the degradative enzymes. Over 100 years ago, Metchnikoff observed using particulate litmus that the ingested organism inside the phagocyte changed from blue to red which meant that an acid reaction within the cell may have been responsible for the death of the ingested organism (46-47). Subsequently, Rous using mammalian leukocytes concluded that the intracellular pH may be as low as 3 (41-42). Later, Sprick (48), Pavlov and Solov'ev (49), Jacques and Bainton (50) found that while the intracellular pH falls, it does not drop as low as originally reported by Rous, but they found it to be pH 4.5-5.5. Jensen and Bainton (47) reported that following ingestion of yeast particles, the pH in rodent polymorphonuclear leukocytes (PMN) drops to 6.5 in 3 min and to 4.0 in 7-15 min. Jacques and Bainton (50) modest changes in pH (6.0-6.5) were also observed by Mandell (51) using human PMN over a period of two hours. Recently, some studies by Segal et al. (52), Geisow et al. (53), Cech and Lehrer (54) and Jiang et al (55) have found an initial rise in pH followed by a modest fall (pH 7.7 to 6.5). More recent studies by Griffiths and Mayorga (43) and Hiddessen et al. (44) confirmed the pH levels (4-5.5) reported by the earlier studies. While the intraphagosomal pH issue is yet to be fully resolved, it is fair to assume that the majority of the published studies agree that the pH does fall to at least pH

5.5. At this pH level, N-chlorotaurine will quickly ($t_{1/2} \sim 1.1$ min) disproportionate to taurine and N-dichlorotaurine (39).

4.4 Conclusions

The contribution of chlorotaurine in the killing of invading bacteria is widely recognized and accepted. There are very few published studies that have focused on the role played by dichlorotaurine. It is conceivable that dichlorotaurine is formed *in vivo* either in the presence of excess HOCl and/or through disproportionation of chlorotaurine in acidic pH conditions. Such conditions are believed to exist at sites of inflammation during phagocytosis. In this study, we have shown that dichlorotaurine reacts 1000 times faster with thiols and ~100 times faster with ascorbate than TauCl. The high reactivity towards thiols suggests that dichlorotaurine may be the reactive species *in vivo*.

4.5 References

1. Calvo, P., Crugeiras, J., Rios, A., Rios, M.A. (2007) Nucleophilic substitution reactions of N-chloramines: evidence for a change in mechanism with increasing nucleophile reactivity, *J. Org. Chem.* 72, 3171-3178.
2. Davies, M. J. (2005) The oxidative environment and protein damage, *Biochim. Biophys. Acta* 1703, 93-109.
3. Pattison, D. I., Davies, M.J., Hawkins, C.L. (2007) Hypochlorous acid-mediated protein oxidation: how important are chloramine transfer reactions and protein tertiary structure? *Biochemistry* 46, 9853-9864.
4. Pattison, D. I., Davies, M.J. (2001) Absolute rate constants for the reaction of hypochlorous acid with protein side chains and peptide bonds, *Chem. Res. Toxicol.* 14, 1453-1464.
5. Armesto, X. L., Canle, M., Garcia, M.V., Santaballa, J. A. (1998) Aqueous chemistry of N-halo-compounds *Chem. Soc. Rev* 27, 435-460.
6. Peskin, A. V., Winterbourn, C.C. (2003) Histamine chloramine reactivity with thiol compounds, ascorbate and methionine and with intracellular glutathione, *Free Radical Biol. Med.* 35, 1252-1260.
7. Peskin, A. V., Winterbourn, C.C. (2001) Kinetics of the reactions of hypochlorous acid and amino acid chloramines with thiols, methionine and ascorbate, *Free Radical Biol. Med.* 30, 572-579.

8. Peskin, A. V., Midwinter, R.G., Harwood, D.T., Winterbourn, C.C. (2004) Chlorine transfer between glycine, taurine and histamine: reaction rates and impact on cellular reactivity, *Free Radical Biol. Med.* 37, 1622-1630.
9. Prutz, W. A. (1998) Reactions of hypochlorous acid with biological substrates are activated catalytically by tertiary amines, *Arch. Biochem. Biophys.* 357, 265-273.
10. Prutz, W. A. (1998) Interactions of hypochlorous acid with pyrimidine nucleotides, and secondary reactions of chlorinated pyrimidines with GSH, NADH and other substrates, *Arch. Biochem. Biophys.* 349, 183-191.
11. McRipley, R. J., Sbarra, A.J. (1967) Role of the phagocyte in host-parasite interactions. XII. Hydrogen peroxide-myeloperoxidase bactericidal system in the phagocyte, *J. Bacteriol.* 94, 1425-1430.
12. Klebanof, S. J. (1968) Myeloperoxidase-halide-hydrogen peroxide antibacterial system, *J. Bacteriol.* 95, 2131-2138.
13. Tilley, F. W., Chapin, R.M. (1930) Germicidal efficiency of chlorine and the N-chloro derivatives of ammonia, methylamine and glycine against antrax spores *J. Bacteriol.* 19, 295-302.
14. Dudani, A. K., Martyres, A., Fliss, H. (2008) Rapid preparation of preventive and therapeutic whole-killed retroviral vaccines using the microbicide taurine chloramine, *Aids Res. Hum. Retroviruses* 24, 635-642.
15. Furnkranz, U., Nagl, M., Gottardi, W., Kohsler, M., Aspöck, H., Walochnik, J. (2008) Cytotoxic activity of N-chlorotaurine on *Acanthamoeba* spp, *Antimicrob. Agents Chemother.* 52, 470-476.

16. Nagl, M., Larcher, C., Gottardi, W. (1998) Activity of N-chlorotaurine against herpes simplex- and adenoviruses, *Antiviral Res.* 38, 25-30.
17. Nagl, M., Hess, M. W., Pfaller, K., Hengster, P., Gottardi, W. (1999) N-chlorotaurine, a product of stimulated leukocytes: Evidence for its antimicrobial function in the human defence system, *Amino Acids* 17, 33.
18. Nagl, M., Hess, M. W., Pfaller, K., Hengster, P., Gottardi, W. (2000) Bactericidal activity of micromolar N-chlorotaurine: Evidence for its antimicrobial function in the human defense system, *Antimicrob. Agents Chemother.* 44, 2507-2513.
19. Nagl, M., Lass-Flörl, C., Neher, A., Gunkel, A., Gottardi, W. (2001) Enhanced fungicidal activity of N-chlorotaurine in nasal secretion, *J. Antimicrob. Chemother.* 47, 871-874.
20. Nagl, M., Gruber, A., Fuchs, A., Lell, C. P., Lemberger, E. M., Borg-Von Zepelin, M., Wuerzner, R. (2002) Impact of N-chlorotaurine on viability and production of secreted aspartyl proteinases of *Candida*, *Antimicrobial agents and chemotherapy* 46, 1996-1999.
21. Peskin, A. V., Winterbourn, C.C. (2006) Taurine chloramine is more selective than hypochlorous acid at targeting critical cysteines and inactivating creatine kinase and glyceraldehyde-3-phosphate dehydrogenase, *Free Radical Biol. Med.* 40, 45-53.
22. Cantin, A. M. (1994) Taurine modulation of hypochlorous acid-induced lung epithelial cell injury in vitro, *J. Clin. Invest.* 93, 606-614.

23. Park, E., Schuller, L.G., Quinn, M.R. (1995) Taurine chloramine inhibits production of nitric oxide and TNF in activated RAW 264.7 cells by mechanisms that involve transcriptional and translational events, *J. Immunol.* 154, 4778-4784.
24. Kim, C., Cha, Y.N. (2009) Production of reactive oxygen and nitrogen species in phagocytes is regulated by taurine chloramine, *Adv. Exp. Med. Biol.* 643, 463-472.
25. Wang, L., Khosrovi, B., Najafi, R. (2008) N-chloro-2,2-dimethyltaurines: a new class of remarkably stable N-chlorotaurines, *Tetrahedron Lett.* 49, 2193-2195.
26. Nagl, M., Gottardi, W. (2010) N-chlorotaurine, a natural antiseptic with outstanding tolerability, *J. Antimicrob. Chemother.* 65, 399-409.
27. Pattison, D. I., Davies, M.J. (2005) Kinetic analysis of the role of histidine chloramines in hypochlorous acid mediated protein oxidation, *Biochemistry* 44, 7378-7387.
28. Weiss, S. J., Klein, R., Slivka, A., Wei, M. (1982) Chlorination of taurine by human neutrophils, *J. Clin. Invest.* 70, 598-607.
29. Test, S. T., Lampert, M.B., Ossanna, P.J., Thoene, J.G., Weiss, S.J. (1984) Generation of nitrogen-chlorine oxidants by human phagocytes, *J. Clin. Invest.* 74, 1341-1349.
30. Thomas, E. L., Jefferson, M.M., Grisham, M.B. (1982) Myeloperoxidase-catalyzed incorporation of amines into proteins: role of hypochlorous acid and dichloramines, *Biochemistry* 21, 6299-6308.

31. Hawkins, C. L., Pattison, D.I., Davies, M.J. (2003) Hypochlorite-induced oxidation of amino acids, peptides and proteins, *Amino Acids* 25, 259-274.
32. Zgliczynski, J. M., Stelmaszynska, T., Domanski, J., Ostrowski, W. (1971) Chloramines as intermediates of oxidation reaction of amino acids by myeloperoxidase, *Biochim. Biophys. Acta* 235, 419-424.
33. Antelo, J. M., Arce, F., Franco, J., Rodriguez, P., Varela, A. (1989) Stability of N-chloro-3-aminopropanol in aqueous solution. kinetics of decomposition and disproportionation of N-chloro-3-aminopropanol, *Int. J. Chem. Kinet.* 21, 343-354.
34. Antelo, J. M., Arce, F., Parajo, M., Rodriguez, P., Varela, A. (1992) Disproportionation kinetics of N-Cl-n-propylamine and N-Cl-isopropylamine, *Int. J. Chem. Kinet.* 24, 991-997.
35. Valentine, R. L., Jafvert. (1988) General acid catalysis of monochloramine disproportionation, *Environ. Sci. Technol.* 22, 691-696.
36. Gottardi, W., Nagl, M. (2002) Chemical properties of N-chlorotaurine sodium, a key compound in the human defense system, *Arch. Pharm.* 9, 411-421.
37. Winterbourn, C. C., Peskin, A.V. (2001) Kinetics of the reactions of hypochlorous acid acid and amino acid chloramines with thiols, methionine, and ascorbate, *Free Radical Biol. Med.* 30, 572-579.

38. Thomas, E. L., Jefferson, M.M., Grisham, M.B., Melton, D.F. (1985) Evidence for a role of taurine in the in vitro oxidative toxicity of neutrophils towards erythrocytes, *J. Biol. Chem.* 260, 3321-3329.
39. Gottardi, W., Nagl, M., Hagleitner, M. (2005) N,N-Dichlorotaurine: Chemical and bactericidal properties, *Arch. Pharm.* 338, 473-483.
40. Coker, M. S. A., Hu, W., Senthilmohan S.T., Kettle, A.J. (2008) Pathways for the decay of organic dichloramines and liberation of antimicrobial chloramines gases, *Chem. Res. Toxicol.* 21, 2334-2343.
41. Rous, P. (1925) The relative reaction within living mammalian tissues. II. On the mobilization of acid material within cells, and the reaction as influenced by the cell state *J. Exp. Med.* 41, 399-411.
42. Rous, P. (1925) The relative reaction within living mammalian tissues. I. General features of vital staining with litmus, *J. Exp. Med.* 41, 379-397.
43. Griffiths, G., Mayorga, L. (2007) Phagosome proteomes open the way to a better understanding of phagosome function, *Genome biology* 8, 1-4.
44. Hiddessen, A. L., Sulchek, T.A., Shen, N., Thomas, C., Woo, Y., Blanchette, C.D. (2009) Decoupling internalization, acidification and phagosomal-endosomal/lysosomal fusion during phagocytosis of InA coated beads in epithelial cells, *Plos One* 4, 1-13.
45. Test, S. T., Weiss, S.J. (1986) The generation and utilization of chlorinated oxidants by human neutrophils, *Adv. Rad. Biol. Med.* 2, 91-116.

46. Metchnikoff, E. (1968) *Lectures on the comparative pathology of inflammation*, Dover Publications, New York.
47. Jensen, M. S., Bainton, D.F. (1973) Temporal changes in pH within the phagocytic vacuole of the polymorphonuclear neutrophilic leukocyte, *J. Cell Biol.* 56, 379-388.
48. Sprick, M. G. (1956) Phagocytosis of *M. tuberculosis* and *M. smegmatis* stained with indicator dyes, *Am. Rev. Tuberc.* 74, 552-565.
49. Pavlov, E. P., Solov'ev, V.N. (1967) Changes in pH of the cytoplasm during phagocytosis of microorganisms stained with indicator dyes *Bulletin Exp Biol Med* 63, 78-81.
50. Jacques, Y. V., Bainton, D.F. (1978) Changes in pH within the phagocytic vacuoles of human neutrophils and monocytes, *Lab. Invest.* 39, 179-185.
51. Mandell, G. L. (1970) Intraphagosomal pH of human polymorphonuclear neutrophils *Proc. Soc. Exp. Biol. Med* 134, 447-449.
52. Segal, A. W., Geisow, M., Garcia, R., Harper, A., Miller, R. (1981) The respiratory burst of phagocytic cells is associated with a rise in the vacuolar pH, *Nature* 290, 406-409.
53. Geisow, M. J., D'Arcy, H.P., Young, M.R. (1981) Temporal changes of lysosome and phagosome pH during phagolysosome formation in macrophages: studies by fluorescence spectroscopy *J. Cell Biol.* 89, 645-652.
54. Lehrer, R. I., Cech, P. (1984) Phagolysosomal pH of human neutrophils, *Blood* 63, 88-95.

55. Jiang, Q., Griffin, D.A., Barofsky, D.F., Hurst, J.K. (1997) Intraphagosomal chlorination dynamics and yields determined using unique fluorescent bacterial mimics, *Chem. Res. Toxicol.* 10, 1080-1089.

CHAPTER 5: REPAIR OF CELLULAR DAMAGE AND RECOVERY OF ENZYME ACTIVITY BY SCN⁻ FOLLOWING TREATMENT WITH HOCl

5.1 Introduction

Optical cellular imaging is one of the most popular techniques used in biological research to explore microscopic structures at cellular and sub-cellular levels (1). During the past few decades, there has been a surge in the development of fluorescent probes which can be used as biomarkers (2). Owing to its versatility and noninvasiveness, fluorescence microscopy is emerging as one of the preferred imaging techniques for real-time monitoring of protein and enzyme activities in vitro and in vivo (3-7). Fluorescent detection offers several advantages which include high sensitivity, low cost and easy handling over other techniques (8). Unfortunately, only a limited number of fluorescent probes have been successfully developed thus far for the detection of HOCl and chloramines in living cells (9). However, rhodamine-based fluorescent probes are promising and are currently attracting considerable attention (10-11).

Reactive oxygen species including HOCl are employed by activated neutrophils as part of the immune arsenal (12-14). HOCl is believed to be the major microbiocidal agent in the phagolysosomes of neutrophils, but its excessive extraphagosomal production leads to host tissue damage and has been implicated in the progression of a number of inflammatory diseases (12-13, 15-16). The design of some of the probes that have been proposed is based on

oxidation reactions of p-methoxyphenol to benzoquinone, dibenoylhydrazine to dibenzoyl diimide, thiol to sulfonate derivative and p-alkoxyaniline by HOCl (9-11, 17-18) . While most of these probes have demonstrated reasonable selectivity for HOCl over other reactive oxygen species, the need for better probes that are highly selective and more reactive towards HOCl still exists. Recently, Tae et al. described the successful synthesis of a new highly selective and sensitive fluorescent probe for HOCl detection in aqueous media (19). The new probe is rhodamine-hydroxamic acid-based and is designed in a way that HOCl selectively and irreversibly oxidizes the hydroxamic acid unit of the probe, resulting in ring opening and the production of a highly fluorescent compound (Figure 5.1).

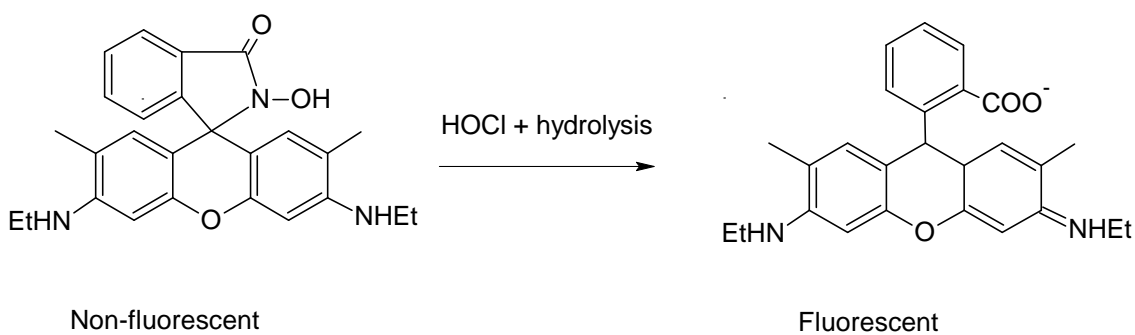


Figure 5.1. HOCl-induced oxidation of the fluorescent probe

An increase in fluorescence intensity was observed when the probe was mixed with HOCl solutions but not with other ROS at pH 7.4 (19). A549 cancer cells and zebra fish, were used to investigate whether the new probe could be used to detect “HOCl” in living cells. In these biological studies, a strong fluorescence in both A549 cells and zebra fish was observed after the exposure to HOCl and the new probe. The two issues that piqued our interest about this study were the claim that this probe was selective for HOCl (*in vitro and in vivo*) and also that it could be applied to detect HOCl in biological systems (19). There are other biologically relevant two-electron oxidants (e.g. HOBr and chloramines) that were not tested by the authors which we believed could react just as well as HOCl with the probe. Also, HOCl is highly reactive towards biological molecules with second-order rate constants of (10^5 - 10^7 M⁻¹s⁻¹) for sulfur-containing groups and (10^3 - 10^5 M⁻¹s⁻¹) for amino groups (20). The authors used a time-scale (i.e., the cells were incubated with HOCl for 20 min) which is long enough for all of the HOCl to react with the cellular components both on the surface and inside the cells thus making the claim for *in vivo* HOCl detection suspicious. We were more inclined to believe that the authors were observing the reaction of cellular chloramines (which are secondary products of the reaction of HOCl with amino groups) with the probe. Chloramines are less reactive and more selective than HOCl (21-22).

In this study we demonstrate that contrary to the claims by the authors, the probe is not as selective for HOCl as it was observed to react with chloramines. We recently published a study that demonstrated using kinetic and spectroscopic techniques that chloramines react with thiocyanate (SCN^-) to produce hypothiocyanite (OSCN^-) (23). This reaction is potentially important *in vivo* since it is our assertion that SCN^- plays a repair role on proteins that are damaged by HOCl. Herein, we employed an optical cellular imaging technique using the new probe to demonstrate the reaction of cellular chloramines with SCN^- . We further extended our study to investigate whether the reaction of chloramines with SCN^- could restore enzyme activity and cellular function.

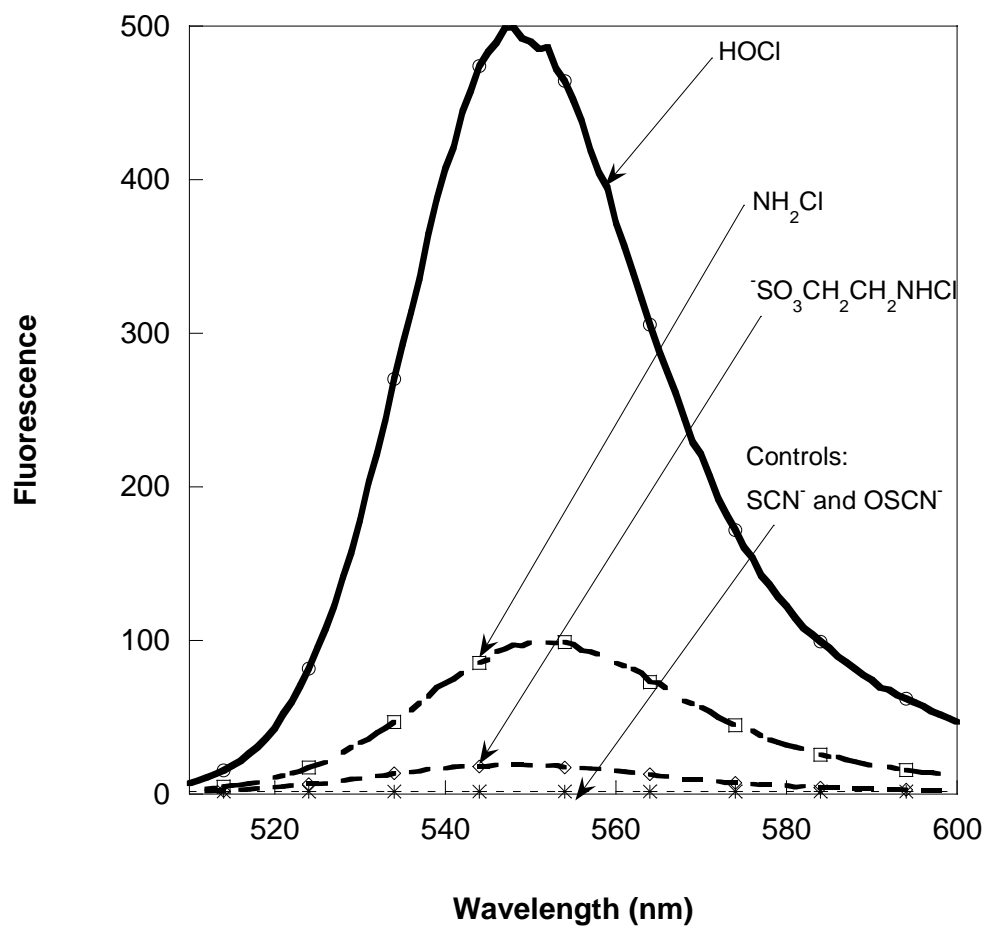
5.2 Results and discussion

5.2.1 In vitro study of the reactions of the probe with HOCl and chloramines

A closer inspection of the other reactive oxygen species (24) that were tested by Tae et al. for their ability to oxidize the rhodamine-probe reveals that with the exception of H_2O_2 , all were one-electron species. The reactive species that were investigated includes nitric oxide (NO^\bullet), hydroxyl ($\bullet\text{OH}$), alkylperoxy radical (ROO^\bullet) and superoxide ($\bullet\text{O}_2^-$) radicals. Hypochlorous acid (HOCl) reacts with amines with a second-order rate constant of 10^3 - $10^5 \text{ M}^{-1}\text{s}^{-1}$ at physiological pH conditions to produce chloramines. It is therefore unexpected that after 20 min of incubation of the A549 cells with HOCl and the washing of residual HOCl, there would be any HOCl present. Accordingly, we investigated whether inorganic and

organic chloramines (NH_2Cl and $\text{SO}_3\text{CH}_2\text{CH}_2\text{NHCl}$) were able to oxidize the rhodamine probe by monitoring changes in fluorescence intensities. Figure 5.2 (a-b) shows the fluorescence spectra of the rhodamine probe (10 μM) and its reaction with 50 and 100 μM HOCl, NH_2Cl , $\text{SO}_3\text{CH}_2\text{CH}_2\text{NHCl}$, SCN^- and OSCN^- at pH 7.4. The spectra were measured 10 min after the respective solutions were mixed. Not surprising, under both concentration conditions, there was significant fluorescence enhancement when the probe was treated with HOCl due to the rapid oxidation of the probe by HOCl. Relatively lower fluorescence intensity changes were observed in the case of NH_2Cl and $\text{SO}_3\text{CH}_2\text{CH}_2\text{NHCl}$. This is due to HOCl reacting faster with the probe than chloramines. In addition to HOCl and the chloramines, we investigated whether SCN^- and OSCN^- would react with the rhodamine probe. As shown in Figure 5.3, no enhancement of the fluorescence intensity in the presence of SCN^- or OSCN^- was observed which indicates that they do not oxidize the rhodamine probe. Based on these results, it appears that contrary to the claim of Tae et al. the rhodamine fluorescent probe may not be selective for HOCl as it also reacts with other electrophilic two-electron oxidants (i.e. chloramines).

(a)



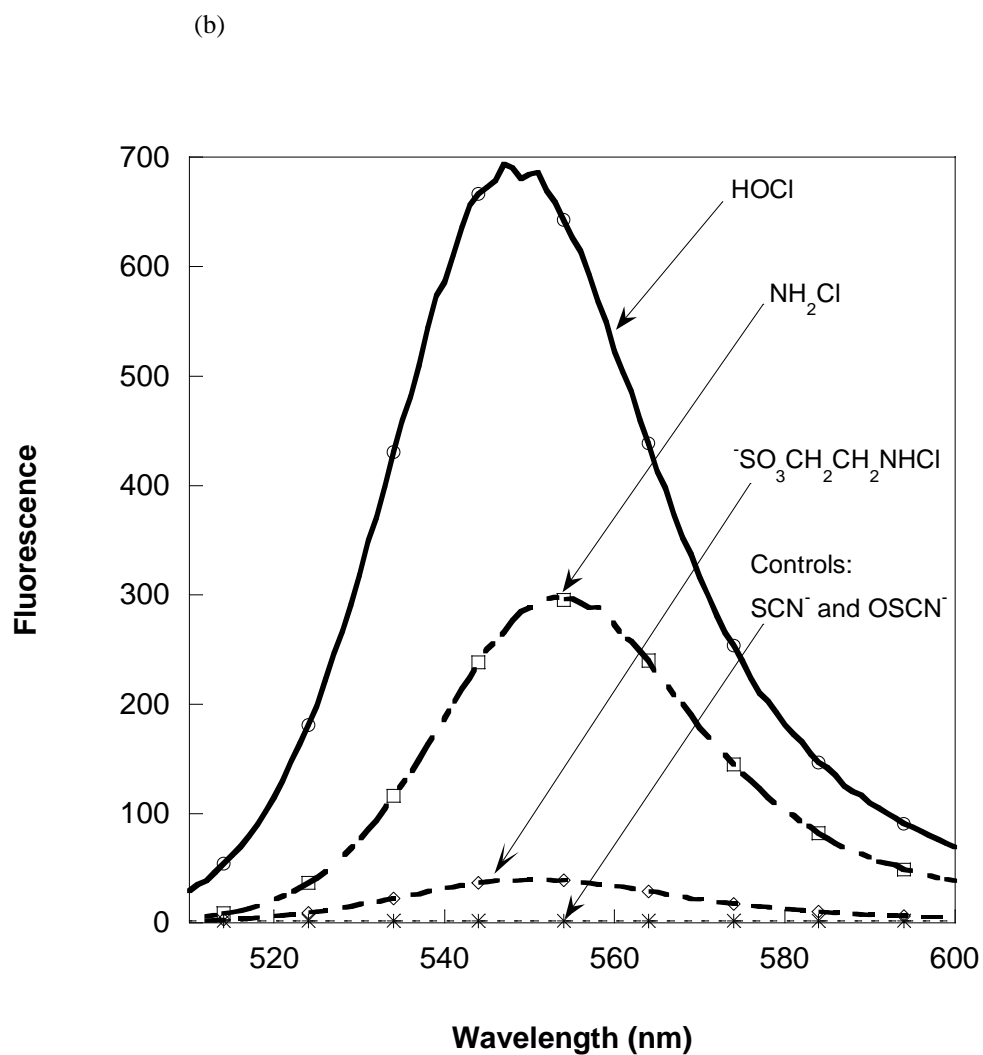


Figure 5.2. Fluorescence response of the probe (10 μM) 10 min after the addition of (a) 50 μM ; (b) 100 μM HOCl, NH_2Cl and $\text{SO}_3\text{CH}_2\text{CH}_2\text{NHCl}$

5.2.2 Cellular imaging studies with A549 cancer cells

Tae et al. evaluated the possible biological application of the rhodamine probe as a fluorescence chemosensor for HOCl detection in living cells using A549 lung cancer cells (19). After incubating the cells with HOCl, washing and treating them with the probe, the cells were imaged using a confocal fluorescence microscope. It was observed that the cells that were not exposed to HOCl showed no fluorescence but those treated with HOCl exhibited a strong red fluorescence. Using the protocol of Tae et al., we sought to reproduce their results by conducting the same experiments at pH 7.4. We treated the A549 cells with various amounts of HOCl and then stained them with 10 μM of the fluorescent probe. As shown in Figure 5.3, (a) in the absence of HOCl treatment, no fluorescence was observed (b) 50 μM HOCl treatment displayed red fluorescence (c) 100 μM HOCl treatment showed an even stronger red fluorescence. These results are consistent with those of Tae et al. who observed that increasing the concentration of HOCl resulted in the corresponding increase in fluorescence intensity.

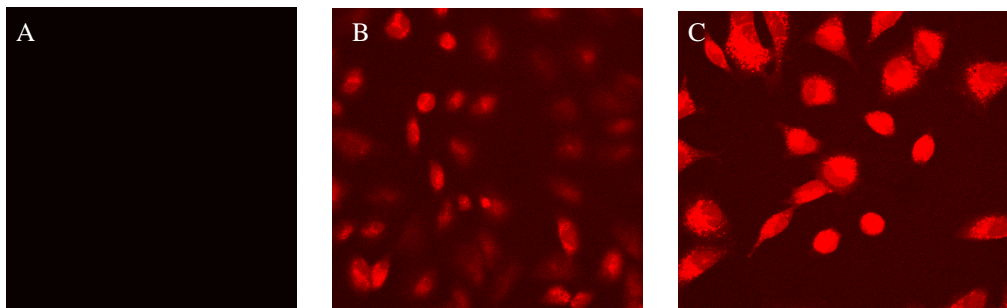


Figure 5.3. Fluorescence images of A549 cells (A) untreated; (B) treated with 50 μM HOCl; (C) treated with 100 μM HOCl

We further investigated the reaction of the rhodamine fluorescent probe with A549 cells that were treated with SCN^- subsequent to incubation with HOCl. The purpose of these experiments was to evaluate whether the optical imaging technique could be used to study the reaction of cellular chloramines with SCN^- . A549 cells were incubated with 50 μM HOCl in culture medium for 20 min at 37 $^\circ\text{C}$ and washed with the medium to remove residual HOCl, the cells were then incubated for an additional 20 min at 37 $^\circ\text{C}$ with 50 μM SCN^- and washed again with the medium. The HOCl and SCN^- treated cells were then incubated with the fluorescent probe (10 μM) in the medium for 10 min at 37 $^\circ\text{C}$. Immediately after incubation, the cells were imaged using a confocal fluorescence microscope. Control experiments included untreated cells, cells treated with HOCl, SCN^- and OSCN^- (Table 5.1). For qualitative comparisons of relative fluorescence intensities, we used the sample treated with HOCl as a baseline/reference for setting the microscope. This implies that the Z-series was adjusted based upon the HOCl treated sample and was not changed when imaging of the other samples was conducted. As expected, the HOCl treated sample showed an intense red fluorescence, indicating the reaction of the probe with cellular chloramines (Figure 5.4 b). No fluorescence was detected in any of the control experiments (i.e. no treatment; SCN^- and OSCN^- treatment). Interestingly, the sample that was subsequently treated with SCN^- following HOCl treatment did not show any fluorescence (Figure 5.4 c). The absence of fluorescence in this sample suggests that the chloramines reacted with SCN^- to form OSCN^- which does not oxidize the rhodamine probe.

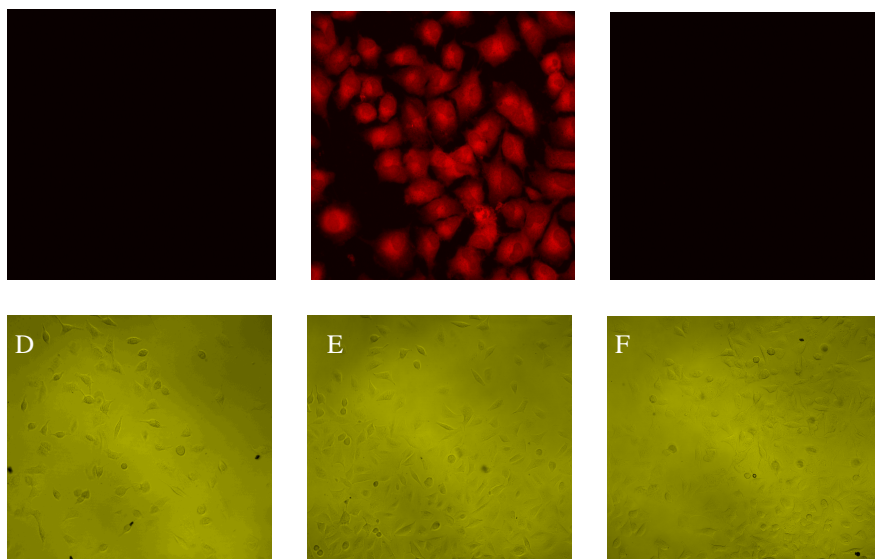


Figure 5.4. Fluorescence images of A549 cells (A) untreated; (B) treated with 50 μM HOCl; (C) treated with 50 μM SCN^- subsequent to treatment with 50 μM HOCl; (D-F) the corresponding transmission images

In addition to fluorescence images, we took transmittance images in order to confirm that despite the absence of fluorescence, the A549 cells were present in all the samples. The corresponding transmittance images show that in each chamber A549 cells were present during fluorescence imaging. A recent study published by Hawkins et al. reports that hypothiocyanous acid was found to induce apoptosis and necrosis with greater efficacy, and at lower concentrations, than HOCl or HOBr (25). We further extended the imaging studies to include investigation into possible morphological changes following each treatment (with HOCl, OSCN⁻ or SCN⁻). Morphological examination shows that most of the cells were not detached and no visible differences in cell shapes were observed in

each experiment (Figure 5.5). No signs of “popcorn-like” blebs which are typical of cells undergoing apoptosis (26).

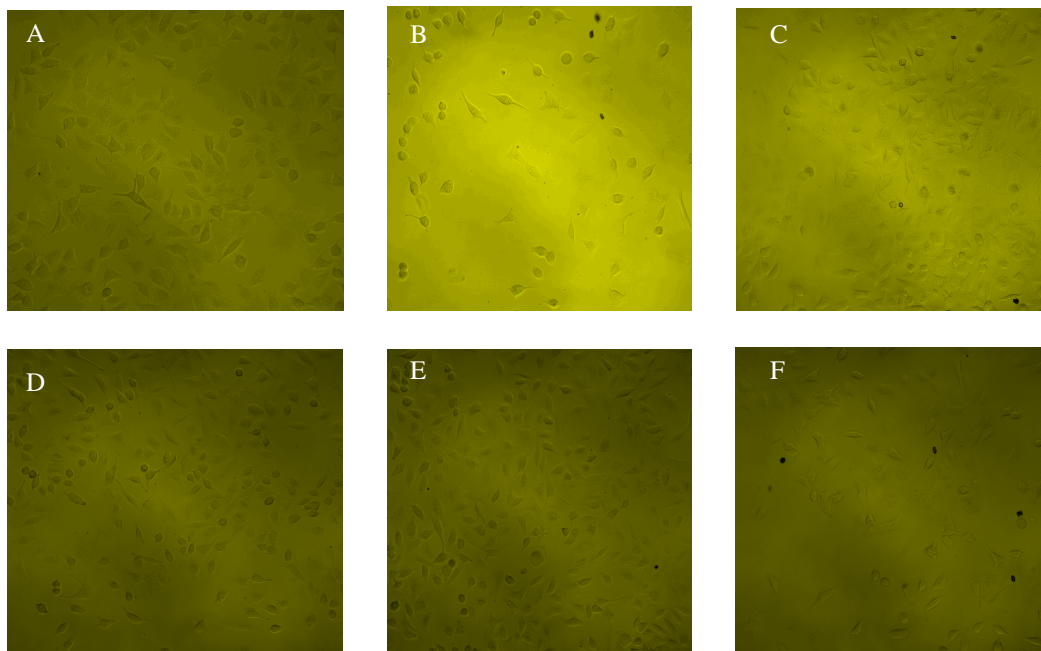
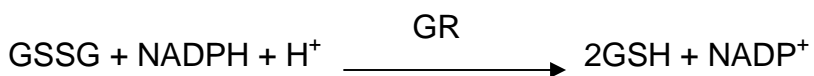


Figure 5.5. Morphological changes to A549 cells (A) control (untreated); (B) exposed to 50 μM HOCl; (C) exposed to 50 μM SCN⁻; (D) exposed to 50 μM SCN⁻ subsequent to treatment with 50 μM HOCl; (E) exposed to 50 μM OSCN⁻; (F) exposed to 50 μM SCN⁻ and then treated with 50 μM HOCl;

5.2.3 Inhibition glutathione reductase (GR) and the recovery of enzyme activity after SCN⁻ treatment

We investigated the possible recovery of the activity of selected housekeeping enzymes by SCN⁻ after they were treated with HOCl. We selected glutathione reductase (GR) an important component of the glutathione redox cycle, which catalyzes the reduction of oxidized glutathione (GSSG) to glutathione (GSH) by NADPH.



GR is a dimer with identical subunits and has a molecular weight of 100 kDa (27). The active site of this enzyme is located between the subunits. The prevailing understanding of the catalytic cycle of GR is that it involves a cascade of electron transfer reactions which are initiated by NADPH.

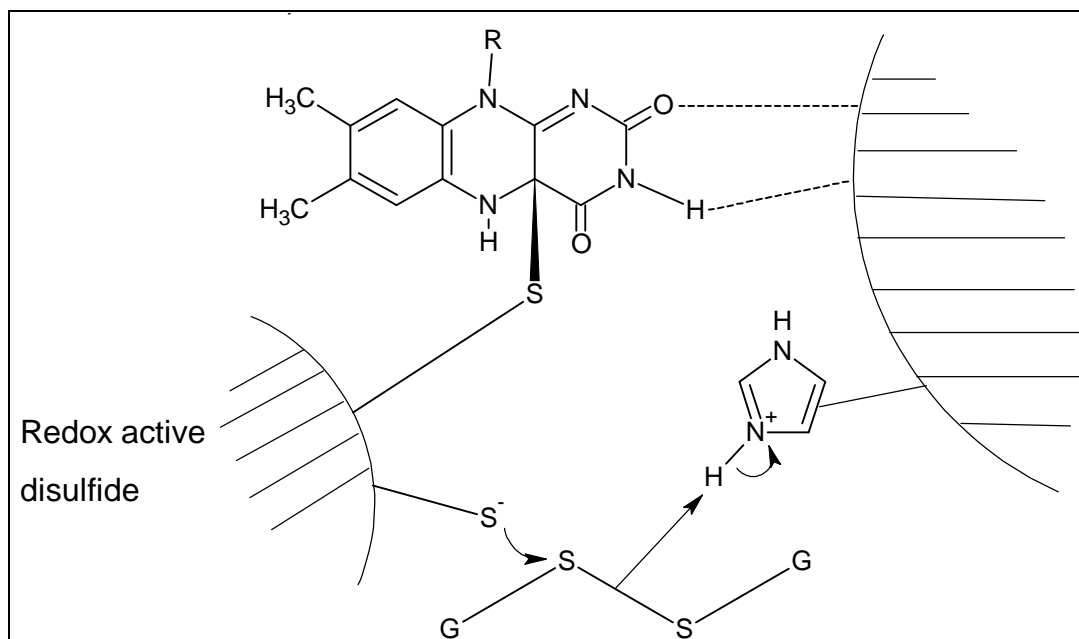


Figure 5.6. Scheme of the GR active site

First, NADPH binds to and reduces the tightly bound FAD to FADH⁻. After transferring the hydride to FAD, NADPH leaves as FADH⁻ quickly reduces the active site disulfide Cys58-Cys63. The reduction of the disulfide likely takes place via the formation of a transient adduct between flavin and the sulfur of Cys63 plus a nucleophilic Cys58. In the next step of the catalytic cycle, the Cys58 nucleophile attacks GSSG to form a mixed protein-glutathione disulfide (GS-Cys58) while releasing the first glutathione molecule. Another important residue in the catalytic cycle is histidine (His467) which by acting as a proton acceptor and/or donor facilitates the Cys58 nucleophilic attack. In the final step, Cys63

reduces the mixed disulfide which releases the second GSH molecule and reoxidizes cysteine to the disulfide (Cys58-Cys63).

Glutathione is a major non-protein thiol in cells where up to millimolar concentrations have been reported in some cells (28). One of its cellular functions is to serve as an antioxidant and thus it is essential for cell survival especially during conditions of oxidative stress. Many of the important residues in the active site of GR including cysteines (Cys-58 and Cys-63), histidine (His467) and tyrosine (Tyr197) are susceptible to HOCl attack. The oxidation of these residues results in the inhibition of the enzyme activity. Under the conditions of our experiments, it is difficult to attribute the inactivation of GR by HOCl to just one of the important residues in the active site of the enzyme. While cysteines may be the primary targets of HOCl, the products of its reactions (i.e. sulfonates, sulfinates and disulfides) are not known to react with SCN^- . As a result if the inactivation of GR by HOCl was exclusively linked to the oxidation of cysteines, the recovery of the enzyme activity by SCN^- would not be expected. In our experiments, the activity of GR was monitored by following the depletion of NADPH at $\lambda = 340 \text{ nm}$ as it reduces GSSG to GSH (Figure 5.7).

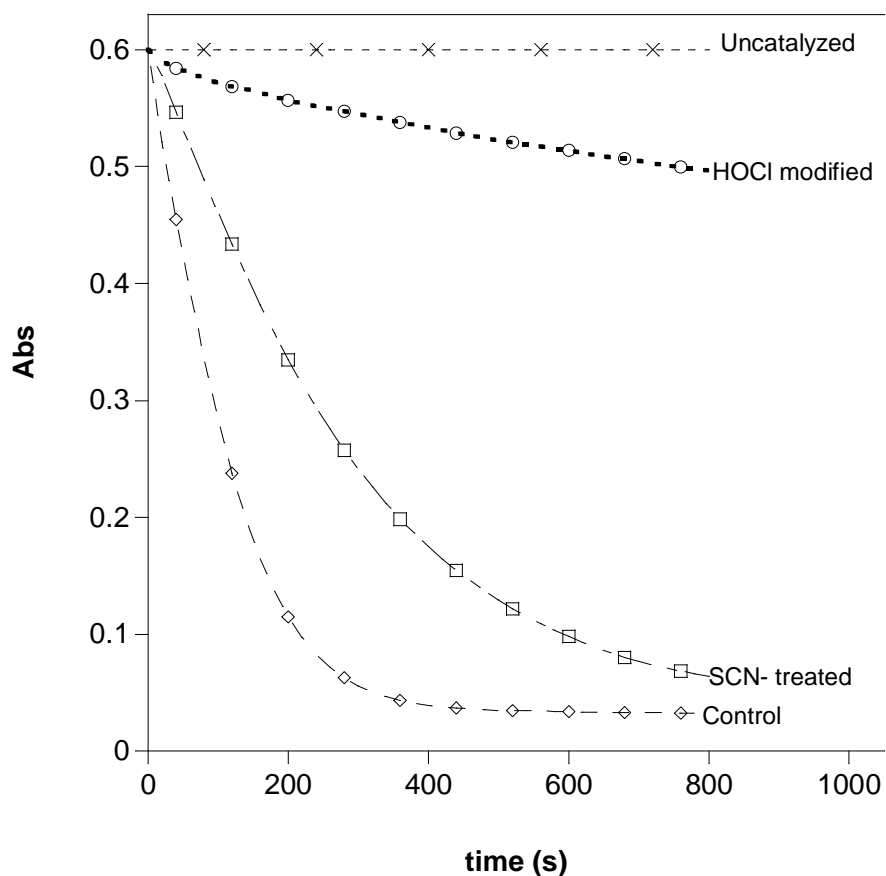


Figure 5.7. Kinetic traces at $\lambda = 340\text{nm}$ depicting the GR-catalyzed reduction of GSSG by NADPH. Conditions: (A) $[\text{GSSG}]_0 = 1 \text{ mM}$, $[\text{NADPH}]_0 = 0.1 \text{ mM}$, $[\text{GR}] = 0.025 \text{ U/mL}$, $[\text{PBS}] = 0.1 \text{ M}$, $\text{pH } 7.4$ and $T = 25 \text{ }^\circ\text{C}$; (B) GR incubated with $40 \text{ }\mu\text{M HOCl}$ for 20 min and then treated with $160 \text{ }\mu\text{M SCN}^-$ for another 20 min. (c) GR incubated with $40 \text{ }\mu\text{M HOCl}$ for 20 min and then treated with phosphate buffer for an additional 20 min. Each line represents an average of five data sets and only 10% of the data are illustrated.

The GR activity (mU/mL) was estimated using the linear portion of each of the curves in Figure 5.8. We calculated the rate of decrease of the absorbance (A_{340}/min) from the slope of each line and then divided it by the molar absorptivity of GR (6.22×10^{-3} nmol/mL) to get the activity in (mU/mL). Lastly we corrected each measurement for the sample dilution in the assay by multiplying the mU/mL by 20 (*i.e.*, 50 μL was diluted to 1000 μL).

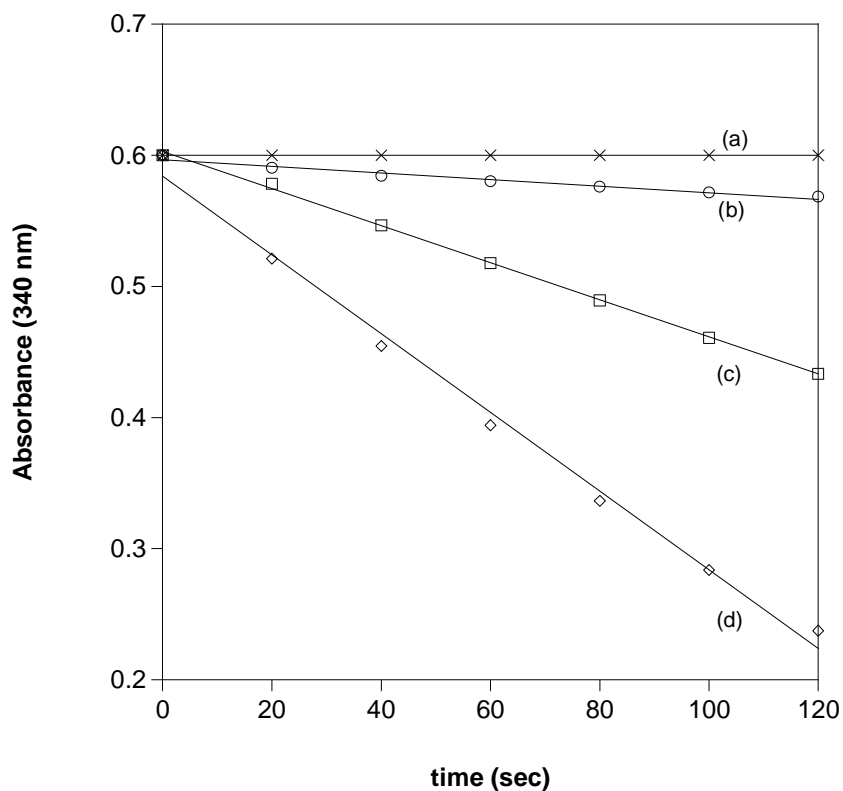


Figure 5.8. Enzyme activity estimated using the rate of change in the A_{340} and the molar absorptivity (6.22×10^{-3} nmol/mL) of GR. (a) Uncatalyzed: 0, (b) HOCl modified: 0.405, (c) SCN^- treated: 2.25 and control: 4.82 (mU/mL)

The activity of un-modified GR is 4.82 (mU/mL) (control, Figure 5.8). However, the treatment of GR (~ 1.3 nM) with 40 μ M HOCl resulted in severe loss (~ 92 %) of the enzyme activity. Since the experiment was done under conditions of large HOCl excess, the loss of activity is presumably due to the oxidation of one or more of the critical residues in the active site of GR. The observed activity (~ 8 %) of the HOCl-modified GR presumably indicates that 40 μ M HOCl was not enough to completely inactivate GR under the conditions of our experiment or indicates the reaction of NADPH with chlorinated GR. Surprisingly when the HOCl modified GR was subsequently treated with 160 μ M SCN⁻ for 20 min, most of the lost enzyme activity (~ 47 %) was recovered. We believe that the reactivation of GR by SCN⁻ suggests possible involvement of the histidine residue. When HOCl reacts with His467, the enzyme is modified through the formation of histidine chloramine which presumably inactivates the enzyme. Boggaram and Mannervik published a study in which it was shown that GR was inactivated by treatment with ethoxyformic anhydride through the modification of particularly the histidine residue (29). It was concluded that the histidine residue was essential for the catalytic activity of GR. Pattison and Davies showed that histidine containing compounds readily form imidazole chloramines ($k = 1.6 \times 10^6 \text{ M}^{-1}\text{s}^{-1}$) and that these chloramines can rapidly chlorinate other target molecules such as amino groups via inter- or intramolecular chlorine transfer reactions ($k = 10^{-3}\text{-}10^{-4} \text{ M}^{-1}\text{s}^{-1}$) (20). Transhalogenation reactions are typically very slow reactions ($k = 10^{-2} \text{ M}^{-1}\text{s}^{-1}$) for the reaction of chlorotaurine with benzylamine (30). Given how fast the imidazole chloramine forms and also how fast it reacts with

other amino groups, it is conceivable that this chloramine in the active site of GR is capable of oxidizing SCN^- to OSCN^- .

5.3 Detection of apoptosis and necrosis by flow cytometry

We investigated the changes in the proportion of live, apoptotic and necrotic A549 cells after treating the cells with SCN^- for 1 h following a 20 min and 1 h exposure to HOCl. The preliminary data of cells incubated with HOCl for 20 min indicates that SCN^- treatment results in a significant increase in the number of live cells and a decrease in the number of necrotic cells (Figure 5.9).

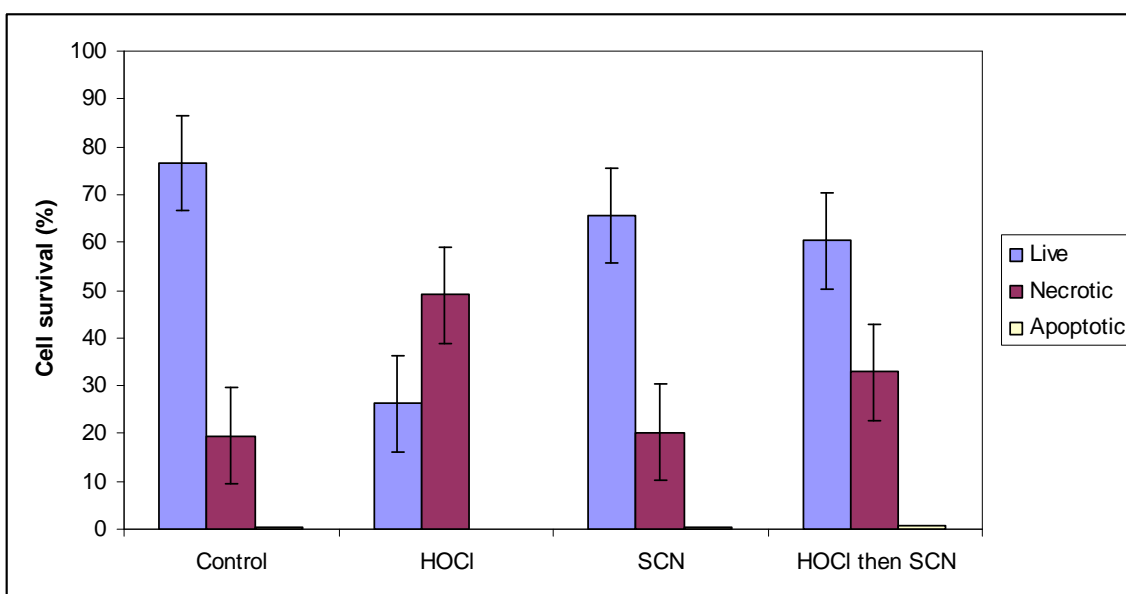


Figure 5.9. Proportion between living, apoptotic and necrotic cells after 20 min incubation with HOCl

The proportion distribution changed significantly when the cells were incubated with HOCl for 1 h (Figure 5.10). The subsequent treatment of the cells with SCN- did not have any positive effect on both the live and necrotic cells.

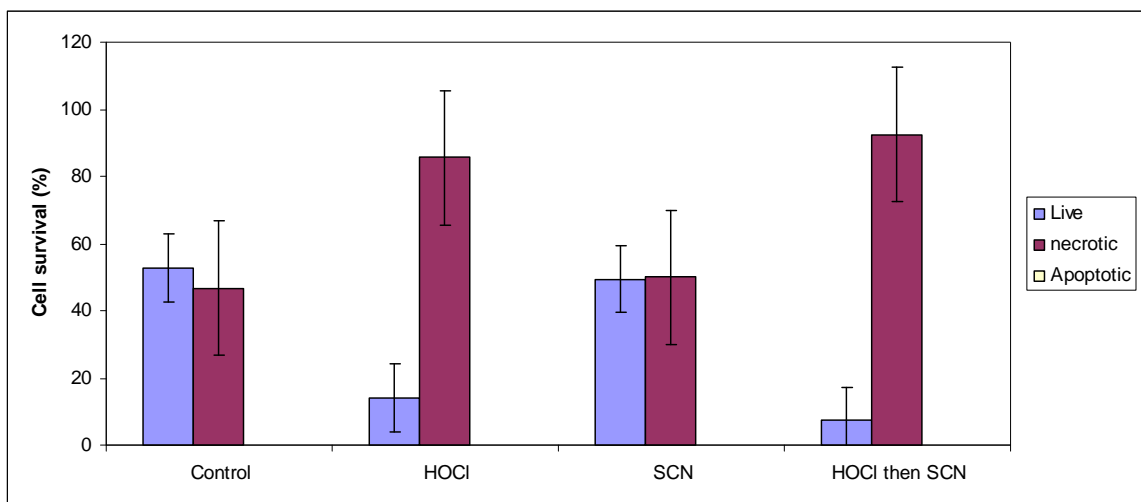


Figure 5.10. Proportion between living, apoptotic and necrotic cells after 1 h incubation with HOCl

We observed that in both cases, the fraction of apoptotic cells remained below 0.7 %. This was unexpected given that some studies have suggested that HOCl and chloramines trigger apoptosis (24, 31-32). Our data are however consistent with the findings of Robaszkievicz et al. who also observed low levels of apoptotic cells (< 8 %) after incubation (24 h) A549 cells with 500 μ M HOCl (33).

5.4 Possible biological significance of these findings

Chloramines are a major fraction of the secondary reactive intermediates produced by the reaction between HOCl and amino groups (23). In the absence of other functional groups (e.g. thiols) that can react with chloramines *in vivo*, they decompose to form aldehydes which and other products that can lead to permanent alteration of protein structure and function and cellular dysfunction. The reaction of chloramines with thiocyanate (SCN^-) has received some attention recently, mainly because this reaction was found to produce hypothiocyanite (OSCN^-), a species that is not lethal to mammalian cells (14, 23). The present study demonstrates that this reaction is effective at partially restoring the activity of glutathione reductase (GR) inactivated by HOCl and also may prevent cell death. Given the significant role of GR as a housekeeping enzyme for redox homeostasis (normally maintains cytosolic glutathione ca. 98% in its reduced state GSH), its inactivation makes the cellular contents vulnerable to attack by oxidants. In this work we observed that GR inactivated by HOCl can be reactivated by incubation with SCN^- . These results, confirm that the histidine (His467) residue in the GR active site is involved in its catalytic activity. When SCN^- reacts with the histidine chloramine, the result is the restoration of some of the GR activity. In a recent study Bozonet et al. observed no morphology changes on endothelial cells treated with low concentrations of OSCN^- ($\leq 200 \mu\text{M}$) and the cells remained viable (34). It was also reported that at these levels, OSCN^- appears to block the initiation of apoptosis. These findings are applicable to this study since the reaction of cellular chloramines with SCN^- produces low

concentrations of OSCN⁻. The preliminary flow cytometry data shows that the exposure to SCN⁻ (50 μM) for 1 h of A549 cells that were pre-incubated with HOCl (50 μM) for 20 min, results in the slight reduction of necrotic cells and an increase of viable cells. This positive effect is attributable to both the reduction of the cellular chloramines by SCN⁻ and the formation of the lower concentration of OSCN⁻. The results of this study suggest that the reaction of chloramines with SCN⁻ may play a role in determining the outcome of inflammatory diseases.

5.5 Conclusions

This work began with the aim of disproving the claim made in a study published by Tae et al. that they had synthesized a rhodamine fluorescent probe which was selective for HOCl. The authors of this study did not investigate possible reactions of chloramines with the new rhodamine probe. This was rather a puzzling omission given that chloramines are the main products of the reaction of HOCl with amines. Our investigation reveals that both the inorganic and organic chloramines are capable of oxidizing the rhodamine probe as confirmed by an increase in fluorescence intensity. We then extended our study to include the reaction of chloramines with SCN⁻ using the fluorescent probe by optical imaging techniques. Images of A549 cells treated only with HOCl showed strong red fluorescence while those treated with SCN⁻ subsequent to HOCl did not show any fluorescence. It appears that the fluorescent rhodamine probe can be applied in biological systems not only to detect HOCl but its secondary products such as chloramines. We also found in this work that SCN⁻ is effective at repairing

damage inflicted by HOCl on cells and GR enzyme. Approximately 47 % of GR was recovered by treating HOCl-modified enzyme with SCN^- . Confocal images of A549 cells treated with SCN^- subsequent to HOCl show the quenching of fluorescence by SCN^- and preliminary flow cytometry data confirms this observation as the number of viable cells increased.

5.6 References

1. Shaw, P. (1994) Deconvolution in 3-D optical microscopy, *Histochem. J.* 26, 687-694.
2. Tong, A., Xiang, Y. (2006) A new rhodamine-based chemosensor exhibiting selective Fe(III)-amplified fluorescence, *Org. Lett.* 8, 1549-1552.
3. Fang, X. H., Li, J.W.J., Perlette, J., Tan, W.H., Wang, K.M. (2000) Molecular beacons: novel fluorescent probes, *Anal. Chem.* 72, 747A-753A.
4. Zheng, Q., Xu, G., Prasad, P.N. (2008) Conformationally restricted dipyrromethene boron difluoride (BODIPY) dyes: high fluorescent, multicolored probes for cellular imaging, *Chem.Eur. J.* 14, 5812-5819.
5. Uttamchandani, M., Lu, C.H.S., Yao, S.Q. (2009) Next generation chemical proteomic tools for rapid enzyme profiling, *Acc. Chem. Res.* 42, 1183-1192.
6. Kamiya, M., Kobayashi, H., Hama, Y., Koyama, Y., Bernardo, M., Nagano, T., Choyke, P.L., Urano, Y. (2007) An enzymatically activated fluorescence probe for targeted tumor imaging, *J. Am. Chem. Soc.* 129, 3918-3929.
7. Stephens, D. J., Allan, V.J. (2003) Light microscopy techniques for live cell imaging, *Science* 300, 82-86.
8. Xing, B., Ang, C., Jiang, T., Yang, Y., Shao, Q., Aw, J. (2010) Synthesis and characterization of 2-(2-hydroxy-5-chlorophenyl)-6-chloro-4(3H)-

- quinazolinine-based fluorogenic probes for cellular imaging of monoamine oxidases, *Chem.--Asian J.* 5, 1317-1321.
9. Chen, X., Wang, X., Wang, S., Shi, W., Wang, K., Ma, H. (2008) A highly selective and sensitive fluorescence probe for the hypochlorite anion, *Chemistry-A-European Journal* 14, 4719-4724.
 10. Kenmoku, S., Urano, Y., Kojima, H., Nagano, T. (2007) Development of a highly specific rhodamine-based fluorescence probe for hypochlorous acid and its application to real-time imaging of phagocytosis, *J. Am. Chem. Soc.* 129, 7313-7318.
 11. Shepherd, J., Hilderbrand, S.A., Waternan, P., Heinecke, J.W., Weissleder, R., Libby, P. (2007) A fluorescent probe for the detection of myeloperoxidase activity in atherosclerosis-associated macrophages, *Chem. Biol.* 14, 1221-1231.
 12. Pullar, J. M., Visser, M.C.M., Winterbourn, C.C. (2000) Living with a killer: the effects of hypochlorous acid on mammalian cells, *Int. Union Biochem. Mol. Biol.* 50, 259-266.
 13. Winterbourn, C. C., Kettle, A.J. (2000) Biomarkers of myeloperoxidase-derived hypochlorous acid, *Free Radical Biol. Med.* 29, 403-409.
 14. Ashby, M. T., Carlson, A. C., Scott, M. J. (2004) Redox buffering of hypochlorous acid by thiocyanate in physiologic fluids, *J. Am. Chem. Soc.* 126, 15976-15977.
 15. Crugeiras, J., Calvo, P., Rios, A., Rios, M.A. (2007) Nucleophilic substitution reactions of N-chloramines: Evidence for a change in

- mechanism with increasing nucleophile reactivity, *J. Org. Chem.* **72**, 3171-3178.
16. Segal, A. W. (2005) How neutrophils kill microbes, *Annu. Rev. Immunol.* **23**, 197-223.
 17. Bizyukin, A. V., Korkina, L.G., Velichkovskii, B.T. (1995) Comparative use of 2,7-dichlorofluorescein diacetate, dihydrorhodamine 123, and hydroethidine to study oxidative metabolism in phagocytic cells, *Bull. Exp. Biol. Med.* **119**, 347-351.
 18. Sun, Z., Liu, F., Chen, Y., Tam, P.K.H., Yang, D. (2008) A highly specific BODIPY-based fluorescent probe for the detection of hypochlorous acid, *Org. Lett.* **10**, 2171-2174.
 19. Tae, J., Yang, Y., Cho, H.J., Lee, J., Shin, I. (2009) A rhodamine-hydroxamic acid-based fluorescent probe for hypochlorous acid and its applications to biological imagings, *Org. Lett.* **11**, 859-861.
 20. Pattison, D. I., Davies, M.J. (2006) Evidence for rapid inter- and intramolecular chlorine transfer reactions of histamine and carnosine chloramines: implications for the prevention of hypochlorous-acid-mediated damage, *Biochemistry* **45**, 8152-8162.
 21. Weiss, S. J., Lampert, M.B., Test, S.T. (1983) Long-lived oxidants generated by human neutrophils: characterization and bioactivity, *Science* **222**, 625-628.
 22. Thomas, E. L., Grisham, M.B., Jefferson, M.M. (1986) Cytotoxicity of chloramines, *Method Enzymol* **132**, 585-593.

23. Ashby, M. T., Xulu, B.A. (2010) Small molecular, macromolecular and cellular chloramines react with thiocyanate to give the human defense factor hypothiocyanite, *Biochemistry* 49, 2068-2074.
24. Whiteman, M., Chu, S., Siau, J., Rose, P., Sabapathy, K., Schantz, J., Cheung, N., Spencer, J., Armstrong, J. (2007) The pro-inflammatory oxidant hypochlorous acid induces Bax-dependent mitochondrial permeabilisation and cell death through AIF-/EndoG-dependent pathways, *Cell Signal.* 19, 705-714.
25. Hawkins, C. L., Davies, M.J., van Reyk, D.M., Lloyd, M.M. (2008) Hypothiocyanous acid is a more potent inducer of apoptosis and protein thiol depletion in murine macrophage cells than hypochlorous acid or hypobromous acid, *Biochem. J.* 414, 271-280.
26. Vissers, M. C. M., Pullar, J.M., Hampton, M.B. (1999) Hypochlorous acid causes caspase activation and apoptosis or growth arrest in human endothelial cells, *Biochem. J.* 344, 443-449.
27. Torchinsky, Y. M. (1981) *Sulfur in proteins*, Pergamon, Oxford.
28. Ashby, M. T., Nagy, P. (2007) Kinetics and mechanism of the oxidation of the glutathione dimer by hypochlorous acid and catalytic reduction of the chloroamine product by glutathione reductase, *Chem. Res. Toxicol.* 20, 79-87.
29. Boggaram, V., Mannervik, B. (1978) An essential histidine residue in the catalytic mechanism of mammalian glutathione reductase, *Biochem. Biophys. Res. Commun.* 83, 558-564.

30. Crugeiras, J., Calvo, P., Rios, A., Rios, M.A. (2009) Nucleophilic substitution reactions of N-Chloramines: evidence for a change in mechanism with increasing nucleophile reactivity, *J. Org. Chem.* **72**, 3171-3178.
31. Emerson, D., McCormick, M., Schmidt, J., Knudson, C. (2005) Taurine monochloramine activates a cell death pathway involving Bax and Caspase-9, *J. Biol. Chem.* **280**, 3233-3241.
32. Oyake, J., Otaka, M., Matsushashi, T., Jin, M., Odashima, M., Komatsu, K., Wada, I., Horikawa, Y., Ohba, R., Hatakeyama, N., Itoh, H., Watanabe, S. (2006) Over-expression of 70-kDa heat shock protein confers protection against monochloramine-induced gastric mucosal cell injury, *Life Sci.* **79**, 300-305.
33. Robaszekiewicz, A., Bartosz, G., Soszynski, M. (2010) N-Chloroamino acids mediate the action of hypochlorite on A549 lung cancer cells in culture, *Toxicology* **270**, 112-120.
34. Bozonet, S. M., Scott-Thomas, A.P., Nagy, P., Vissers, M.C.M. (2010) Hypothiocyanous acid is a potent inhibitor of apoptosis and caspase 3 activation in endothelial cells, *Free Radical Biol. Med.* **49**, 1054-1063.

CHAPTER 6: CONCLUDING REMARKS AND RECOMMENDATIONS FOR FUTURE WORK

The main findings of this work include:

- We successfully identified for the first time OSCN^- as the product of the reaction of SCN^- with chloramines (small molecular, protein and cellular). The product was identified by UV-visible spectroscopy and also kinetically by stopped-flow methods. Furthermore, we found that chloramines react faster with OSCN^- than SCN^- . Protein-bound chloramines eventually decompose by mechanisms that could irreversibly alter the structure and function of the protein. We surmise that the reactions of chloramines with SCN^- and OSCN^- has a potential biological significance as they may repair some of the damage inflicted by HOCl on proteins.
- Dichloramines (e.g. dichlorotaurine) are formed when monochloramines (e.g. chlorotaurine) disproportionates under slightly acidic conditions. We found that under pseudo-first-order conditions, chlorotaurine reacts with thiols with a second-order rate constant of $10^2 \text{ M}^{-1}\text{s}^{-1}$ while dichlorotaurine reacts much faster, with a second-order rate constant of $10^6 \text{ M}^{-1}\text{s}^{-1}$ at pH 7.4. The rate constant for dichlorotaurine is only three orders of magnitude lower than that for the reaction of HOCl with cysteine thiolate ($10^9 \text{ M}^{-1}\text{s}^{-1}$). We extended our investigation to include information about the mechanism of the reaction of dichlorotaurine with TNB. We found that the

reaction proceeds by a pathway involving the deprotonated TNB thiolate (nucleophile) and TauCl_2 (electrophile) over $6.5 \leq \text{pH} \leq 7.5$ range. These results suggest that dichloramines may be contributing towards the oxidative killing of invading pathogens.

- We demonstrated using A549 lung cancer cells and the rhodamine-hydroxamic acid-based fluorescent probe that SCN^- quenches cellular chloramines. Cells that were treated with HOCl and the probe showed strong fluorescence while after treating the cells with SCN^- no fluorescence was observed. We further probed the effects of the reaction of SCN^- with cellular chloramines on the viability of A549 cells. Using flow-cytometry, we observed that when cells that were pretreated with sublethal concentration of HOCl were now treated with SCN^- , the result was an increase in the proportion of live cells accompanied by a decrease in the proportion of necrotic cells. We believe that these experiments provide some evidence of SCN^- repairing and reversing the damage caused by HOCl on the A549 cells.
- We further investigated whether SCN^- was capable of restoring some activity of glutathione reductase (GR) that was inactivated by HOCl. We recovered approximately close to half of the GR activity. Since GR has a histidine residue in its active site, we suspect that the modification by HOCl affects this residue which leads to the formation of histidine chloramine. We believe therefore that the observed recovery of GR activity is due to the reaction of SCN^- with the histidine chloramine.

Recommended future studies:

- The reaction of OSCN^- with chloramines requires further investigation. We only measured the rate constant but never characterized the reaction products nor conducted a detailed mechanistic investigation. This reaction may be important in vivo because we observed that chloramines react faster with OSCN^- than with SCN^- .
- A more detailed mechanistic investigation for the reaction of dichlorotaurine with thiols is recommended. The work reported in this dissertation is a snapshot of a more complex mechanism. It is still unclear why dichlorotaurine reacts so much faster with TNB than chlorotaurine. To bolster the case for possible involvement of dichloramines in the killing of pathogens by neutrophils, future endeavors should also focus on finding evidence for the presence of dichloramines in vivo as this information is very scarce.
- A detailed investigation of the reaction of HOCl inactivated GR with SCN^- is required. We speculated in our work that it was the reaction between the histidine chloramine of GR and SCN^- that resulted in the restoration of GR activity. We however, do not have concrete evidence for this conclusion. Also, other housekeeping enzymes should be considered in future studies.

- The apparent ability of SCN^- to recover some of the GR activity following HOCl treatment should be further demonstrated in cell lysate. Our attempts fell short due to the low GR concentration and lack of specificity of the assay we used. New assays that are more specific and sensitive should be employed.

APPENDIX

LIST OF ABBREVIATIONS

A.C.S	American Chemical Society
BODIPY	Dipyrrromethene boron difluoride
CF	Cystic fibrosis
DIC	Differential interference contrast
DTNB	5,5-Dithio-bis (2-nitrobenzoic acid)
EDTA	Ethylenediaminetetraacetic acid
FAD	Flavin adenine dinucleotide
GR	Glutathione reductase
GSH	Reduced glutathione
GSSG	Oxidized glutathione
LPO	Lactoperoxidase
MPO	Myeloperoxidase
NADPH	Nicotinamide adenine dinucleotide phosphate
NCT	N-chlorotaurine
NDCT	N-dichlorotaurine
NFK	N-formylkynurenine
OSCN ⁻	Hypothiocyanite
PMN	Polymorphonuclear leukocytes
RNS	Reactive nitrogen species
ROS	Reactive oxygen species
RPMI	Roswell Park Memorial Institute
SCN ⁻	Thiocyanate
SNAPF	Sulfonaphthoaminophenyl fluorescein
TNB	5-Thio-2-nitrobenzoic acid
Ub*Cl	Ubiquitin chloramines